frontiers | Frontiers in Nutrition

ORIGINAL RESEARCH
published: 14 June 2022
doi: 10.3389/fnut.2022.898782

Plasma Metabolic Signatures of Healthy Overweight Subjects Challenged With an Oral Glucose Tolerance Test

Jarlei Fiamoncini[1,2], Carlos M. Donado-Pestana[2], Graziela Biude Silva Duarte[2], Milena Rundle[3], Elizabeth Louise Thomas[4], Yoana Kiselova-Kaneva[5], Thomas E. Gundersen[6], Diana Bunzel[7], Jean-Pierre Trezzi[8,9], Sabine E. Kulling[7], Karsten Hiller[8,9], Denise Sonntag[10], Diana Ivanova[5], Lorraine Brennan[11], Suzan Wopereis[12], Ben van Ommen[12], Gary Frost[3], Jimmy Bell[4], Christian A. Drevon[6,13] and Hannelore Daniel[1]*

[1] Department Food and Nutrition, Technische Universität München, Freising, Germany, [2] Food Research Center, Department of Food Science and Experimental Nutrition, School of Pharmaceutical Sciences, University of São Paulo, São Paulo, Brazil, [3] Division of Diabetes, Endocrinology and Metabolism, Department of Medicine, Imperial College London, London, United Kingdom, [4] Research Centre for Optimal Health, School of Life Sciences, University of Westminster, London, United Kingdom, [5] Department of Biochemistry, Molecular Medicine and Nutrigenomics, Medical University, Varna, Bulgaria, [6] Vitas Ltd., Oslo Science Park, Oslo, Norway, [7] Department of Safety and Quality of Fruit and Vegetables, Federal Research Institute of Nutrition and Food, Max Rubner-Institut, Karlsruhe, Germany, [8] Braunschweig Integrated Centre of Systems Biology, University of Braunschweig, Braunschweig, Germany, [9] Department of Computational Biology of Infection Research, Helmholtz Centre for Infection Research, Braunschweig, Germany, [10] biocrates life sciences AG, Innsbruck, Austria, [11] UCD School of Agriculture and Food Science, Institute of Food and Health, Conway Institute, University College Dublin, Dublin, Ireland, [12] Netherlands Organisation for Applied Scientific Research, Netherlands Institute for Applied Scientific Research, Microbiology and Systems Biology, Zeist, Netherlands, [13] Department of Nutrition, Faculty of Medicine, Institute of Basic Medical Sciences, University of Oslo, Oslo, Norway

OPEN ACCESS

Edited by:
Rikard Landberg,
Chalmers University of Technology, Sweden

Reviewed by:
Cherlyn Ding,
Nestlé Research Center, Switzerland
Sergio Polakof,
Institut National de la Recherche Agronomique (INRA), France

***Correspondence:**
Hannelore Daniel
contact@hdaniel.de

Specialty section:
This article was submitted to Nutrition and Metabolism, a section of the journal Frontiers in Nutrition

Received: 17 March 2022
Accepted: 05 May 2022
Published: 14 June 2022

Citation:
Fiamoncini J, Donado-Pestana CM, Duarte GBS, Rundle M, Thomas EL, Kiselova-Kaneva Y, Gundersen TE, Bunzel D, Trezzi J-P, Kulling SE, Hiller K, Sonntag D, Ivanova D, Brennan L, Wopereis S, van Ommen B, Frost G, Bell J, Drevon CA and Daniel H (2022) Plasma Metabolic Signatures of Healthy Overweight Subjects Challenged With an Oral Glucose Tolerance Test. Front. Nutr. 9:898782. doi: 10.3389/fnut.2022.898782

Insulin secretion following ingestion of a carbohydrate load affects a multitude of metabolic pathways that simultaneously change direction and quantity of interorgan fluxes of sugars, lipids and amino acids. In the present study, we aimed at identifying markers associated with differential responses to an OGTT a population of healthy adults. By use of three metabolite profiling platforms, we assessed these postprandial responses of a total of 202 metabolites in plasma of 72 healthy volunteers undergoing comprehensive phenotyping and of which half enrolled into a weight-loss program over a three-month period. A standard oral glucose tolerance test (OGTT) served as dietary challenge test to identify changes in postprandial metabolite profiles. Despite classified as healthy according to WHO criteria, two discrete clusters (A and B) were identified based on the postprandial glucose profiles with a balanced distribution of volunteers based on gender and other measures. Cluster A individuals displayed 26% higher postprandial glucose levels, delayed glucose clearance and increased fasting plasma concentrations of more than 20 known biomarkers of insulin resistance and diabetes previously identified in large cohort studies. The volunteers identified by canonical postprandial responses that form cluster A may be called pre-pre-diabetics and defined as "at risk" for development of insulin resistance. Moreover, postprandial changes in selected fatty acids and complex lipids, bile acids, amino acids, acylcarnitines and sugars like mannose revealed marked differences in the responses seen in cluster A and cluster B individuals that sustained over the entire challenge test period of 240 min. Almost all metabolites, including glucose and insulin, returned to baseline values at the end of the test (at 240 min), except a variety of amino acids and here those that have been linked to diabetes development. Analysis of the corresponding metabolite profile in a fasting blood sample may therefore allow for early identification of these subjects at risk for insulin resistance without the need to undergo an OGTT.

Keywords: dietary challenge test, metabotypes, OGTT, postprandial metabolism, insulin resistance

INTRODUCTION

Subjects with insulin resistance display impaired phenotypic flexibility as a consequence of a reduced capacity for insulin-stimulated glucose uptake into muscle and adipose tissue and insufficient suppression of hepatic gluconeogenesis (1, 2). The oral glucose tolerance test (OGTT) is an effective assessment method for identification of an insulin resistant state, a pre-stage for multiple chronic diseases, including diabetes type II. Insulin by its pleiotropic actions affects interorgan fluxes of almost all nutrient classes and in turn, insulin resistance results in impaired metabolite partitioning and that may therefore contribute to metabolic dysregulation (3, 4).

The application of metabolic profiling attempts in human studies are often limited to biosamples that can be easily collected such as urine or plasma/serum. Yet, these metabolite patterns can provide insights into physiological control processes or the establishment of diseases (5, 6). Metabolic profiling techniques applied in human studies have led to the identification of plasma metabolite signatures associated with insulin resistance dominated by branched-chain amino acids (BCAA), acylcarnitines, gluconeogenesis precursors, bile acids (BA), ketone bodies and specific lipid groups (7–9). When applied together with a dietary challenge such as the OGTT these techniques may identify adaptive response patterns as well as biomarkers and pathways that describe the flexibility of the metabolic system or its impairment and role in the development of non-communicable chronic diseases (6, 10). Following digestion of food and absorption of nutrients, individual organs are provided with these substrates in processes mostly regulated by insulin. These processes also reveal a high individual variability with the term "metabotype" introduced to describe the different patterns of metabolic response or different "metabolic phenotypes" (11, 12). The characterization and classification may contribute to the development of new interventions in the framework of personalized nutrition (13). Unfortunately, most human studies that employ metabolite profiling technologies, assess subjects in the overnight fasting condition only, therefore lacking phenotypical information derived from the response to a meal. This creates a significant gap of information as humans with safe access to food spend most of their waking hours in the postprandial state.

We previously identified distinct metabotypes within a healthy study population, identified based on their response to a mixed meal, revealing a co-regulation of different physiologic processes, allowing early detection of metabolic impairments and susceptibility to the beneficial effects of energy restriction (14). In the present study, we aimed at identifying markers associated with differential responses to an OGTT in the same population of healthy adults. In this exercise, we describe the close association of several metabolites in plasma with the insulin-dependent postprandial responses employing 3 metabolite profiling platforms. The analysis enabled the identification of new biomarkers to be identified that are linked to the body's insulin-responsiveness.

MATERIALS AND METHODS

Ethics Approval and Study Registration

The intervention study was conducted under the umbrella of the "NutriTech" project and was carried out at NIHR/Wellcome Trust Imperial Clinical Research Facility at Hammersmith Hospital of Imperial College London. The study was approved by the Brent Ethics Committee (REC ref: 12/LO/0139) and registered at clinicaltrials.gov record: NCT01684917. NutriTech was funded by the European Union Framework 7 program.

Study Population and Experimental Design

The data presented here was obtained from one out of the three dietary challenges (OGTT) performed in the NutriTech study. Participants attended a health-screening visit at the research facility that included measurements of height, weight, body composition by bioelectric impedance, blood pressure, electrocardiogram and markers of clinical chemistry: glucose, insulin, glycated hemoglobin, plasma lipids, hematocrit, liver and kidney functions. A total of 72 subjects (38 women and 34 men) that displayed no signs of metabolic diseases judged by the clinical assessment during screening completed the study. All female participants were post-menopausal. The individuals were overweight/ obese, with BMI ranging from 24.7 to 35.5.

All volunteers underwent an oral glucose tolerance test (OGTT). Subjects were instructed to avoid alcohol consumption and strenuous exercise prior to each study visit. The OGTT started at 09:00 am following a 12-h fasting. Upon arrival, participants had a catheter placed in the antecubital vein by a trained nurse and a fasting blood sample was obtained. The test consisted in the ingestion of 75 g of glucose dissolved in 250 mL of water and blood sampling at 0, 15, 30, 60, 90, 120 and 240 min. The cannula was flushed with saline between blood collections and 3 mL of waste was drawn first to allow for the saline diluted blood before the blood was taken for analysis. Plasma (from heparin coated tubes) and serum were separated after centrifugation at 1,800 rpm and stored at −80°C for future analyses.

Measurement of Markers of Intermediate Metabolism and Inflammation

Serum insulin concentration was measured by radioimmunoassay using a Human Specific Insulin RIA Kit (Millipore Corporation) accordingly to manufacturer's instructions. Glucose levels in serum were measured by an enzymatic method using an Abbott Architect ci8200 analyzer. Plasma glucagon was measured with a RIA kit (GL-32K Sigma-Aldrich). PYY and GLP-1 were also measured using RIA, following previously established methods (15, 16). Non-esterified fatty acids (NEFA), albumin, ammonia, urea, creatine, aspartate aminotransferase, gamma-glutamyl transpeptidase, total cholesterol, HDL-cholesterol, LDL-cholesterol, triacylglycerides, and uric acid levels, where measured using standard enzymatic methodology according to manufacturer's instructions. Leptin levels in plasma were assayed by a sandwich enzyme immunoassay (ELISA) (BioVendor, Czech Republic). The cytokines and other inflammation markers like CRP, IL-8, IL-10-, IL-18, ICAM-1, MCP-1 were measured by Vitas AS (www.vitas.no) using ELISA technology. IL-8, ICAM-1, IL-10, sE-selectin, TNF-α, CRP, adiponectin and IL-1β in plasma were analyzed using ELISA kits (Invitrogen Corporation, USA). MCP-1 and sVCAM-1 in plasma were analyzed using ELISA kits (Life Technologies, USA).

Plasma fatty acids (FA) were measured by 2 independent groups with different methodologies. One of the groups (Vitas AS, Oslo, Norway) quantified FA in the fasting state using GC-FID providing data expressed as μg/mL and a FA profile expressed in percentage (17), while the other group analyzed FA concentrations in plasma sampled during the OGTT using GC-MS.

Assessment of Body Composition and Physical Activity

Adipose tissue content and distribution, as well as liver and muscle fat content were assessed using magnetic resonance imaging (MRI) and spectroscopy (MRS), on a 1.5T Phillips multinuclear system as previously described (18). Briefly, single voxel spectra (2 x 2 x 2 cm^3; TE/TR= 135/1500 ms) were obtained from the liver using a PRESS sequence for measurement of intrahepatocellular lipid (IHCL). Spectra were also acquired from the Soleus and Tibialis muscles to measure intra-myocellular lipid (IMCL). Body fat was assessed using a whole-body rapid T1-weighted spin echo sequence. Participants were scanned from head to toes by acquiring 10 mm thick transverse images with 10 mm gaps between slices.

In order to assess the level of physical activity, participants were asked to wear an accelerometer (BodyMedia SenseWear, USA) on the non-dominant arm for 7 days. Final value was presented as day average in metabolic equivalents (METs).

Mass Spectrometry-Based Plasma Metabolite Profiling

All plasma samples were randomized to exclude batch variation. Quality control plasma samples (Recipe chemicals and instruments, Munich, Germany) were included into each set of samples to control for instrument drifting and other technical issues during measurements.

Acylcarnitines (19) amino acids (20), biogenic amines (12), glycerophospholipids (90), and sphingolipids (15) were quantified in plasma using the LC-MS/MS based AbsoluteIDQ® p180 Kit (biocrates life sciences AG, Innsbruck, Austria), following the manufacturer's protocol and excluding metabolites below the limit of detection. Additional acylcarnitines (21) were quantified after sample extraction with methanol in the presence of deuterated standards and butylated prior to analysis using LC-MS/MS coupled to a Sciex 5500 MS (Sciex, USA) following a previously described method (22). The 13 most abundant bile acids in plasma were quantified using an adaptation of the method previously described. Briefly, 10 μL of plasma were mixed with deuterated internal standards and after methanolic extraction, the samples were evaporated to dryness, reconstituted in methanol:water (1:1) and injected into the LC-MS/MS system as described (23).

For the GC-MS analysis, metabolites were extracted from 40 μL plasma aliquots using ice-cold methanol:H_2O (8:1) in a ratio of 1:10 (sample:solvent). After centrifugation (13,200 g, 4 min, 4°C), 200 μL of supernatant was completely dried under vacuum. A 2-step derivatization was performed using an autosampler (Agilent 7693, Agilent Technologies, Germany) by incubating the samples with methoxyamine hydrochloride (20 mg/mL in pyridine) for 30 min at 45°C, followed by the addition of N-methyl-N-trimethylsilyl-triflouroacetamide, and a second incubation for 30 min at 45°C. Each sample was thereafter immediately submitted to GC–MS analysis (Agilent 6890N GC coupled to an Agilent 5975C inert XL - Agilent Technologies, Germany). The gas chromatograph was equipped with a 30 m DB-35MS capillary column (Agilent J&W GC Column). Metabolites were eluted by a temperature gradient starting at 80°C and rising by 11°C/min to 325°C with 5 min hold at 325°C. Metabolite identification and quantification was accomplished using the Metabolite Detector software. Metabolites were identified according to their retention time and spectra similarity against the Golm metabolome database.

Data Analysis

The aim of this study was to assess metabolic differences in subjects that display differential glucose responses to an OGTT. Our first approach was to check for different patterns of glycemic response to the OGTT using a hierarchical cluster analysis (HCA) based on glucose concentrations measured at 7 time points during the test. The analysis identified 2 clear clusters of subjects or patterns of response (**Supplementary Figure 1**). Cluster A was comprised of 33 subjects of whom 14 were female (42%), whereas cluster B had 39 subjects of whom 24 were females (61% female). A Chi-square test ruled out the gender discrepancy between the two groups ($p = 0.10$, **Table 1**).

A partial least squares discriminant analysis (PLS-DA) was performed including all measured variables, except for glucose and insulin to compare clusters A and B and identify discriminant variables. A list with all metabolites and other variables used in the analysis is presented in **Supplementary Table 1**. The model was built with 1,222 variables classified into the following 14 categories: bile acids, acylcarnitines, oxidative stress markers, amino acid metabolism markers, signaling molecules, biogenic amines, body composition, lipid metabolism markers, inflammation, leucocytes, markers of glucose metabolism, glycerophospholipids and sphingomyelins (**Supplementary Table 1**). In case of variables measured in all 7 plasma samples collected during the OGTT, each data point was considered as an independent variable. The variables with Variable Importance in the Projection (VIP) value ≥ 1 were further analyzed in univariate statistical analysis, except when only one data point of a given metabolite measured during the OGTT received a VIP value >1. In these cases, the metabolite was not considered of relevance and was not further analyzed. The selected variables are presented as line graphs, if considered different between the clusters after a mixed-effects analysis. Additionally, a Pearson's correlation analysis was performed between all selected variables that were statistically different between clusters A and B with the average glucose concentration during the OGTT (postprandial glycaemia).

Depending on the nature of comparisons, ordinary one-way ANOVA or a mixed-effects analysis (in case of variables measured in samples collected during the OGTT) were used to test differences between the groups. Multiple comparisons were tested using Tukey's *post-hoc* test. Differences with $p < 0.05$ were considered as significant. Shapiro-Wilk test was used to assess normality ($p < 0.05$). In cases where outliers were removed, their detection was done using the ROUT method. Pearson's

TABLE 1 | Characteristics of the study population.

	A			**B**			***t* test**
	Mean	**SD**	**N**	**Mean**	**SD**	**N**	***p*-Value**
Age (years)	60.2	3.26	33	58.3	4.66	39	0.063
BMI (kg/m^2)	29.39	3.02	33	29.01	2.53	39	0.565
TAT (kg)	31.52	10.20	29	30.97	7.93	39	0.806
TAT (%BW)	36.00	9.32	29	37.92	9.05	39	0.395
DBP (mmHg)	77.89	6.76	33	77.31	10.14	39	0.778
SBP (mmHg)	126.64	10.38	33	126.74	14.08	39	0.971
Fasting glucose (mmol/L)	5.58	0.42	33	4.81	0.39	39	<0.000001
Fasting insulin (mIU/L)	19.09	8.42	31	13.12	4.13	39	0.0002
HOMA-IR	4.53	1.79	30	2.81	0.90	39	0.000002
Cholesterol (mmol/L)	4.83	0.93	32	4.90	0.83	37	0.736
HDL-chol (mmol/L)	1.62	0.15	32	1.69	0.20	37	0.088
LDL-chol (mmol/L)	2.53	0.86	32	2.69	0.77	37	0.414
GGTP (U/L)	28.72	21.79	32	22.22	22.08	37	0.224
AST (U/L)	20.84	7.06	32	21.76	9.60	37	0.659
AP (IU/L)	77.44	20.44	32	72.32	23.18	37	0.338
Uric acid (μmol/L)	319.94	90.28	32	286.32	72.04	37	0.090
TSH (mUI/L)	1.68	0.76	32	1.81	0.96	39	0.546
T4 (pmol/L)	13.47	1.46	32	13.23	1.37	39	0.481
Leptin (ng/mL)	15.72	8.32	32	14.53	8.02	38	0.547
TNF-α (pg/mL)	3.31	1.12	33	3.57	2.08	39	0.526
IL-18 (pg/mL)	266.42	88.40	33	235.82	105.30	39	0.191
VCAM (ng/mL)	1,909.76	980.45	33	1,674.46	709.51	39	0.243
CRP (ng/mL)	674.61	709.68	33	1,198.10	2,529.50	39	0.254
Female (N)	14 (42%)			24 (61%)			X2 *p*-value = 0.10

As a recruitment criterion, participants of the study were considered healthy after a medical assessment. Data presented as mean ± standard devdiation. The bottom row provides the gender distribution in each cluster, which was found not to be different, according to a Chi square test (p = 0.10). AST, aspartate aminotransferase; AP, alkaline phosphatase; BMI, body mass index; CRP, C-reactive protein; DBP, diastolic blood pressure; GGTP, gamma-glutamyl transpeptidase; HDL, high density lipoproteins; HOMA-IR, Homeostatic model assessment for insulin resistance; IL-18, interleukin 18; LDL, low density lipoproteins; SBP, systolic blood pressure; TAT, total adipose tissue; TNF-a, tumor necrosis factor-alpha; TSH, thyroid-stimulating hormone; T4, thyroxine; VCAM, vascular cell adhesion molecule.

multiple correlation analysis was performed assuming that most of the variables followed a normal distribution. GraphPad Prism Software (version 9.0) was used for these analyses and preparing most of the figures. PLS-DA was performed using SIMCA software (version 16) after data scaling using unit variance.

RESULTS

The study population was considered overweight/obese according to the WHO (average BMI = 29.2), but did not present high blood pressure nor hyperlipidemia, despite the mean age of 59.2 years old. The presence of obese individuals (BMI > 29.9) was proportional in both groups: 45% in group A and 36% in group B. There were also no differences in the plasma concentrations of thyroid hormones, leptin or inflammatory markers between clusters A and B (**Table 1**).

The focus of this study was to identify markers of metabolic responses to an OGTT, and the chosen approach included a hierarchical cluster analysis considering glucose concentrations measured throughout the test, resulting in the identification of two groups of volunteers, named clusters A and B. As seen in **Figure 1**, cluster A displayed higher fasting and postprandial plasma glucose levels and an exaggerated insulin response, indicating a certain state of insulin resistance, also confirmed by the HOMA-IR values that were 60% higher than those of individuals in cluster B (**Table 1**). A PLS-DA model comparing clusters A and B in search of discriminant variables revealed differences between these 2 groups (the model has 1 component, $R^2 = 0,5$ and $Q^2 = 0,27$). A cross-validation performed using the K-fold method (**Supplementary Figure 1**) indicates robust differences between the two groups and the analyses of variance of the cross-validated residuals returned a *p* value = 0.000028 as statistical significance of the model.

The next step of our analysis was an univariate statistical test among the variables that received a VIP value > 1 in the PLS-DA model. **Table 2** reports these variables obtained in the overnight fasting state only. Despite the absence of differences in the BMI between groups (**Table 1**), the content of intra-abdominal adipose tissue (IAAT) was 35% higher in cluster A as well as internal body fat and liver fat associated with cluster A. Liver fat content appeared as particularly relevant, as it revealed a strong correlation with the average glucose concentrations during the test (r = 0.69; *p* = 1.77E-10) and was 3.1-fold higher

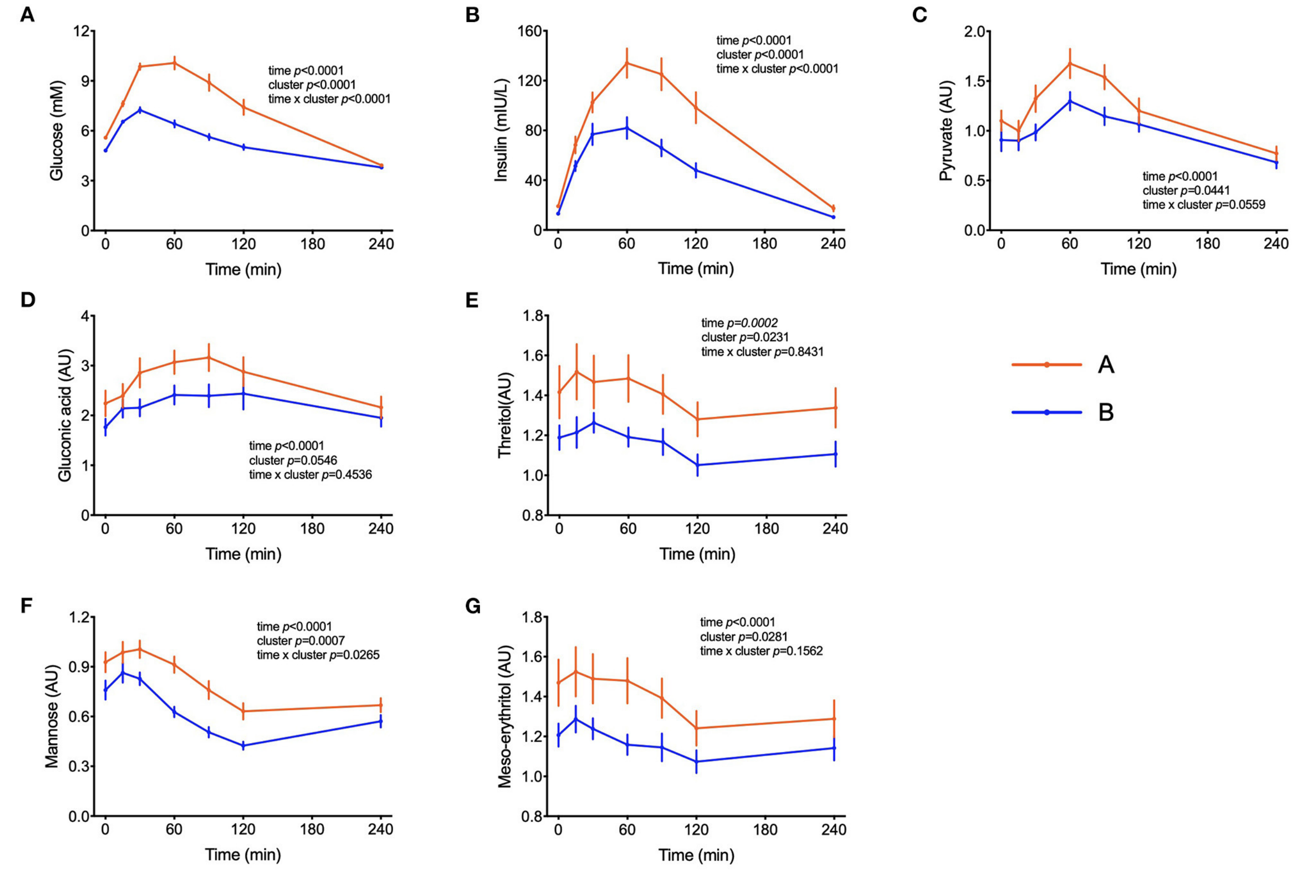

FIGURE 1 | Handling of glucose and other sugars and sugar-derivatives. **(A–G)** Plasma glucose and insulin concentrations during the OGTT and levels of pyruvate, gluconate, threitol, mannose and meso-erythritol (AU = arbitrary units). Data are presented as the means and standard errors of the mean. Results from mixed-effects analysis indicated in each graph.

TABLE 2 | Discriminant variables measured in fasting state.

	A			**B**			***t* test**		**Pearson corr x Glucose**		**A/B**
	Mean	**SEM**	**N**	**Mean**	**SEM**	**N**	***p*-Value**	**q value**	**rho**	***p*-Value**	
Plasma fatty acids (μg/ml)											
C14:0	37.48	2.99	33	23.49	1.79	39	0.0001	0.0007	0.44	0.0001	1.60
C15:0	7.13	0.36	33	5.79	0.29	39	0.0040	0.0072	0.31	0.0077	1.23
C16:0	766.45	39.79	33	606.54	22.03	39	0.0005	0.0024	0.40	0.0005	1.26
C16:1 n-7	86.85	6.20	33	60.05	4.97	39	0.0011	0.0038	0.33	0.0044	1.45
C18:0	218.52	8.92	33	187.38	4.94	39	0.0022	0.0056	0.31	0.0091	1.17
C18:1 c11	61.94	3.49	33	51.18	2.20	39	0.0089	0.0131	0.30	0.0109	1.21
C18:1 c9	707.03	38.67	33	566.62	19.66	39	0.0012	0.0038	0.40	0.0005	1.25
C18:1 t6-11	41.58	3.19	33	32.67	2.29	39	0.0236	0.0258	0.23	0.0486	1.27
C18:3 n-3	24.12	2.08	33	18.87	0.81	39	0.0149	0.0203	0.31	0.0081	1.28
C20:1 n-9	5.10	0.28	33	4.33	0.17	39	0.0190	0.0220	0.33	0.0049	1.18
C20:2 n-6	7.89	0.50	33	6.51	0.32	39	0.0190	0.0220	0.25	0.0349	1.21
C20:3 n-6	44.21	2.17	33	38.49	1.72	39	0.0398	0.0402	0.24	0.0406	1.15
C22:5 n-3	21.36	1.02	33	17.26	0.53	39	0.0004	0.0023	0.31	0.0081	1.24
C22:6 n-3	80.73	4.95	33	69.13	2.82	39	0.0380	0.0394	0.14	0.2343	1.17
Plasma fatty acids (%)											
C14:0	1.07	0.05	33	0.79	0.04	39	2.30E-05	0.0004	0.49	1.15E-05	1.37
C16:0	22.45	0.29	33	20.77	0.25	39	2.80E-05	0.0004	0.50	9.91E-06	1.08
C16:1,n-7	2.51	0.12	33	2.00	0.13	39	0.0057	0.0089	0.28	0.0198	1.25
C18:1,c9	20.58	0.46	33	19.46	0.32	39	0.0458	0.0440	0.38	0.0012	1.06
C18:2,n-6	22.24	0.52	33	25.13	0.50	39	0.0002	0.0011	−0.45	0.0001	0.89
C20:0	0.26	0.01	33	0.28	0.01	39	0.0187	0.0220	−0.34	0.0042	0.91
C22:0	0.58	0.02	33	0.67	0.02	39	0.0036	0.0068	−0.39	0.0008	0.87
C23:0	0.29	0.01	33	0.34	0.01	39	0.0054	0.0088	−0.39	0.0008	0.85
C24:0	0.63	0.02	33	0.71	0.02	39	0.0081	0.0123	−0.38	0.0011	0.88
C24:1,n-9	1.12	0.04	33	1.38	0.04	39	4.10E-05	0.0004	−0.49	1.37E-05	0.81
Body composition/anthropometric variables											
Waist (cm)	102.24	1.77	33	97.30	1.70	39	0.0489	0.0459	0.39	0.0008	1.05
IAAT (%BW)	5.37	0.28	29	4.14	0.22	39	0.0009	0.0038	0.46	0.0001	1.30
IAAT (%TBF)	15.78	1.02	29	11.70	0.84	39	0.0028	0.0062	0.43	0.0003	1.35
IAAT (kg)	4.70	0.29	29	3.48	0.23	39	0.0012	0.0038	0.52	6.50E-06	1.35
IAAT:ASAT	0.80	0.07	29	0.53	0.05	39	0.0016	0.0046	0.39	0.0010	1.51
Internal (%TBF)	26.96	1.45	29	21.34	1.14	39	0.0030	0.0062	0.39	0.0011	1.26
Internal (%BW)	9.19	0.36	29	7.65	0.29	39	0.0014	0.0042	0.39	0.0010	1.20
Internal (kg)	8.04	0.42	29	6.38	0.33	39	0.0023	0.0056	0.47	0.0001	1.26
Internal: subcutaneous	0.38	0.03	29	0.28	0.02	39	0.0032	0.0063	0.37	0.0018	1.37
Liver lipids	7.40	1.15	29	2.38	0.28	38	0.00001	0.0004	0.69	1.77E-10	3.11
NAIAT (%TBF)	11.18	0.56	29	9.65	0.38	39	0.0225	0.0254	0.22	0.0702	1.16
NAIAT (kg)	3.34	0.17	29	2.90	0.13	39	0.0454	0.0440	0.27	0.0246	1.15
Soleus m. IMCL	18.06	1.58	29	14.73	0.88	39	0.0534	0.0480	0.21	0.0950	1.23
Tibialis m. IMCL	8.11	0.61	29	6.72	0.42	39	0.0582	0.0504	0.18	0.1507	1.21
ASAT (%TBF)	21.08	0.70	29	22.99	0.50	39	0.0260	0.0276	−0.21	0.0931	0.92
NASAT (%TBF)	51.96	1.01	29	55.67	1.00	39	0.0127	0.0179	−0.38	0.0014	0.93
SAT (%TBF)	73.04	1.45	29	78.66	1.14	39	0.0030	0.0062	−0.39	0.0011	0.93
Metabolism markers											
HbA1c (mmol/mol Hb)	37.64	0.61	28	35.53	0.43	38	0.0049	0.0084	0.38	0.0017	1.06
MDA (μmol/L)	2.44	0.15	32	1.96	0.13	38	0.0186	0.0220	0.36	0.0025	1.24
s-E-Selectin (ng/mL)	41.85	3.81	33	29.33	3.52	39	0.0185	0.0220	0.34	0.0032	1.43
Adiponectin (μg/mL)	13.32	0.96	33	16.67	1.39	39	0.0589	0.0504	−0.40	0.0007	0.80

Only variables with a VIP value > 1 in the PLS-DA model are depicted in this table. The differences between the two clusters were tested with a T-test and their correlation (Pearson) with the average glucose concentration during the OGTT presented. The right (last) column presents the ratio of each variable between clusters A and B individuals. Highlighted rows indicate variables associated with cluster B. Variables that were not considered different between the two clusters after the T-test are not included in the table. ASAT, abdominal subcutaneous adipose tissue; AT, adipose tissue; IAAT, intra-abdominal adipose tissue; IMCL, intramyocellular lipids; MDA, malondialdehyde; NAIAT, non-abdominal internal adipose tissue; NASA, non-abdominal subcutaneous adipose tissue; SAT, subcutaneous adipose tissue. Total internal AT (Internal) was subdivided into Intra-abdominal AT (IAAT) and non-abdominal internal AT (NAIAT). Total Subcutaneous AT (SAT) was subdivided into abdominal subcutaneous AT (ASAT) and non-abdominal subcutaneous AT, with the abdominal region defined as the region between the top of the liver and the femoral heads. Adipose tissue was expressed relative to total body weight (%BW) or relative to total fat mass (%TBF).

in subjects from cluster A, as compared to cluster B individuals. Interestingly, the proportion of non-abdominal subcutaneous adipose tissue (NASAT) to total body fat was higher in cluster B, suggesting that given the same amount of body fat, its higher presence in the subcutaneous depot may provide some protection from insulin resistance (**Table 2**). As expected, higher HbA1c concentrations were associated with cluster A, as it was also the case for malondialdehyde and s-E-selectin concentrations.

Several fatty acids (FA) displayed higher overnight fasting concentrations in cluster A as compared to cluster B subjects. Myristic acid (C14:0) deserves particular attention, as its concentration, despite corresponding to only ∼1% of total FA, was 60% higher in cluster A and had the highest correlation among FA with the average glucose concentrations during the test ($r = 0.44$; $p = 0.0001$). Palmitic acid (C16:0) revealed a similar behavior, but even oleic (C18:1c9) and linolenic (C18:3n3) acids - often classified as beneficial FA - were most abundant in cluster A (**Table 2**). In the composition of the FA profile (as % of total), very long chain fatty acids such as lignoceric (C24:0) and nervonic (C24:1n9) had around 15% higher concentration than cluster A and their level was negatively correlated ($r = -0.38$ and -0.49; $p < 0.001$) with the average glucose concentrations during the OGTT (**Table 2**).

Peak plasma glucose reached Cmax at $t = 30$ min in both groups but individuals in cluster A displayed a 77% increase in comparison to fasting values, whereas in cluster B it increased by only 50%. After 120 min, plasma glucose levels in individuals from cluster B already returned to fasting values, whereas in cluster A these values were still 32% higher ($p = 0.0001$) than fasting levels (**Figure 1A**). Plasma insulin concentrations reached also Cmax at 30 min in cluster B but kept increasing till $t = 60$ min in cluster A, reaching values 65% higher ($p = 0.0005$) than in cluster B (**Figure 1B**). The concentrations of pyruvate, mannose, gluconic acid, threitol and meso-erythritol were also higher in individuals from cluster A (**Figure 1** and **Table 3**).

We previously reported that markers of lipid catabolism in response to mixed meal tolerance test could be used as the basis for the separation of individuals into different metabotypes (14). In the present dataset, a similar observation was made. Postprandial plasma concentration of non-esterified fatty acids (NEFA) as well as individual FA such as palmitic and oleic acids and 3-hydroxy-butyrate ranked highest amongst metabolites that discriminate clusters A and B (**Figure 2**). As seen in **Table 3**, palmitate and stearate were ∼17% higher in cluster A during the OGTT and were positively correlated to postprandial glucose concentration ($r = 0.31$, $p = 0.008$). Plasma concentration of several acylcarnitines derived from metabolization of FA displayed similar responses. Of note, miristoylcarnitine (C14) and hexanoylcarnitine (C6) displayed throughout the OGTT consistently lower plasma concentrations in cluster B, in comparison to cluster A, but positively correlated with postprandial glycaemia (**Figure 2** and **Table 3**).

The amino acids BCAA, glutamate, tyrosine, tryptophan, alanine and phenylalanine were found at higher concentrations in plasma of individuals in cluster A (**Figure 3**) and confirm that they are linked to insulin action. These amino acids all displayed strong correlations with postprandial glucose concentration with r-values ranging from 0.3 for phenylalanine to 0.64 for glutamate (**Table 3**). Similarly, plasma concentration of those acylcarnitines that are derived from the degradation of amino acids such as propionylcarnitine (C3), isovaleryl-carnitine (3-M-C4) and succinylcarnitine (C4-DC) had higher levels in subjects from cluster A than from cluster B (**Figure 4**). Isovalerylcarnitine plasma levels were 25% higher in the plasma of subjects from cluster A and displayed a strong correlation with postprandial glucose levels ($r = 0.56$, $p = 0.0000004$) (**Table 3**). Finally, glutamine, glycine and serine, showed 8–17% lower plasma concentration in subjects from cluster A than B, confirming also previous findings in their association with insulin sensitivity (**Figure 3** and **Table 3**). Amongst the biogenic amines spermidine and spermine were also found in higher concentrations in cluster A, as it was the case for urea, suggesting an altered amino acid handling during the OGTT in cluster A or B individuals. The average concentration of these metabolites across all 7 samples collected during the OGTT are given in **Table 3**.

Several bile acids (BA) were amongst the metabolites identified in the PLS-DA model as most discriminant between clusters A and B. In both groups, the sum of BA reached Cmax at $t = 60$ min. While concentrations started to decrease in cluster A participants after this time, in cluster B the concentration of total BA were kept at maximum levels until the end of the test, remaining 38% higher in comparison to cluster A ($p = 0.02$) as shown in **Figure 5**. A similar pattern was observed for the sum of glycine-conjugated and secondary BA as well as for the unconjugated and glycine-conjugated forms of cholic, chenodeoxycholic, deoxycholic and ursodeoxycholic acids and the taurine-conjugated forms of deoxycholic and lithocholic acids. Interestingly, individuals from cluster A displayed a higher proportional (percentual) fraction of unconjugated BA, deoxycholic and tauroursodeoxycholic acids (**Figure 5**), and a lower fraction of glycine-conjugated BA and a lower ratio of conjugated: unconjugated BA (**Figure 4**). Glycine-conjugated BA were negatively correlated to postprandial glycaemia ($r = -0.26$, $p = 0.02$) (**Table 3**).

In addition to metabolites other differences between clusters were observed in blood cell sub-populations during the OGTT. In both groups of subjects, the numbers of leucocytes in blood increased during the test, with total counts of white blood cells (WBC) reaching 23% higher counts in the 4th h of the test as compared to the fasting values ($p < 0.0001$) (**Figure 6**). On average across the 7 blood samples collected from each subject, 26% higher counts of WBC were found in cluster A and 37 and 27% higher numbers of neutrophils and monocytes, respectively. The levels of s-E-selectin were 43% higher in subjects from cluster A in comparison to cluster B ($p = 0.018$).

Figure 7 displays summary of the major differences between groups A and B considering anthropometric and body composition data, markers of clinical chemistry, and metabolites assessed in different metabolomics platforms. It clearly indicates which metabolites or other phenotypical features could be used for the "diagnosis" of glucose homeostasis. It compiles well known markers such as glucose concentration itself and liver lipids, but also less discussed markers such as different classes of BA or very long chain fatty acids.

TABLE 3 | Discriminant variables measured during the OGTT.

	A			**B**			***t* test**		**Pearson corr x Glucose**		**A/B**
	Mean	**SEM**	**N**	**Mean**	**SEM**	**N**	***p*-Value**	**q value**	**rho**	***p*-value**	
Bile acids											
TUDCA (%)	0.33	0.06	30	0.20	0.02	35	0.021	0.087	0.06	0.6505	1.67
Unconj. BA (%)	38.59	2.83	33	31.36	2.67	39	0.068	0.132	0.24	0.0414	1.23
Conj./ Unconj. BA	2.95	0.41	33	4.44	0.53	39	0.034	0.088	−0.31	0.0079	0.66
Gly-conj. BA (%)	51.85	2.26	33	60.36	2.28	39	0.011	0.068	−0.28	0.0179	0.86
Gly-conj. BA (nmol/L)	1,597.61	127.71	33	2,345.40	273.06	39	0.022	0.087	−0.26	0.0262	0.68
GCDCA (nmol/L)	853.72	79.15	33	1,164.85	106.33	39	0.026	0.087	−0.25	0.0380	0.73
Fatty acid-derived acylcarnitines											
C14 (μmol/L)	0.02	0.00	33	0.02	0.00	39	0.028	0.087	0.35	0.0028	1.18
C16 (μmol/L)	0.11	0.01	33	0.10	0.00	39	0.033	0.088	0.39	0.0007	1.14
C18 (μmol/L)	0.03	0.00	33	0.02	0.00	39	0.039	0.096	0.31	0.0083	1.16
C3 (μmol/L)	0.34	0.02	33	0.26	0.01	39	0.004	0.055	0.47	3.13E-05	1.28
C4 (μmol/L)	0.07	0.01	33	0.05	0.00	39	0.018	0.087	0.37	0.0014	1.37
C6 (μmol/L)	0.04	0.00	33	0.03	0.00	39	0.018	0.087	0.39	0.0008	1.34
Amino acids and amino acid-related metabolites											
Isovaleryl-carnitine (μmol/L)	0.08	0.01	33	0.06	0.00	39	0.011	0.068	0.56	4.00E-07	1.25
Spermidine (μmol/L)	0.18	0.03	33	0.12	0.01	39	0.041	0.097	0.41	0.0004	1.53
Spermine (μmol/L)	0.25	0.06	33	0.13	0.01	39	0.031	0.087	0.33	0.0052	1.90
Urea (mmol/L)	5.94	0.21	33	5.34	0.20	39	0.047	0.100	0.13	0.2626	1.11
Free carnitine (μmol/L)	39.65	1.49	33	35.94	1.30	39	0.064	0.129	0.26	0.0290	1.10
Glu (μmol/L)	51.52	4.43	33	31.41	2.39	39	0.0001	0.0017	0.64	1.39E-09	1.64
Ile (μmol/L)	59.61	2.20	33	53.16	1.90	39	0.029	0.087	0.56	3.31E-07	1.12
Leu (μmol/L)	114.85	4.51	33	101.89	3.12	39	0.018	0.087	0.52	2.21E-06	1.13
Phe (μmol/L)	53.84	1.38	33	49.93	1.09	39	0.028	0.087	0.30	0.0114	1.08
Trp (μmol/L)	54.19	1.26	33	49.66	1.20	39	0.011	0.068	0.33	0.0051	1.09
Val (μmol/L)	202.08	6.18	33	186.47	4.78	39	0.046	0.100	0.53	1.30E-06	1.08
Gln (μmol/L)	575.08	11.52	33	622.93	12.04	39	0.006	0.056	−0.29	0.0140	0.92
Gly (μmol/L)	206.06	9.64	33	247.27	12.05	39	0.011	0.068	−0.31	0.0077	0.83
Ser (μmol/L)	92.49	2.74	33	101.72	3.18	39	0.035	0.088	−0.22	0.0602	0.91
Glucose metabolism											
Glucose (mmol/L)	7.62	0.21	33	5.64	0.09	39	<0.000001	<0.000001	1		1.35
Insulin (mIU/L)	80.99	5.94	33	49.65	4.13	39	0.00003	0.00130	0.56	2.87E-07	1.63
Mannose (AU)	0.82	0.05	33	0.69	0.05	39	0.056	0.116	0.47	2.95E-05	1.18
Meso-Erythritol (AU)	1.42	0.10	33	1.18	0.05	39	0.030	0.087	0.24	0.0413	1.20
Threitol (AU)	1.41	0.10	33	1.17	0.04	39	0.023	0.087	0.27	0.0225	1.21
Pyruvate (AU)	1.22	0.10	33	0.98	0.07	39	0.042	0.097	0.37	0.0013	1.25
Lipids											
Palmitic acid (AU)	2.35	0.12	33	2.01	0.09	39	0.029	0.087	0.31	0.0080	1.17
Stearic acid (AU)	2.13	0.09	33	1.81	0.07	39	0.005	0.055	0.32	0.0060	1.18
Cholesterol (AU)	2.57	0.19	33	2.09	0.14	37	0.045	0.100	0.16	0.1951	1.23
Triglycerides (mmol/L)	1.52	0.08	33	1.09	0.06	39	0.0001	0.0017	0.52	2.37E-06	1.39
Leucocytes											
Monocytes (giga/L)	0.50	0.03	33	0.39	0.02	39	0.005	0.055	0.25	0.0340	1.27
Neutrophils (giga/L)	3.88	0.46	33	2.83	0.14	39	0.023	0.087	0.23	0.0518	1.37
White blood cells (giga/L)	6.31	0.49	33	4.98	0.18	39	0.008	0.068	0.27	0.0206	1.27

The variables measured in samples collected during the OGTT that received a VIP value > 1 in the PLS-DA model at a minimum of two time points are presented with the average concentration during the test. The differences between the 2 clusters were tested with a T-test and their correlation (Pearson) with the average glucose concentration during the OGTT is presented. The right (last) column presents the ratio of each variable between cluster A and B individuals. Highlighted rows indicate variables predominantly associated with cluster B. Variables not considered different between the two clusters after the T-test were not included in the table.

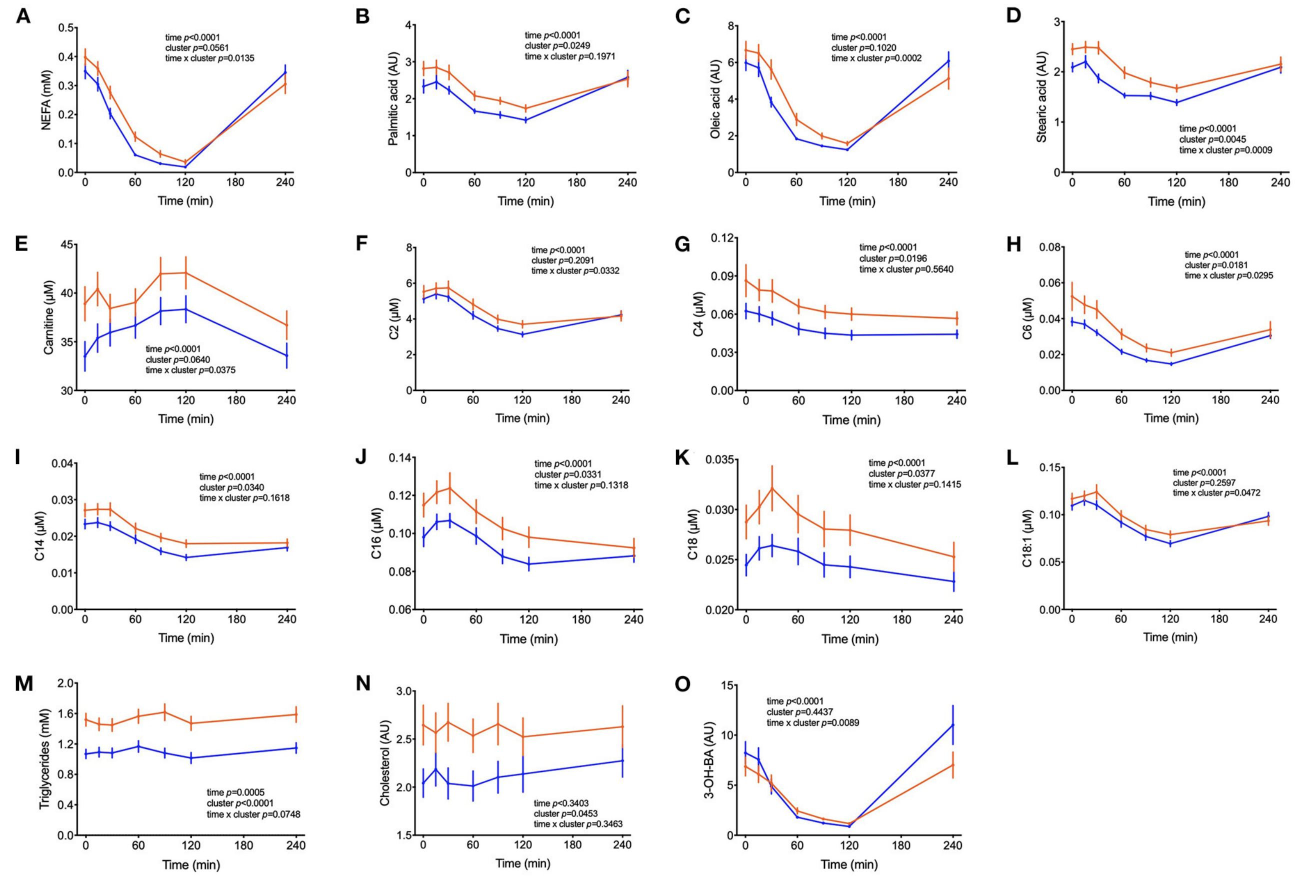

FIGURE 2 | Lipid metabolism. **(A–O)** Plasma concentrations of the sum of non-esterified fatty acids, free palmitic, oleic and stearic acids, free carnitine and fatty acid-derived acylcarnitines, triglycerides, cholesterol and 3-hydroxy-butyric acid (AU = arbitrary units). Data are presented as means and standard errors of mean. Results from mixed-effects analysis indicated in each graph.

DISCUSSION

According to the Word Health Organisation, impaired fasting glycemia (IFG) is characterized by fasting glucose levels between 6.1 and 7 mmol/L, while impaired glucose tolerance (IGT) is diagnosed when glucose levels are > 7 mmol/L at fasting and between 7.8 and 11 mmol/L at t = 120 minutes after the intake of 75 g glucose (24). Based on the WHO classification, only 3 subjects (4.6% of the study population) could be classified as impaired fasting glucose (IFG) and nobody fulfilled the criteria for IGT. Nevertheless, the PLS-DA model revealed 2 clear clusters that displayed distinct glucose concentrations after an overnight fasting and in the postprandial state (**Table 1** and **Figure 1**).

All volunteers were thoroughly phenotyped including anthropometrics, clinical parameters, whole body MRI. The comprehensive metabolite profiling with hundreds of metabolites from various chemical classes revealed as one of the key findings that cluster A individuals–separated from cluster B solely by the glycemic response–had altered plasma levels of almost all known biomarkers of insulin resistance previously identified in large cohorts including increased levels of the BCAA and related acylcarnitines, reduced glycine levels and numerous altered lipid species.

Other additional marker metabolites, seldom included in other metabolite platforms are sugars and sugar-derivatives such as mannose, meso-erythritol, threitol, gluconate and pyruvate. Mannose has recently been identified in an OGTT as a monosaccharide that behaving like glucose with insulin-dependence and altered levels in prediabetic and diabetic volunteers (20). Mannose levels were strongly correlated with glycaemia (r = 0.47, $p < 0.0001$) and such a correlation between plasma mannose and glucose in the fasting state was previously described and response of plasma levels of mannose to an OGTT has also been reported (19, 25, 26). Meso-erythritol was recently associated with adiposity gain in healthy subjects and pyruvate is the ultimate precursor of liver gluconeogenesis which is important for glycemic homeostasis in the fasting state (21, 27). In both clusters, during the OGTT, pyruvate reached C_{max} at t = 60 min and thus 30 min later than the glucose peak with average postprandial pyruvate concentration exceeding those in cluster B individuals by 25% in subjects from cluster A (**Table 3**) as also observed by Meyer et al. (28) and Wang et al. (29).

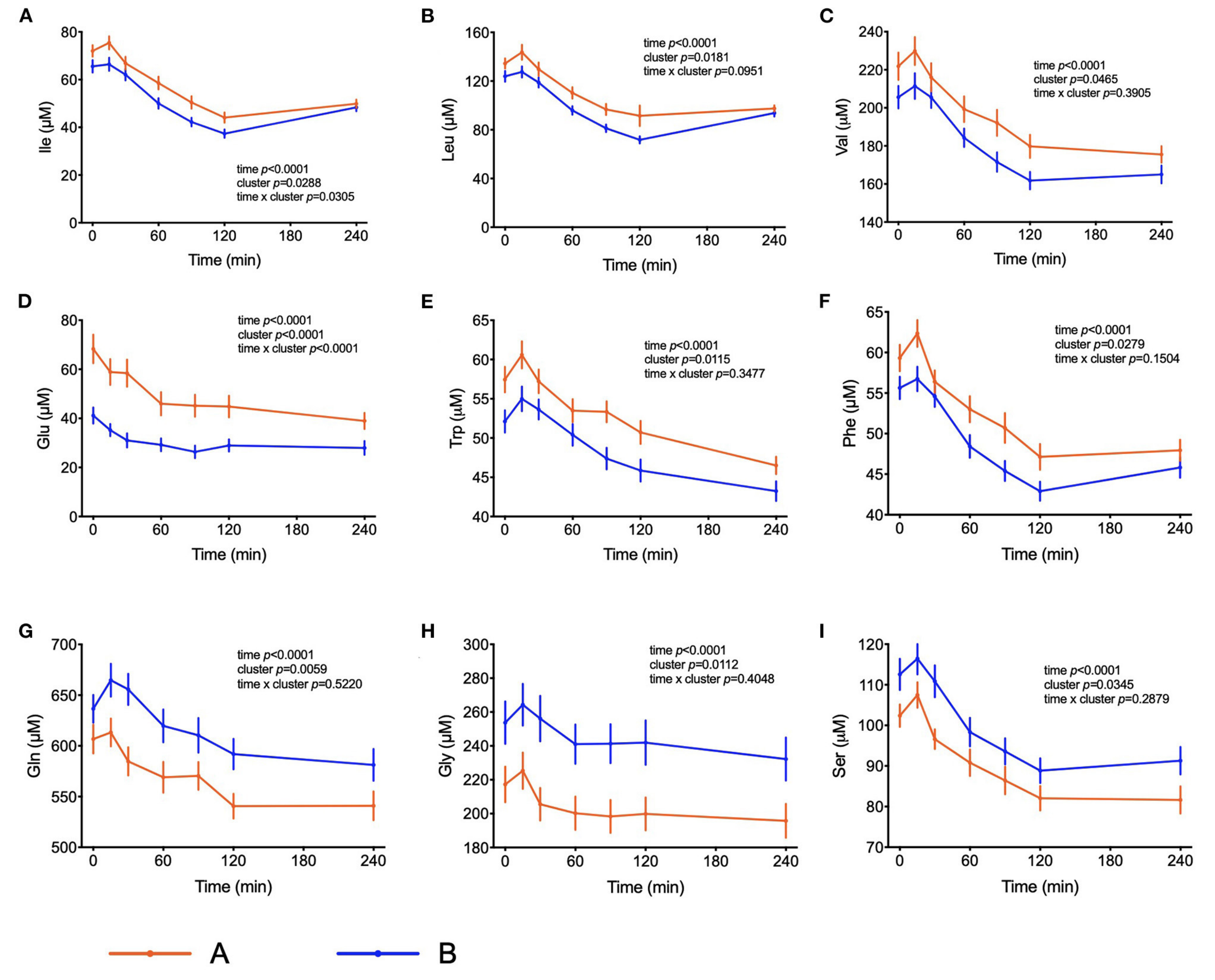

FIGURE 3 | Amino acid metabolism. **(A–F)** Plasma concentrations of selected amino acids that may serve as markers of insulin resistance. **(G–I)** Plasma concentrations of amino acids associated with insulin sensitivity. Data presented as the means and the standard errors of mean. Results from mixed-effects analysis indicated in each graph.

The higher postprandial insulin increase as well as its delayed return to fasting concentrations in subjects from cluster A might have a direct effect on the postprandial concentration of markers of lipolysis and catabolism of fatty acids. Elevated insulin concentrations suppress lipolysis in the adipose tissue, leading to a decrease in NEFA levels during an OGTT that reach their nadir at t = 120 min, followed by a rebound to fasting levels at t = 240 min. This characteristic postprandial kinetic profile of fatty acid and their catabolic products is due to the coordinated regulation of hormone sensitive lipase (HSL) and lipoprotein lipase (LPL), both timely altered in activity by insulin in the postprandial period (30). Levels of NEFA, palmitic, oleic, and stearic acids were all higher in cluster A compared to B in the early phase of the OGTT (until t = 120 min) whereas after reaching the nadir, the rebound was faster in cluster B individuals. Both observations are suggestive of a more efficient and precise regulation of lipolysis by insulin, or higher metabolic flexibility in cluster B individuals. Acylcarnitines derived from fatty acid β-oxidation and 3-OH-butyrate (**Figure 2**) also revealed this higher responsiveness in cluster B. Fatty acids and fatty acid-derived acylcarnitines in the fasting state were increased in patients with impaired glucose tolerance as compared to individuals with normal glucose tolerance (31, 32). Nowak et al. (33) observed a decline in plasma levels of fatty acids and acylcarnitines during a glucose challenge that was blunted in participants with insulin resistance as compared to insulin sensitive individuals (33).

The increased glucose uptake into muscle, adipose tissue and liver followed by storage in glycogen (liver and muscle) or conversion into long-chain FA (liver and adipose) but also increased flux through glycolysis and TCA, cause a transient increase in plasma levels of long-chain acyl-carnitines

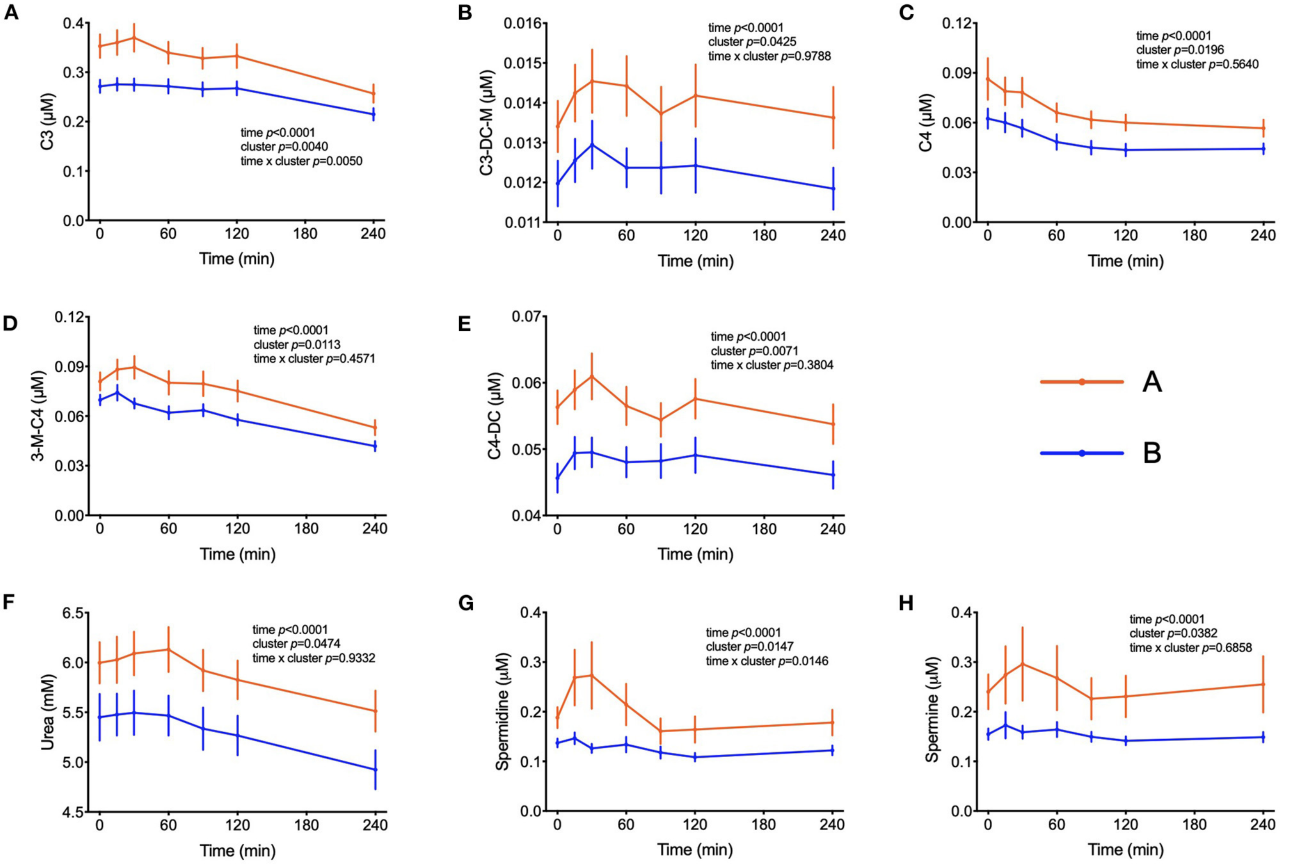

FIGURE 4 | Amino acid degradation. **(A–E)** Plasma concentrations of acylcarnitines derived from the degradation of amino acids. **(F)** Plasma concentrations of urea. **(G,H)** Plasma concentration of spermidine and spermine. Data presented as means and standard errors of mean. Results from mixed-effects analysis indicated in each graph.

(>16 carbon) although levels of the corresponding free FA decline simultaneously by inhibition of lipolysis. The efflux of mitochondrial-derived acylcarnitines into plasma seems to represent an overflow of substrates for oxidation (9). Although the carnitine palmitoyl transferase (CPT)-system in the inner mitochondrial membrane operates as an exchanger, the transport pathway for the cellular exit is less effective but it may also be of an exchange character as it was previously shown that free carnitine and acyl-carnitines in plasma under anabolic and catabolic conditions always behave mirror-like (4).

Elevated plasma BCAA levels and their degradation-derived acylcarnitines (C3 and C5) are established markers of insulin resistance, prediabetes and future onset of type 2 diabetes associated with an altered flux through BCAA catabolic pathways in obesity (34, 35). BCAA play a central role in insulin resistance and appear detrimental to insulin sensitivity in animals and humans (36). Amino acids may also affect a variety of other processes involved in glucose homeostasis (37). It has also been shown that amino acids influence the distribution of GLUT4-containing vesicles indicating that the insulin-dependent glucose influx mediated by an increase of GLUT4 density in the plasma membrane may already be compromised (38). It is interesting to note that troglitazone was able to increase amino acid uptake into preadipocytes, suggesting that amino acid uptake into adipose tissue is under insulin control (39). The response to the OGTT is characterized by a rapid decrease in circulating BCAA levels. We observed higher plasma BCAA concentrations among the individuals from cluster A compared to cluster B in the fasting state, which was subsequently maintained throughout the entire challenge, with the exception of the time point t = 240 min, when the differences among the two groups were no longer visible. Yet, plasma levels 4 h after the intake of glucose were still considerably below initial fasting levels. These effects may be due to a dysregulated BCAA uptake via system A transporters in the plasma membranes of insulin target organs and by changes in activity of BCAA catabolizing enzymes (40). A previous study identified expression of genes that regulate the initial, rate-limiting steps of BCAA oxidation (including BCAA transaminase 2 and inner-mitochondrial enzymes from the branched-chain alpha-ketoacid dehydrogenase complex) as dependent on the degree of insulin resistance in subjects (41). Since plasma levels of several amino acids decrease in circulation up to t = 120 min and start increasing after that time point only in individuals from cluster B, we can speculate that the absence

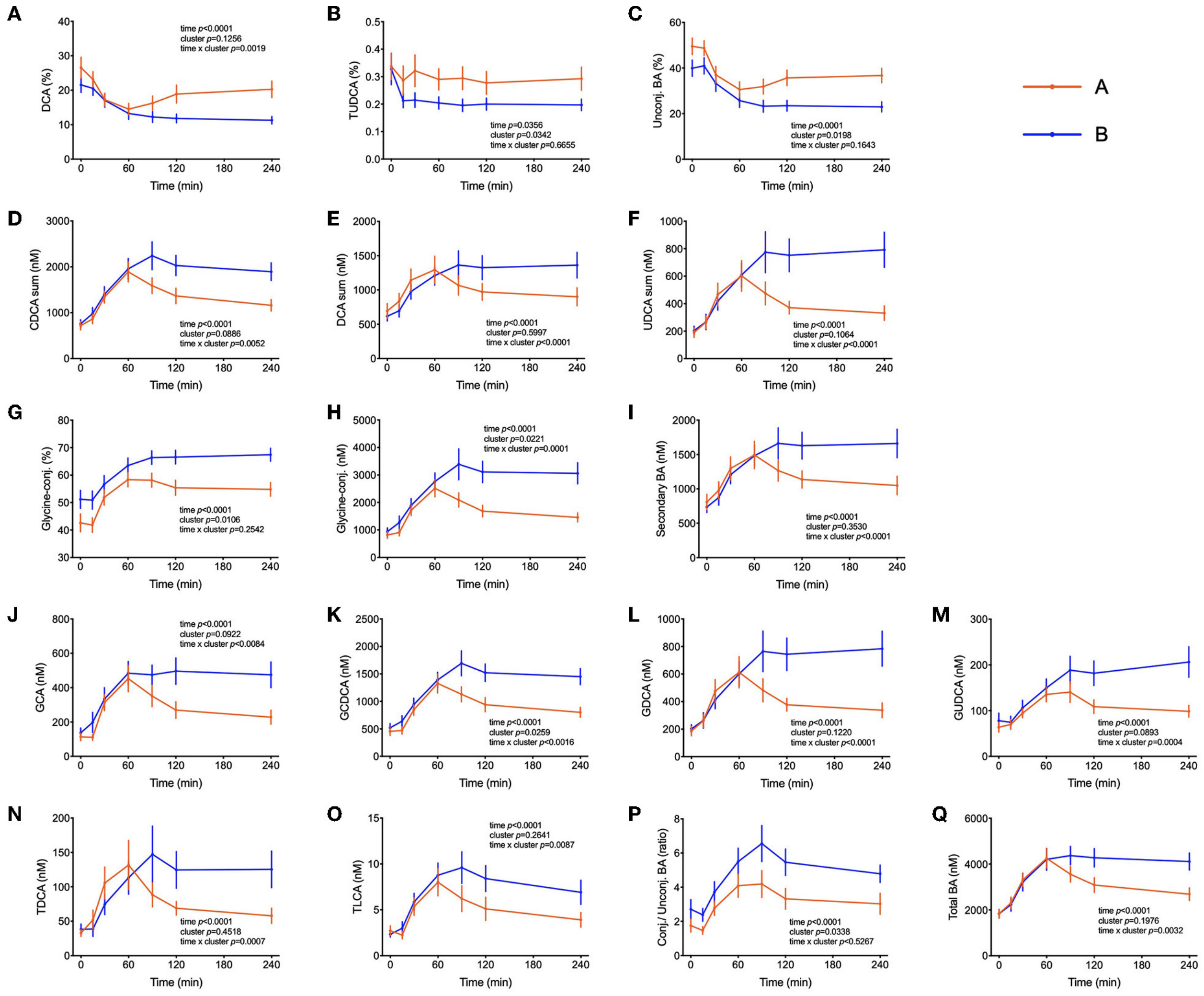

FIGURE 5 | Bile acids postprandial kinetics. **(A–C)** Bile acids associated with cluster A provided as % of the total pool of plasma bile acids. **(D–Q)** Plasma concentrations of most abundant bile acids in subjects from cluster B. Data are presented as means and standard errors of the mean. Results from mixed-effects analysis indicated in each graph.

of a rebound in subjects from cluster A is a response to the higher levels of insulin. It is possible that the higher levels of insulin that are kept higher for a longer time in these subjects is keeping the values of some amino acids (Ile, Leu and Phe) at a lower concentration even at t = 240 min. Impaired sensitivity to insulin could also be the reason behind such responses, given that membrane density and/or translocation of amino acid transporters is insulin dependent.

The PLS-DA model also identified significantly elevated plasma levels of glutamate, tryptophan and phenylalanine in cluster A subjects (**Figure 3**). Mean glutamate concentrations during the OGTT were 64% higher in subjects from cluster A compared to cluster B and were positively correlated with postprandial glycemic profile ($r = 0.64$, $p = 1.39E\text{-}09$) (**Table 3**). Aromatic amino acids in plasma are also related to insulin resistance, and emerged as predictors of future development of type 2 diabetes (42, 43). We found reduced levels of glycine and serine in cluster A as compared to cluster B individuals. Elevated levels of plasma glycine and serine have previously been linked to increased insulin sensitivity, with an association between high plasma glycine and decreased odds of abnormal HOMA-IR. In a recent review, White et al. (44) postulated a mechanism underlying the inverse association between glycine and BCAA levels which is based on increased nitrogen load in tissues by elevated BCAA levels which is dissipated by using glutamate to form alanine from pyruvate by alanine transaminase (44). The depletion of pyruvate in these pathways can be replenished from glycine by serine dehydratase and serine hydroxymethyl transferase, thereby reducing glycine and serine levels during insulin resistance or obesity.

Higher plasma triglyceride concentrations as observed in cluster A subjects confirm and extend previous findings with

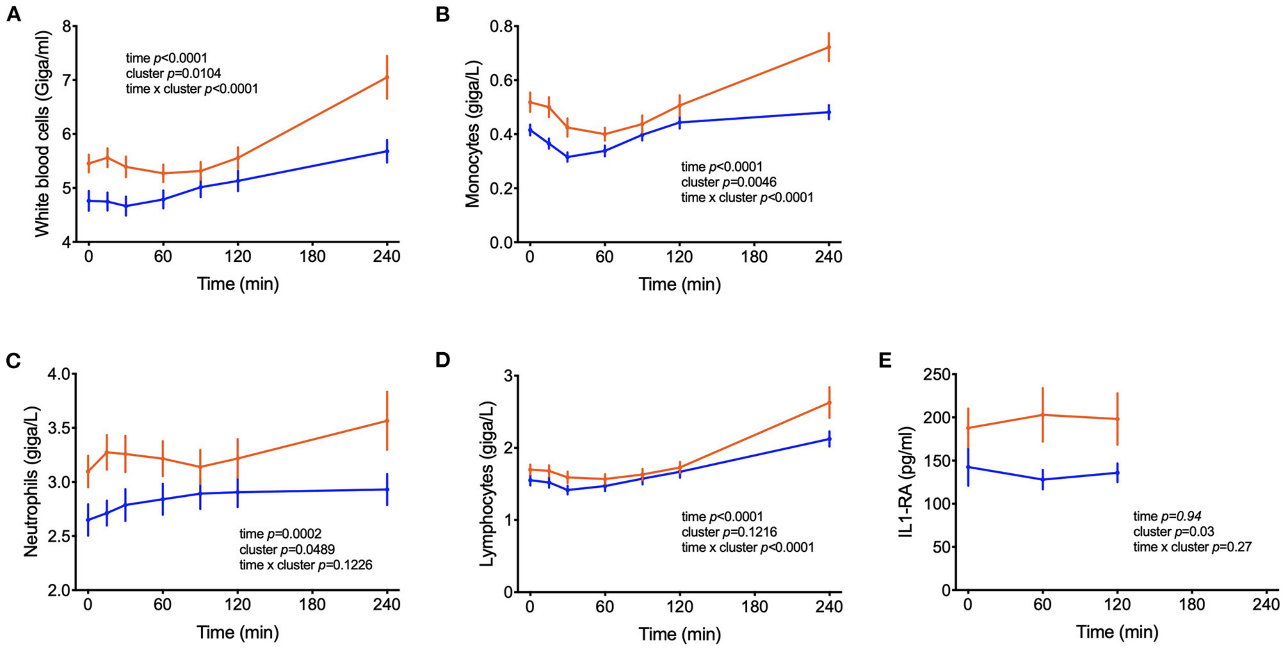

FIGURE 6 | Counts of circulating leucocytes. **(A–D)** Cell counts of white blood cells, monocytes, neutrophils, lymphocytes; **(E)** IL1-RA levels in postprandial blood. Data are presented as means and standard errors of the mean. Results from mixed-effects analysis indicated in each graph.

higher levels and predictive quality for insulin resistance (45, 46). Although cluster A subjects had higher concentrations (μg/mL) of NEFA in the fasting state, very long-chain fatty acids (VLCFA) were consistently more abundant among individuals from cluster B and displayed a negative correlation with the average glucose concentration during the OGTT (**Table 2**). These observations can also be extended to linoleic acid. Previous studies have described such an association between VLCFA and lower incidence of diabetes, but we here show that even in healthy individuals, the percentage of these compounds within the entire plasma fatty acid profile is associated with an improved glycemic response during the OGTT (47, 48). Whereas, mechanistic explanations are still missing, the higher proportion of VLCFA has been linked to lower *de novo* lipogenesis or changes in sphingolipid metabolism (49).

High-fat and high-carbohydrate meals can trigger an acute increase of plasma inflammatory biomarkers such as IL-6 and TNF-α in the first hours of the postprandial period (50, 51). In parallel, the number of leucocytes such as macrophages and neutrophils increase, probably participating in this transient inflammatory response to the meal (52–54). This postprandial inflammation might be an important risk factor for the development of chronic diseases such as type 2 diabetes and cardiovascular disease and depends on meal composition and lifestyle factors (52, 55, 56). We report increased numbers of WBC, monocytes, lymphocytes and neutrophils in the subjects from cluster A compared to cluster B, suggesting increased inflammation in the first group. Although changes in the plasma levels of inflammatory cytokines were not observed in our study (**Table 1**), s-E-selectin concentrations were higher in subjects from cluster A in comparison to B, supporting the notion of an inflammatory state in cluster A individuals (**Table 2**). Previous reports identified an association between s-E-selectin with obesity, insulin resistance and metabolic inflexibility (57–59).

BA are released from the gallbladder following a meal by contraction mediated primarily by cholecystokinin. That glucose can elicit as well a BA secretion with an increase in plasma that follows glucose appearance has been shown before and BA are now considered to play an important role in coordinating metabolic responses during the postprandial period (60). In addition to their well-established function in facilitating dietary lipid emulsification and absorption, BA may be important signaling molecules able to exert pleiotropic physiological effects on different organs (61). Insulin resistance has been previously associated with increased plasma levels of deoxycholic acid and its conjugated forms and increments in the ratio of unconjugated/conjugated BA were attributed to subjects with high plasma concentrations of insulin, NEFA, and triglyceride levels (62). Other studies have reported higher levels of BA in diabetic patients in fasting and in the postprandial state and it has been reported that BA hydrophobicity can influence insulin resistance. In fact, DCA (a hydrophobic secondary BA) administration decreased insulin signaling and endoplasmic reticulum homeostasis, exacerbating impaired glucose homeostasis in mice (63–65). The relationship between BA and glucose metabolism is long known, but the mechanisms by which BA affect glucose homeostasis and vice versa are not yet understood. In our present study with healthy individuals, there were no differences in fasting plasma BA concentrations

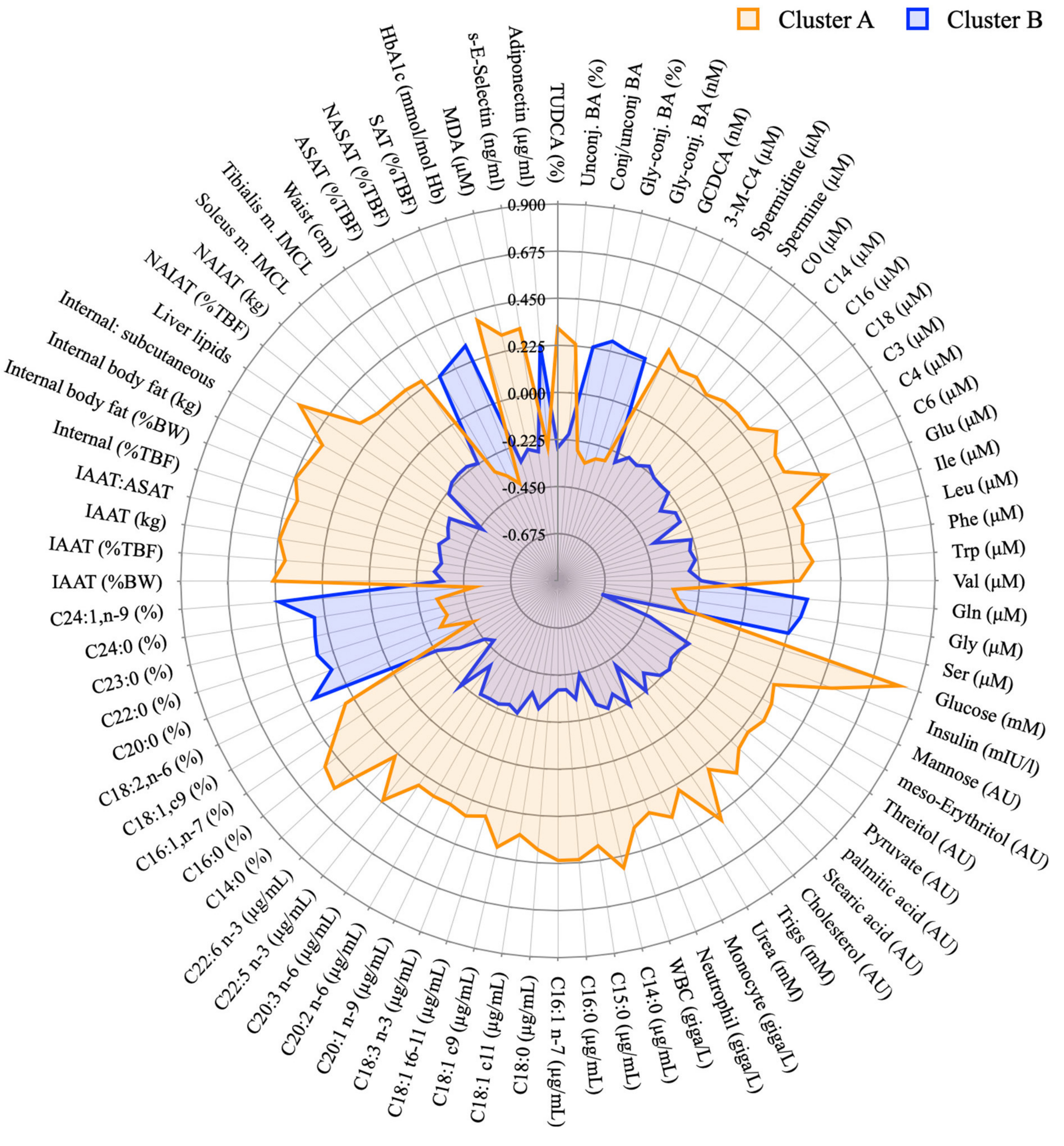

FIGURE 7 | Graphical representation of the phenotypical differences between cluster A and B. Radar plot of the variables identified in the PLS-DA model as discriminant between individuals from cluster A and B and whose concentration was considered different after a T-test. Data presented as z-scores.

between the two groups of individuals, but higher concentrations of BA were observed in subjects with a better glycemic response in the OGTT (cluster B) beginning 1 hour after the start of the OGTT (**Figure 5**). Similar results were observed by Higgins et al. (66), reporting that obese adolescents had reduced postprandial plasma BA concentrations in comparison to lean controls, despite similar fasting BA levels. Mantovani et al. (67) demonstrated also that postprandial BA concentrations were distinctly different between healthy and diabetic individuals (66, 67). Since BA concentrations in plasma increased similar in both clusters in the initial phase of the OGTT (**Figure 1**) their absorption from the intestine seems not to be different between cluster. However, in cluster B individuals BA levels did not decline over time as fast as in cluster A subjects suggesting that either their removal is slower than in less healthy individuals or that there is a higher flux through the enteric-hepatic cycle providing higher plasma BA levels higher throughout the test in more healthy volunteers. To find an explanation for this discrepancy more studies are needed in healthy and compromised individuals with proper reporting of time-dependent changes during an OGTT or a mixed meal test.

CONCLUSION

According to their glycaemia during an OGTT, healthy adult individuals could be classified into two subgroups characterized by a multitude of metabolites with altered plasma levels. These altered metabolite levels included many known markers of obesity, insulin resistance and type 2 diabetes, that were increased in cluster A individuals already in the fasting state. Most of the plasma concentrations of these marker metabolites remained as different during the 240 min of the test, demonstrating that the time-dependent measurements during the OGTT provide no particular benefit for a sub-clustering according to metabotype. Most of the discriminant metabolites can be linked to insulin effects on uptake and utilization of glucose, amino acids and fatty acids with the alterations in plasma levels given as a signature of impaired insulin response. Differences between the clusters also included BA concentrations for which a mechanistic basis for the association cannot be provided. Moreover, higher number of leucocytes were observed in cluster A. These individuals also displayed major differences in body fat stores and fat distribution for which associations with impaired insulin signaling have been reported before. The present study reveals that a panel of metabolites in fasting plasma allows the identification of an individual as "pre-pre-diabetic" and at increased risk for diabetes that is still otherwise classified as healthy according to the definitions of the WHO.

DATA AVAILABILITY STATEMENT

The original contributions presented in the study are included in the article/**Supplementary Material**, further inquiries can be directed to the corresponding author.

ETHICS STATEMENT

The studies involving human participants were reviewed and approved by Brent Ethics Committee (REC ref: 12/LO/0139) and registered at clinicaltrials.gov record: NCT01684917. The patients/participants provided their written informed consent to participate in this study.

AUTHOR CONTRIBUTIONS

BO, HD, JB, LB, SW, DI, CD, and GF designed the research program. JF, MR, ET, TG, DB, and YK-K performed research leading to the findings reported here. ET and JF analyzed data. DS, J-PT, SK, and KH contributed new reagents or specific analytical tools and expertise. JF, CD-P, GD, and HD wrote the manuscript. All authors reviewed the paper.

ACKNOWLEDGMENTS

The excellent technical work of Alexander Haag, Ronny Scheundel, Barbara Gelhaus, Christa Lachermeier, Helene Prunkl, Rita Bäuerle and Claudia Hoffmann is highly appreciated. The authors are thankful for the funding received through the EU 7th Framework Grant number KBBE-2011-5-289511, to all study participants and all members of the NutriTech consortium.

SUPPLEMENTARY MATERIAL

The Supplementary Material for this article can be found online at: https://www.frontiersin.org/articles/10.3389/fnut.2022.898782/full#supplementary-material

Supplementary Figure 1 | Multivariate analysis. **(A)** Graphical representation of hierarchical cluster analysis that generated the classification of the individuals into clusters A and B. **(B)** Score plot showing the separation of cluster A and B. **(C)** Cross-validation, indicating the robustness of the model.

REFERENCES

1. Hatting M, Tavares CDJ, Sharabi K, Rines AK, Puigserver P. Insulin regulation of gluconeogenesis. *Ann N Y Acad Sci.* (2018) 1411:21–35. doi: 10.1111/nyas.13435
2. Galgani JE, Moro C, Ravussin E. Metabolic flexibility and insulin resistance. *Am J Physiol Endocrinol Metab.* (2008) 295:1009–17. doi: 10.1152/ajpendo.90558.2008
3. Legro RS, Castracane D, Kauffman RP. Detecting insulin resistance in polycystic ovary syndrome: purposes and pitfalls. *Obstet Gynecol Surv.* (2004) 59:141–54. doi: 10.1097/01.OGX.0000109523.25076.E2
4. Krug S, Kastenmüller G, Stückler F, Rist MJ, Skurk T, Sailer M, et al. The dynamic range of the human metabolome revealed by challenges. *FASEB J.* (2012) 26:2607–19. doi: 10.1096/fj.11-198093
5. Zhao X, Fritsche J, Wang J, Chen J, Rittig K, Schmitt-Kopplin P, et al. Metabonomic fingerprints of fasting plasma and spot urine reveal human pre-diabetic metabolic traits. *Metabolomics.* (2010) 6:362–74. doi: 10.1007/s11306-010-0203-1
6. LaBarre JL, Singer K, Burant CF. Advantages of studying the metabolome in response to mixed-macronutrient challenges and suggestions for future research designs. *J Nutr.* (2021) 151:2868–81. doi: 10.1093/jn/nxab223
7. Rhee EP, Cheng S, Larson MG, Walford GA, Lewis GD, McCabe E, et al. Lipid profiling identifies a triacylglycerol signature of insulin resistance and improves diabetes prediction in humans. *J Clin Investig.* (2011) 121:1402–11. doi: 10.1172/JCI44442
8. Würtz P, Mäkinen VP, Soininen P, Kangas AJ, Tukiainen T, Kettunen J, et al. Metabolic signatures of insulin resistance in 7,098 young adults. *Diabetes.* (2012) 61:1372–80. doi: 10.2337/db11-1355
9. Newgard CB. Metabolomics and metabolic diseases: where do we stand? *Cell Metab.* (2017) 25:43–56. doi: 10.1016/j.cmet.2016.09.018
10. Lépine G, Tremblay-Franco M, Bouder S, Dimina L, Fouillet H, Mariotti F, et al. Investigating the postprandial metabolome after challenge tests to assess metabolic flexibility and dysregulations associated with cardiometabolic diseases. *Nutrients.* (2022) 14:472. doi: 10.3390/nu14030472
11. Gavaghan CL, Holmes E, Lenz E, Wilson ID, Nicholson JK. An NMR-based metabonomic approach to investigate the biochemical consequences of genetic strain differences: application to the C57BL10J and Alpk:ApfCD mouse. *FEBS Lett.* (2000) 484:169–74. doi: 10.1016/S0014-5793(00)02147-5

12. Stella C, Beckwith-Hall B, Cloarec O, Holmes E, Lindon JC, Powell J, et al. Susceptibility of human metabolic phenotypes to dietary modulation. *J Proteome Res.* (2006) 5:2780–8. doi: 10.1021/pr060265y
13. Morris C, O'Grada C, Ryan M, Roche HM, Gibney MJ, Gibney ER, et al. Identification of differential responses to an oral glucose tolerance test in healthy adults. *PLoS ONE*. (2013) 8:e72890. doi: 10.1371/journal.pone.0072890
14. Fiamoncini J, Rundle M, Gibbons H, Thomas EL, Geillinger-Kästle K, Bunzel D, et al. Plasma metabolome analysis identifies distinct human metabotypes in the postprandial state with different susceptibility to weight loss-mediated metabolic improvements. *FASEB J.* (2018) 32:5447–58. doi: 10.1096/fj.201800330R
15. Adrian TE, Ferri GL, Bacarese-Hamilton AJ, Fuessl HS, Polak JM, Bloom SR. Human distribution and release of a putative new gut hormone, peptide YY. *Gastroenterology.* (1985) 89:1070–7. doi: 10.1016/0016-5085(85)90211-2
16. Kreymann B, Williams G, Ghatei M, Bloom S. Glucagon-like peptide-1 7-36: a physiological incretin in man. *The Lancet.* (1987) 5:1300–4. doi: 10.1016/S0140-6736(87)91194-9
17. Vinknes KJ, Elshorbagy AK, Nurk E, Drevon CA, Gjesdal CG, Tell GS, et al. Plasma stearoyl-CoA desaturase indices: association with lifestyle, diet, and body composition. *Obesity.* (2013) 21:E294–302. doi: 10.1002/oby.20011
18. Thomas EL, Parkinson JR, Frost GS, Goldstone AP, Doré CJ, McCarthy JP, et al. The missing risk: MRI and MRS phenotyping of abdominal adiposity and ectopic fat. *Obesity*. (2012) 20, 76–87. doi: 10.1038/oby.2011.142
19. Yoshimura K, Hirano S, Takata H, Funakoshi S, Ohmi S, Amano E, et al. Plasma mannose level, a putative indicator of glycogenolysis, and glucose tolerance in Japanese individuals. *J Diabetes Investig.* (2017) 8:489–95. doi: 10.1111/jdi.12622
20. Mack CI, Ferrario PG, Weinert CH, Egert B, Hoefle AS, Lee Y-M, et al. Exploring the diversity of sugar compounds in healthy, prediabetic, and diabetic volunteers. *Mol Nutr Food Res.* (2020) 64:1–14. doi: 10.1002/mnfr.201901190
21. Hootman KC, Trezzi JP, Kraemer L, Burwell LS, Dong X, Guertin KA, et al. Erythritol is a pentose-phosphate pathway metabolite and associated with adiposity gain in young adults. *Proc Nat Acad Sci.* (2017) 114:E4233–40. doi: 10.1073/pnas.1620079114
22. Giesbertz P, Ecker J, Haag A, Spanier B, Daniel H. An LC-MS/MS method to quantify acylcarnitine species including isomeric and odd-numbered forms in plasma and tissues. *J Lipid Res.* (2015) 56:2029–39. doi: 10.1194/jlr.D061721
23. Fiamoncini J, Yiorkas AM, Gedrich K, Rundle M, Alsters SI, Roeselers G, et al. Determinants of postprandial plasma bile acid kinetics in human volunteers. *Am J Physiol Gastrointest Liver Physiol.* (2017) 313:G300–12. doi: 10.1152/ajpgi.00157.2017
24. Alberti KGMM, Zimmet PZ. Definition, diagnosis and classification of diabetes mellitus and its complications part 1: diagnosis and classification of diabetes mellitus provisional report of a WHO Consultation. *Diab Med*. (1998) 15:539–53. doi: 10.1002/(SICI)1096-9136(199807)15:7<539::AID-DIA668>3.0.CO;2-S
25. Sone H, Shimano H, Ebinuma H, Takahashi A, Yano Y, Iida KT, et al. Physiological changes in circulating mannose levels in normal, glucose-intolerant, and diabetic subjects. *Metabolism.* (2003) 52:1019–27. doi: 10.1016/S0026-0495(03)00153-7
26. Amano E, Funakoshi S, Yoshimura K, Hirano S, Ohmi S, Takata H, et al. Fasting plasma mannose levels are associated with insulin sensitivity independent of BMI in Japanese individuals with diabetes. *Diabetol Metab Syndr.* (2018) 10:1–7. doi: 10.1186/s13098-018-0391-9
27. Dimitriadis GD, Maratou E, Kountouri A, Board M, Lambadiari V. Regulation of postabsorptive and postprandial glucose metabolism by insulin-dependent and insulin-independent mechanisms: an integrative approach. *Nutrients.* (2021) 13:1–33. doi: 10.3390/nu13010159
28. Meyer FL, Mattox H, Bolick M, Macdonald C. Metabolic changes after test meaIs with different carbohydrates: blood levels of pyruvic acid, glucose, and lactic dehydrogenase. *Am J Clin Nutr.* (1971) 24:615–21. doi: 10.1093/ajcn/24.6.615
29. Wang Q, Jokelainen J, Auvinen J, Puukka K, Keinänen-Kiukaanniemi S, Järvelin MR, et al. Insulin resistance and systemic metabolic changes in oral glucose tolerance test in 5340 individuals: an interventional study. *BMC Med.* (2019) 17:1–12. doi: 10.1186/s12916-019-1440-4
30. Frayn KN, Coppack SW, Fielding BA, Humphreys SM. Coordinated regulation of hormone-sensitive lipase and lipoprotein lipase in human adipose tissue *in vivo*: implications for the control of fat storage and fat mobilization. *Adv Enzyme Regul.* (1995) 35:163–78. doi: 10.1016/0065-2571(94)00011-Q
31. Hanefeld M, Koehler C, Fuecker K, Chem D, Henkel E, Schaper F, et al. Insulin secretion and insulin sensitivity pattern is different in isolated impaired glucose tolerance and impaired fasting glucose. *Diabetes Care*. (2003) 26:868–74. doi: 10.2337/diacare.26.3.868
32. Mai M, Tönjes A, Kovacs P, Stumvoll M, Fiedler GM, Leichtle AB. Serum levels of acylcarnitines are altered in prediabetic conditions. *PLoS ONE*. (2013) 8:e82459. doi: 10.1371/journal.pone.0082459
33. Nowak C, Hetty S, Salihovic S, Castillejo-Lopez C, Ganna A, Cook NL, et al. Glucose challenge metabolomics implicates medium-chain acylcarnitines in insulin resistance. *Sci Rep*. (2018) 8:1–10. doi: 10.1038/s41598-018-26701-0
34. Glynn EL, Piner LW, Huffman KM, Slentz CA, Elliot-Penry L, AbouAssi H, et al. Impact of combined resistance and aerobic exercise training on branched-chain amino acid turnover, glycine metabolism and insulin sensitivity in overweight humans. *Diabetologia.* (2015) 58:2324–35. doi: 10.1007/s00125-015-3705-6
35. Gar C, Rottenkolber M, Prehn C, Adamski J, Seissler J, Lechner A. Serum and plasma amino acids as markers of prediabetes, insulin resistance, and incident diabetes. *Crit Rev Clin Lab Sci.* (2018) 55:21–32. doi: 10.1080/10408363.2017.1414143
36. Zhou M, Shao J, Wu CY, Shu L, Dong W, Liu Y, et al. Targeting BCAA catabolism to treat obesity-associated insulin resistance. *Diabetes.* (2019) 68:1730–46. doi: 10.2337/db18-0927
37. Bröer S. Amino acid transporters as modulators of glucose homeostasis. *Trends Endocrinol Metab.* (2022) 33:120–35. doi: 10.1016/j.tem.2021.11.004
38. Bogan JS, Mckee AE, Lodish HF. Insulin-responsive compartments containing GLUT4 in 3T3-L1 and CHO cells: regulation by amino acid concentrations. *Mol Cell Biol.* (2001) 21:4785–806. doi: 10.1128/MCB.21.14.4785-4806.2001
39. Su TZ, Wang M, Oxender DL, Saltiel AR. Troglitazone increases system A amino acid transport in 3T3-L1 cells. *Endocrinology*. (1998) 139:832–7. doi: 10.1210/endo.139.3.5795
40. Gannon NP, Schnuck JK, Vaughan RA. BCAA metabolism and insulin sensitivity – dysregulated by metabolic status? *Mol Nutr Food Res.* (2018) 62:1700756. doi: 10.1002/mnfr.201700756
41. Sears DD, Hsiao G, Hsiao A, Yu JG, Courtney CH, Ofrecio JM, et al. Mechanisms of human insulin resistance and thiazolidinedione-mediated insulin sensitization. *PNAS.* (2009) 3:18745–50. doi: 10.1073/pnas.0903032106
42. Wang TJ, Larson MG, Vasan RS, Cheng S, Rhee EP, McCabe E, et al. Metabolite profiles and the risk of developing diabetes. *Nat Med.* (2011) 17:448–53. doi: 10.1038/nm.2307
43. Floegel A, Stefan N, Yu Z, Mühlenbruch K, Drogan D, Joost HG, et al. Identification of serum metabolites associated with risk of type 2 diabetes using a targeted metabolomic approach. *Diabetes.* (2013) 62:639–48. doi: 10.2337/db12-0495
44. White PJ, McGarrah RW, Herman MA, Bain JR, Shah SH, Newgard CB. Insulin action, type 2 diabetes, and branched-chain amino acids: a two-way street. *Mol Metab.* (2021) 52:101261. doi: 10.1016/j.molmet.2021.101261
45. Khan SH, Sobia F, Niazi NK, Manzoor SM, Fazal N, Ahmad F. Metabolic clustering of risk factors: evaluation of triglyceride-glucose index (TyG index) for evaluation of insulin resistance. *Diabetol Metab Syndr.* (2018) 10:1–8. doi: 10.1186/s13098-018-0376-8
46. Mazidi M, Kengne AP, Katsiki N, Mikhailidis DP, Banach M. Lipid accumulation product and triglycerides/glucose index are useful predictors of insulin resistance. *J Diabetes Complications.* (2018) 32:266–70. doi: 10.1016/j.jdiacomp.2017.10.007
47. Lemaitre RN, Fretts AM, Sitlani CM, Biggs ML, Mukamal K, King IB, et al. Plasma phospholipid very-long-chain saturated fatty acids and incident diabetes in older adults: the cardiovascular health study. *Am J Clin Nutr.* (2015) 101:1047–54. doi: 10.3945/ajcn.114.101857
48. Fretts AM, Imamura F, Marklund M, Micha R, Wu JHY, Murphy RA, et al. Associations of circulating very-long-chain saturated fatty acids and incident type 2 diabetes: A pooled analysis of prospective cohort studies. *Am J Clin Nutr.* (2019) 109:1216–23. doi: 10.1093/ajcn/nqz005

49. Lemaitre RN, King IB. Very long-chain saturated fatty acids and diabetes and cardiovascular disease. *Curr Opin Lipidol.* (2022) 33:76–82. doi: 10.1097/MOL.0000000000000806
50. Herieka M, Erridge C. High-fat meal induced postprandial inflammation. *Mol Nutr Food Res.* (2014) 58:136–46. doi: 10.1002/mnfr.201300104
51. Meessen ECE, Warmbrunn MV, Nieuwdorp M, Soeters MR. Human postprandial nutrient metabolism and low-grade inflammation: a narrative review. *Nutrients.* (2019) 11:3000. doi: 10.3390/nu11123000
52. Margioris AN. Fatty acids and postprandial inflammation. *Curr Opin Clin Nutr Metab Care.* (2009) 12:129–37. doi: 10.1097/MCO.0b013e3283232a11
53. Gregor MF, Hotamisligil GS. Inflammatory mechanisms in obesity. *Annu Rev Immunol.* (2011) 29:415–45. doi: 10.1146/annurev-immunol-031210-101322
54. Kardinaal AFM, van Erk MJ, Dutman AE, Stroeve JHM, van de Steeg E, Bijlsma S, et al. Quantifying phenotypic flexibility as the response to a high-fat challenge test in different states of metabolic health. *FASEB J.* (2015) 29:4600–13. doi: 10.1096/fj.14-269852
55. Hotamisligil GS. Inflammation, metaflammation and immunometabolic disorders. *Nature.* (2017) 542:177–85. doi: 10.1038/nature21363
56. Rogero MM, Calder PC. Obesity, inflammation, toll-like receptor 4 and fatty acids. *Nutrients.* (2018) 10:432. doi: 10.3390/nu10040432
57. Adamska A, Karczewska-Kupczewska M, Nikołajuk A, Otziomek E, Górska M, Kowalska I, et al. Relationships of serum soluble E-selectin concentration with insulin sensitivity and metabolic flexibility in lean and obese women. *Endocrine.* (2014) 45:422–9. doi: 10.1007/s12020-013-0025-9
58. Mulhem A, Moulla Y, Klöting N, Ebert T, Tönjes A, Fasshauer M, et al. Circulating cell adhesion molecules in metabolically healthy obesity. *Int J Obes.* (2021) 45:331–6. doi: 10.1038/s41366-020-00667-4
59. Lee CH, Kuo FC, Tang WH, Lu CH, Su SC, Liu JS, et al. Serum E-selectin concentration is associated with risk of metabolic syndrome in females. *PLoS ONE.* (2019) 14:e0222815. doi: 10.1371/journal.pone.0222815
60. Kuipers F, Bloks VW, Groen AK. Beyond intestinal soap - bile acids in metabolic control. *Nat Rev Endocrinol.* (2014) 10:488–98. doi: 10.1038/nrendo.2014.60
61. Perino A, Demagny H, Velazquez-Villegas L, Schoonjans K. Molecular physiology of bile acid signaling in health, disease, and aging. *Physiol Rev.* (2021) 101:683–731. doi: 10.1152/physrev.00049.2019
62. Haeusler RA, Astiarraga B, Camastra S, Accili D, Ferrannini E. Human insulin resistance is associated with increased plasma levels of 12a-hydroxylated bile acids. *Diabetes.* (2013) 62:4184–91. doi: 10.2337/db13-0639
63. Wewalka M, Patti ME, Barbato C, Houten SM, Goldfine AB. Fasting serum taurine-conjugated bile acids are elevated in type 2 diabetes and do not change with intensification of insulin. *J Clin Endocrinol Metab.* (2014) 99:1442–51. doi: 10.1210/jc.2013-3367
64. Sonne DP, van Nierop FS, Kulik W, Soeters MR, Vilsbøll T, Knop FK. Postprandial plasma concentrations of individual bile acids and FGF-19 in patients with type 2 diabetes. *J Clin Endocrinol Metab.* (2016) 101:3002–9. doi: 10.1210/jc.2016-1607
65. Zaborska KE, Lee SA, Garribay D, Cha E, Cummings BP. Deoxycholic acid supplementation impairs glucose homeostasis in mice. *PLoS ONE.* (2018) 13:e0200908. doi: 10.1371/journal.pone.0200908
66. Higgins V, Asgari S, Hamilton JK, Wolska A, Remaley AT, Hartmann B, et al. Postprandial dyslipidemia, hyperinsulinemia, and impaired gut peptides/bile acids in adolescents with obesity. *J Clin Endocrinol Metab.* (2020) 105:1228–41. doi: 10.1210/clinem/dgz261
67. Mantovani A, Dalbeni A, Peserico D, Cattazzo F, Bevilacqua M, Salvagno GL, et al. Plasma bile acid profile in patients with and without type 2 diabetes. *Metabolites.* (2021) 11:1–14. doi: 10.3390/metabo11070453

Conflict of Interest: TG is the CEO and stockowner in Vitas Ltd. CD is a founder, stockowner, board member and consultant in Vitas Ltd. DS was an employee of biocrates life sciences AG.

The remaining authors declare that the research was conducted in the absence of any commercial or financial relationships that could be construed as a potential conflict of interest.

Supplemental Table 1. Variables included in the PLS-DA model. Variables are presented with their respective VIP values and loadings, method of detection and units.

Variables included in the PLS-DA model in alphabetical order

Primary ID	Sampling time	Unit	Category	Method	VIP	Loadings
2-M-C3	0	µM	Acylcarnitine	LC-MS/MS	0,633	0,0181
2-M-C3	120	µM	Acylcarnitine	LC-MS/MS	1,160	0,0332
2-M-C3	15	µM	Acylcarnitine	LC-MS/MS	0,648	0,0185
2-M-C3	240	µM	Acylcarnitine	LC-MS/MS	1,051	0,0300
2-M-C3	30	µM	Acylcarnitine	LC-MS/MS	0,581	0,0166
2-M-C3	60	µM	Acylcarnitine	LC-MS/MS	0,973	0,0278
2-M-C3	90	µM	Acylcarnitine	LC-MS/MS	1,221	0,0349
2-M-C4	0	µM	Acylcarnitine	LC-MS/MS	0,912	-0,0261
2-M-C4	120	µM	Acylcarnitine	LC-MS/MS	0,827	-0,0237
2-M-C4	15	µM	Acylcarnitine	LC-MS/MS	0,919	-0,0263
2-M-C4	240	µM	Acylcarnitine	LC-MS/MS	0,811	-0,0232
2-M-C4	30	µM	Acylcarnitine	LC-MS/MS	0,989	-0,0283
2-M-C4	60	µM	Acylcarnitine	LC-MS/MS	0,927	-0,0265
2-M-C4	90	µM	Acylcarnitine	LC-MS/MS	0,857	-0,0245
3-Hydroxybutyric acid	0	AU	Lipid metabolism	GC-MS	0,627	0,0179
3-Hydroxybutyric acid	120	AU	Lipid metabolism	GC-MS	1,526	-0,0436
3-Hydroxybutyric acid	15	AU	Lipid metabolism	GC-MS	0,696	0,0199
3-Hydroxybutyric acid	240	AU	Lipid metabolism	GC-MS	1,116	0,0319
3-Hydroxybutyric acid	30	AU	Lipid metabolism	GC-MS	0,187	-0,0053
3-Hydroxybutyric acid	60	AU	Lipid metabolism	GC-MS	1,284	-0,0367
3-Hydroxybutyric acid	90	AU	Lipid metabolism	GC-MS	1,818	-0,0520
3-M-C4	0	µM	Acylcarnitine	LC-MS/MS	1,260	-0,0360
3-M-C4	120	µM	Acylcarnitine	LC-MS/MS	1,568	-0,0449
3-M-C4	15	µM	Acylcarnitine	LC-MS/MS	1,285	-0,0368
3-M-C4	240	µM	Acylcarnitine	LC-MS/MS	1,294	-0,0370
3-M-C4	30	µM	Acylcarnitine	LC-MS/MS	1,894	-0,0541
3-M-C4	60	µM	Acylcarnitine	LC-MS/MS	1,438	-0,0411
3-M-C4	90	µM	Acylcarnitine	LC-MS/MS	1,305	-0,0373
8-hydroxy-2'-deoxyguanosine	fasting	pg/ml	Oxidative stress	x	0,418	-0,0119
Ac-Orn	0	µM	Amino acid metabolism	Biocrates	0,444	-0,0127
Ac-Orn	120	µM	Amino acid metabolism	Biocrates	0,445	-0,0127
Ac-Orn	15	µM	Amino acid metabolism	Biocrates	0,617	-0,0176
Ac-Orn	240	µM	Amino acid metabolism	Biocrates	0,432	-0,0124
Ac-Orn	30	µM	Amino acid metabolism	Biocrates	0,365	-0,0104
Ac-Orn	60	µM	Amino acid metabolism	Biocrates	0,377	-0,0108
Ac-Orn	90	µM	Amino acid metabolism	Biocrates	0,452	-0,0129
Activity level	7 days assessm.	MET/ day	General	Accelerometer	1,125	0,0322
Adiponectin	fasting	µg/ml	Signalling/ hormone	ELISA	1,249	0,0357
ADMA	0	µM	Biogenic amine	Biocrates	0,838	0,0240
ADMA	120	µM	Biogenic amine	Biocrates	0,763	0,0218
ADMA	15	µM	Biogenic amine	Biocrates	0,539	-0,0154
ADMA	240	µM	Biogenic amine	Biocrates	0,412	0,0118
ADMA	30	µM	Biogenic amine	Biocrates	0,869	-0,0249
ADMA	60	µM	Biogenic amine	Biocrates	0,193	-0,0055
ADMA	90	µM	Biogenic amine	Biocrates	0,314	-0,0090
Ala	0	µM	Amino acid metabolism	Biocrates	1,161	-0,0332
Ala	120	µM	Amino acid metabolism	Biocrates	0,439	-0,0125
Ala	15	µM	Amino acid metabolism	Biocrates	1,169	-0,0334
Ala	240	µM	Amino acid metabolism	Biocrates	0,936	-0,0268
Ala	30	µM	Amino acid metabolism	Biocrates	0,791	-0,0226
Ala	60	µM	Amino acid metabolism	Biocrates	1,148	-0,0328
Ala	90	µM	Amino acid metabolism	Biocrates	0,914	-0,0261
Alkaline phosphatase	fasting	IU/L	General	Enzymatic	0,643	-0,0184
alpha-AAA	0	µM	Biogenic amine	Biocrates	1,252	-0,0358
alpha-AAA	120	µM	Biogenic amine	Biocrates	1,132	-0,0324
alpha-AAA	15	µM	Biogenic amine	Biocrates	0,886	-0,0253
alpha-AAA	240	µM	Biogenic amine	Biocrates	0,805	-0,0230
alpha-AAA	30	µM	Biogenic amine	Biocrates	0,783	-0,0224
alpha-AAA	60	µM	Biogenic amine	Biocrates	0,777	-0,0222
alpha-AAA	90	µM	Biogenic amine	Biocrates	0,444	-0,0127
Arg	0	µM	Amino acid metabolism	Biocrates	0,987	0,0282
Arg	120	µM	Amino acid metabolism	Biocrates	0,303	0,0087
Arg	15	µM	Amino acid metabolism	Biocrates	0,094	0,0027
Arg	240	µM	Amino acid metabolism	Biocrates	0,033	0,0010
Arg	30	µM	Amino acid metabolism	Biocrates	0,731	0,0209
Arg	60	µM	Amino acid metabolism	Biocrates	0,343	-0,0098
Arg	90	µM	Amino acid metabolism	Biocrates	0,274	0,0078
ASAT	fasting	%BW	Body composition	MRI	0,926	0,0265

Supplemental Table 1. Variables included in the PLS-DA model. Variables are presented with their respective VIP values and loadings, method of detection and units.

ASAT	fasting	%TBF	Body composition	MRI	1,451	0,0415
Primary ID	**Sampling time**	**Unit**	**Category**	**Method**	**VIP**	**Loadings**
ASAT	fasting	kg	Body composition	MRI	0,265	0,0076
Asn	0	µM	Amino acid metabolism	Biocrates	1,083	0,0310
Asn	120	µM	Amino acid metabolism	Biocrates	0,653	0,0187
Asn	15	µM	Amino acid metabolism	Biocrates	0,970	0,0277
Asn	240	µM	Amino acid metabolism	Biocrates	0,823	0,0235
Asn	30	µM	Amino acid metabolism	Biocrates	1,543	0,0441
Asn	60	µM	Amino acid metabolism	Biocrates	0,069	0,0020
Asn	90	µM	Amino acid metabolism	Biocrates	0,533	0,0153
Asp	0	µM	Amino acid metabolism	Biocrates	0,543	-0,0155
Asp	120	µM	Amino acid metabolism	Biocrates	0,665	-0,0190
Asp	15	µM	Amino acid metabolism	Biocrates	0,610	-0,0174
Asp	240	µM	Amino acid metabolism	Biocrates	0,467	0,0134
Asp	30	µM	Amino acid metabolism	Biocrates	0,262	-0,0075
Asp	60	µM	Amino acid metabolism	Biocrates	0,462	0,0132
Asp	90	µM	Amino acid metabolism	Biocrates	0,075	-0,0021
Aspartate aminotrans.	fasting	U/L	General	Enzymatic	0,320	0,0092
BA conj/unconj	0	ratio	Bile acid	LC-MS/MS	0,878	0,0251
BA conj/unconj	120	ratio	Bile acid	LC-MS/MS	1,380	0,0395
BA conj/unconj	15	ratio	Bile acid	LC-MS/MS	1,269	0,0363
BA conj/unconj	240	ratio	Bile acid	LC-MS/MS	1,470	0,0420
BA conj/unconj	30	ratio	Bile acid	LC-MS/MS	0,743	0,0212
BA conj/unconj	60	ratio	Bile acid	LC-MS/MS	0,784	0,0224
BA conj/unconj	90	ratio	Bile acid	LC-MS/MS	1,132	0,0324
BA prim/sec	0	ratio	Bile acid	LC-MS/MS	0,315	0,0090
BA prim/sec	120	ratio	Bile acid	LC-MS/MS	0,200	-0,0057
BA prim/sec	15	ratio	Bile acid	LC-MS/MS	0,079	-0,0023
BA prim/sec	240	ratio	Bile acid	LC-MS/MS	0,288	-0,0082
BA prim/sec	30	ratio	Bile acid	LC-MS/MS	0,199	-0,0057
BA prim/sec	60	ratio	Bile acid	LC-MS/MS	0,173	-0,0049
BA prim/sec	90	ratio	Bile acid	LC-MS/MS	0,217	-0,0062
BA primary	0	%	Bile acid	LC-MS/MS	0,575	0,0165
BA primary	120	%	Bile acid	LC-MS/MS	0,514	0,0147
BA primary	15	%	Bile acid	LC-MS/MS	0,363	0,0104
BA primary	240	%	Bile acid	LC-MS/MS	0,638	0,0182
BA primary	30	%	Bile acid	LC-MS/MS	0,076	-0,0022
BA primary	60	%	Bile acid	LC-MS/MS	0,015	-0,0004
BA primary	90	%	Bile acid	LC-MS/MS	0,158	0,0045
BA primary	0	nM	Bile acid	LC-MS/MS	0,414	0,0118
BA primary	120	nM	Bile acid	LC-MS/MS	1,472	0,0421
BA primary	15	nM	Bile acid	LC-MS/MS	0,502	0,0144
BA primary	240	nM	Bile acid	LC-MS/MS	1,745	0,0499
BA primary	30	nM	Bile acid	LC-MS/MS	0,322	0,0092
BA primary	60	nM	Bile acid	LC-MS/MS	0,327	0,0094
BA primary	90	nM	Bile acid	LC-MS/MS	1,085	0,0310
BA secondary	0	%	Bile acid	LC-MS/MS	0,575	-0,0165
BA secondary	120	%	Bile acid	LC-MS/MS	0,514	-0,0147
BA secondary	15	%	Bile acid	LC-MS/MS	0,363	-0,0104
BA secondary	240	%	Bile acid	LC-MS/MS	0,638	-0,0182
BA secondary	30	%	Bile acid	LC-MS/MS	0,076	0,0022
BA secondary	60	%	Bile acid	LC-MS/MS	0,015	0,0004
BA secondary	90	%	Bile acid	LC-MS/MS	0,158	-0,0045
BA secondary	0	nM	Bile acid	LC-MS/MS	0,401	-0,0115
BA secondary	120	nM	Bile acid	LC-MS/MS	1,346	0,0385
BA secondary	15	nM	Bile acid	LC-MS/MS	0,381	-0,0109
BA secondary	240	nM	Bile acid	LC-MS/MS	1,535	0,0439
BA secondary	30	nM	Bile acid	LC-MS/MS	0,279	-0,0080
BA secondary	60	nM	Bile acid	LC-MS/MS	0,064	-0,0018
BA secondary	90	nM	Bile acid	LC-MS/MS	0,935	0,0267
BA total	0	nM	Bile acid	LC-MS/MS	0,076	0,0022
BA total	120	nM	Bile acid	LC-MS/MS	1,558	0,0446
BA total	15	nM	Bile acid	LC-MS/MS	0,218	0,0062
BA total	240	nM	Bile acid	LC-MS/MS	1,817	0,0519
BA total	30	nM	Bile acid	LC-MS/MS	0,127	0,0036
BA total	60	nM	Bile acid	LC-MS/MS	0,229	0,0066
BA total	90	nM	Bile acid	LC-MS/MS	1,105	0,0316
BA unconj.	0	nM	Bile acid	LC-MS/MS	0,328	-0,0094
BA unconj.	120	nM	Bile acid	LC-MS/MS	0,016	0,0005
BA unconj.	15	nM	Bile acid	LC-MS/MS	0,451	-0,0129
BA unconj.	240	nM	Bile acid	LC-MS/MS	0,104	0,0030

Supplemental Table 1. Variables included in the PLS-DA model. Variables are presented with their respective VIP values and loadings, method of detection and units.

BA unconj.	30	nM	Bile acid	LC-MS/MS	0,049	-0,0014
BA unconj.	60	nM	Bile acid	LC-MS/MS	0,049	0,0014
Primary ID	**Sampling time**	**Unit**	**Category**	**Method**	**VIP**	**Loadings**
BA unconj.	90	nM	Bile acid	LC-MS/MS	0,007	-0,0002
BA unconjugated	0	%	Bile acid	LC-MS/MS	1,035	-0,0296
BA unconjugated	120	%	Bile acid	LC-MS/MS	1,532	-0,0438
BA unconjugated	15	%	Bile acid	LC-MS/MS	0,795	-0,0227
BA unconjugated	240	%	Bile acid	LC-MS/MS	1,852	-0,0530
BA unconjugated	30	%	Bile acid	LC-MS/MS	0,223	-0,0064
BA unconjugated	60	%	Bile acid	LC-MS/MS	0,403	-0,0115
BA unconjugated	90	%	Bile acid	LC-MS/MS	1,007	-0,0288
BMI	fasting	kg/m2	Body composition	Scale	0,448	-0,0128
C0	0	µM	Amino acid metabolism	Biocrates	1,475	-0,0422
C0	120	µM	Amino acid metabolism	Biocrates	1,116	-0,0319
C0	15	µM	Amino acid metabolism	Biocrates	1,420	-0,0406
C0	240	µM	Amino acid metabolism	Biocrates	1,020	-0,0292
C0	30	µM	Amino acid metabolism	Biocrates	0,756	-0,0216
C0	60	µM	Amino acid metabolism	Biocrates	0,785	-0,0225
C0	90	µM	Amino acid metabolism	Biocrates	1,094	-0,0313
C10	0	µM	Acylcarnitine	LC-MS/MS	0,332	-0,0095
C10	120	µM	Acylcarnitine	LC-MS/MS	1,605	-0,0459
C10	15	µM	Acylcarnitine	LC-MS/MS	0,459	-0,0131
C10	240	µM	Acylcarnitine	LC-MS/MS	0,675	-0,0193
C10	30	µM	Acylcarnitine	LC-MS/MS	0,596	-0,0171
C10	60	µM	Acylcarnitine	LC-MS/MS	1,338	-0,0382
C10	90	µM	Acylcarnitine	LC-MS/MS	1,401	-0,0401
C10:1	0	µM	Acylcarnitine	Biocrates	0,550	0,0157
C10:1	120	µM	Acylcarnitine	Biocrates	0,535	0,0153
C10:1	15	µM	Acylcarnitine	Biocrates	0,013	-0,0004
C10:1	240	µM	Acylcarnitine	Biocrates	0,465	0,0133
C10:1	30	µM	Acylcarnitine	Biocrates	0,855	0,0245
C10:1	60	µM	Acylcarnitine	Biocrates	1,133	0,0324
C10:1	90	µM	Acylcarnitine	Biocrates	0,439	0,0126
C10:2	0	µM	Acylcarnitine	Biocrates	0,887	0,0254
C10:2	120	µM	Acylcarnitine	Biocrates	0,289	0,0083
C10:2	15	µM	Acylcarnitine	Biocrates	0,086	-0,0024
C10:2	240	µM	Acylcarnitine	Biocrates	0,475	0,0136
C10:2	30	µM	Acylcarnitine	Biocrates	0,943	0,0270
C10:2	60	µM	Acylcarnitine	Biocrates	1,177	0,0336
C10:2	90	µM	Acylcarnitine	Biocrates	0,082	-0,0023
C12	0	µM	Acylcarnitine	LC-MS/MS	0,408	-0,0117
C12	120	µM	Acylcarnitine	LC-MS/MS	1,663	-0,0475
C12	15	µM	Acylcarnitine	LC-MS/MS	0,608	-0,0174
C12	240	µM	Acylcarnitine	LC-MS/MS	0,791	-0,0226
C12	30	µM	Acylcarnitine	LC-MS/MS	0,913	-0,0261
C12	60	µM	Acylcarnitine	LC-MS/MS	1,376	-0,0394
C12	90	µM	Acylcarnitine	LC-MS/MS	1,600	-0,0457
C12:0	fasting	%	Lipid metabolism	GC-FID	1,326	-0,0379
C12:0VITAS	fasting	µg/mL	Lipid metabolism	GC-FID	1,440	-0,0412
C12:1	0	µM	Acylcarnitine	Biocrates	0,698	0,0200
C12:1	120	µM	Acylcarnitine	Biocrates	0,424	0,0121
C12:1	15	µM	Acylcarnitine	Biocrates	0,333	0,0095
C12:1	240	µM	Acylcarnitine	Biocrates	0,969	0,0277
C12:1	30	µM	Acylcarnitine	Biocrates	0,588	0,0168
C12:1	60	µM	Acylcarnitine	Biocrates	0,780	0,0223
C12:1	90	µM	Acylcarnitine	Biocrates	0,302	0,0086
C12-DC	0	µM	Acylcarnitine	Biocrates	0,950	0,0272
C12-DC	120	µM	Acylcarnitine	Biocrates	0,753	0,0215
C12-DC	15	µM	Acylcarnitine	Biocrates	0,418	0,0120
C12-DC	240	µM	Acylcarnitine	Biocrates	1,268	0,0363
C12-DC	30	µM	Acylcarnitine	Biocrates	0,979	0,0280
C12-DC	60	µM	Acylcarnitine	Biocrates	1,218	0,0348
C12-DC	90	µM	Acylcarnitine	Biocrates	0,368	0,0105
C13	0	µM	Acylcarnitine	LC-MS/MS	0,039	0,0011
C13	120	µM	Acylcarnitine	LC-MS/MS	0,043	-0,0012
C13	15	µM	Acylcarnitine	LC-MS/MS	0,067	0,0019
C13	240	µM	Acylcarnitine	LC-MS/MS	0,548	-0,0157
C13	30	µM	Acylcarnitine	LC-MS/MS	0,206	0,0059
C13	60	µM	Acylcarnitine	LC-MS/MS	0,206	0,0059
C13	90	µM	Acylcarnitine	LC-MS/MS	0,220	0,0063
C14	0	µM	Acylcarnitine	LC-MS/MS	1,141	-0,0326

Supplemental Table 1. Variables included in the PLS-DA model. Variables are presented with their respective VIP values and loadings, method of detection and units.

C14	120	µM	Acylcarnitine	LC-MS/MS	1,853	-0,0530
C14	15	µM	Acylcarnitine	LC-MS/MS	1,198	-0,0342
C14	240	µM	Acylcarnitine	LC-MS/MS	0,667	-0,0191
Primary ID	**Sampling time**	**Unit**	**Category**	**Method**	**VIP**	**Loadings**
C14	30	µM	Acylcarnitine	LC-MS/MS	1,417	-0,0405
C14	60	µM	Acylcarnitine	LC-MS/MS	1,040	-0,0297
C14	90	µM	Acylcarnitine	LC-MS/MS	1,651	-0,0472
C14:0	fasting	%	Lipid metabolism	GC-FID	2,817	-0,0805
C14:0	fasting	µg/mL	Lipid metabolism	GC-FID	2,718	-0,0777
C14:1	0	µM	Acylcarnitine	Biocrates	0,418	-0,0120
C14:1	120	µM	Acylcarnitine	Biocrates	0,448	0,0128
C14:1	15	µM	Acylcarnitine	Biocrates	0,703	-0,0201
C14:1	240	µM	Acylcarnitine	Biocrates	0,386	-0,0111
C14:1	30	µM	Acylcarnitine	Biocrates	0,112	0,0032
C14:1	60	µM	Acylcarnitine	Biocrates	0,666	0,0190
C14:1	90	µM	Acylcarnitine	Biocrates	0,297	-0,0085
C14:1-OH	0	µM	Acylcarnitine	Biocrates	0,228	-0,0065
C14:1-OH	120	µM	Acylcarnitine	Biocrates	0,322	0,0092
C14:1-OH	15	µM	Acylcarnitine	Biocrates	1,058	-0,0303
C14:1-OH	240	µM	Acylcarnitine	Biocrates	0,431	-0,0123
C14:1-OH	30	µM	Acylcarnitine	Biocrates	0,345	0,0099
C14:1-OH	60	µM	Acylcarnitine	Biocrates	0,335	0,0096
C14:1-OH	90	µM	Acylcarnitine	Biocrates	0,236	-0,0067
C14:2	0	µM	Acylcarnitine	Biocrates	0,292	-0,0083
C14:2	120	µM	Acylcarnitine	Biocrates	0,555	0,0159
C14:2	15	µM	Acylcarnitine	Biocrates	0,768	-0,0220
C14:2	240	µM	Acylcarnitine	Biocrates	0,221	-0,0063
C14:2	30	µM	Acylcarnitine	Biocrates	0,501	0,0143
C14:2	60	µM	Acylcarnitine	Biocrates	0,639	0,0183
C14:2	90	µM	Acylcarnitine	Biocrates	0,056	-0,0016
C14:2-OH	0	µM	Acylcarnitine	Biocrates	0,044	0,0013
C14:2-OH	120	µM	Acylcarnitine	Biocrates	0,587	0,0168
C14:2-OH	15	µM	Acylcarnitine	Biocrates	0,296	-0,0085
C14:2-OH	240	µM	Acylcarnitine	Biocrates	0,129	-0,0037
C14:2-OH	30	µM	Acylcarnitine	Biocrates	0,484	0,0138
C14:2-OH	60	µM	Acylcarnitine	Biocrates	0,802	0,0229
C14:2-OH	90	µM	Acylcarnitine	Biocrates	0,057	-0,0016
C15:0	fasting	%	Lipid metabolism	GC-FID	0,634	-0,0181
C15:0	fasting	µg/mL	Lipid metabolism	GC-FID	1,929	-0,0551
C16	0	µM	Acylcarnitine	LC-MS/MS	1,401	-0,0401
C16	120	µM	Acylcarnitine	LC-MS/MS	1,529	-0,0437
C16	15	µM	Acylcarnitine	LC-MS/MS	1,486	-0,0425
C16	240	µM	Acylcarnitine	LC-MS/MS	0,551	-0,0157
C16	30	µM	Acylcarnitine	LC-MS/MS	1,297	-0,0371
C16	60	µM	Acylcarnitine	LC-MS/MS	1,140	-0,0326
C16	90	µM	Acylcarnitine	LC-MS/MS	1,445	-0,0413
C16:0	fasting	%	Lipid metabolism	GC-FID	3,038	-0,0869
C16:0	fasting	µg/mL	Lipid metabolism	GC-FID	2,541	-0,0727
C16:1	0	µM	Acylcarnitine	LC-MS/MS	0,718	-0,0205
C16:1	120	µM	Acylcarnitine	LC-MS/MS	1,557	-0,0445
C16:1	15	µM	Acylcarnitine	LC-MS/MS	0,669	-0,0191
C16:1	240	µM	Acylcarnitine	LC-MS/MS	0,030	0,0009
C16:1	30	µM	Acylcarnitine	LC-MS/MS	1,085	-0,0310
C16:1	60	µM	Acylcarnitine	LC-MS/MS	1,052	-0,0301
C16:1	90	µM	Acylcarnitine	LC-MS/MS	1,495	-0,0428
C16:1 n-7	fasting	µg/mL	Lipid metabolism	GC-FID	2,269	-0,0649
C16:1,n-7	fasting	%	Lipid metabolism	GC-FID	1,868	-0,0534
C16:1-OH	0	µM	Acylcarnitine	Biocrates	0,025	0,0007
C16:1-OH	120	µM	Acylcarnitine	Biocrates	0,632	0,0181
C16:1-OH	15	µM	Acylcarnitine	Biocrates	0,638	-0,0182
C16:1-OH	240	µM	Acylcarnitine	Biocrates	0,250	-0,0071
C16:1-OH	30	µM	Acylcarnitine	Biocrates	0,385	0,0110
C16:1-OH	60	µM	Acylcarnitine	Biocrates	0,841	0,0240
C16:1-OH	90	µM	Acylcarnitine	Biocrates	0,289	-0,0083
C16:2	0	µM	Acylcarnitine	Biocrates	0,561	-0,0161
C16:2	120	µM	Acylcarnitine	Biocrates	0,429	0,0123
C16:2	15	µM	Acylcarnitine	Biocrates	1,007	-0,0288
C16:2	240	µM	Acylcarnitine	Biocrates	0,565	-0,0162
C16:2	30	µM	Acylcarnitine	Biocrates	0,061	0,0017
C16:2	60	µM	Acylcarnitine	Biocrates	0,720	0,0206
C16:2	90	µM	Acylcarnitine	Biocrates	0,660	-0,0189

Supplemental Table 1. Variables included in the PLS-DA model. Variables are presented with their respective VIP values and loadings, method of detection and units.

C16:2-OH	0	µM	Acylcarnitine	Biocrates	0,159	0,0046
C16:2-OH	120	µM	Acylcarnitine	Biocrates	0,738	0,0211
C16:2-OH	15	µM	Acylcarnitine	Biocrates	0,404	-0,0116
C16:2-OH	240	µM	Acylcarnitine	Biocrates	0,014	0,0004
Primary ID	**Sampling time**	**Unit**	**Category**	**Method**	**VIP**	**Loadings**
C16:2-OH	30	µM	Acylcarnitine	Biocrates	0,638	0,0182
C16:2-OH	60	µM	Acylcarnitine	Biocrates	0,958	0,0274
C16:2-OH	90	µM	Acylcarnitine	Biocrates	0,162	-0,0046
C16-OH	0	µM	Acylcarnitine	Biocrates	0,010	-0,0003
C16-OH	120	µM	Acylcarnitine	Biocrates	0,714	0,0204
C16-OH	15	µM	Acylcarnitine	Biocrates	0,326	-0,0093
C16-OH	240	µM	Acylcarnitine	Biocrates	0,040	0,0012
C16-OH	30	µM	Acylcarnitine	Biocrates	0,347	0,0099
C16-OH	60	µM	Acylcarnitine	Biocrates	1,183	0,0338
C16-OH	90	µM	Acylcarnitine	Biocrates	0,218	0,0062
C18	0	µM	Acylcarnitine	LC-MS/MS	1,390	-0,0398
C18	120	µM	Acylcarnitine	LC-MS/MS	1,275	-0,0365
C18	15	µM	Acylcarnitine	LC-MS/MS	1,315	-0,0376
C18	240	µM	Acylcarnitine	LC-MS/MS	0,897	-0,0257
C18	30	µM	Acylcarnitine	LC-MS/MS	1,476	-0,0422
C18	60	µM	Acylcarnitine	LC-MS/MS	1,025	-0,0293
C18	90	µM	Acylcarnitine	LC-MS/MS	1,079	-0,0308
C18:0	fasting	%	Lipid metabolism	GC-FID	0,018	-0,0005
C18:0	fasting	µg/mL	Lipid metabolism	GC-FID	2,114	-0,0604
C18:1	0	µM	Acylcarnitine	LC-MS/MS	0,619	-0,0177
C18:1	120	µM	Acylcarnitine	LC-MS/MS	1,230	-0,0352
C18:1	15	µM	Acylcarnitine	LC-MS/MS	0,479	-0,0137
C18:1	240	µM	Acylcarnitine	LC-MS/MS	0,508	0,0145
C18:1	30	µM	Acylcarnitine	LC-MS/MS	1,012	-0,0290
C18:1	60	µM	Acylcarnitine	LC-MS/MS	0,645	-0,0184
C18:1	90	µM	Acylcarnitine	LC-MS/MS	0,769	-0,0220
C18:1 c11	fasting	µg/mL	Lipid metabolism	GC-FID	1,903	-0,0544
C18:1 c9	fasting	µg/mL	Lipid metabolism	GC-FID	2,336	-0,0668
C18:1 t6-11	fasting	µg/mL	Lipid metabolism	GC-FID	1,622	-0,0464
C18:1,c11	fasting	%	Lipid metabolism	GC-FID	0,766	-0,0219
C18:1,c9	fasting	%	Lipid metabolism	GC-FID	1,459	-0,0417
C18:1,t6-11	fasting	%	Lipid metabolism	GC-FID	0,643	-0,0184
C18:1-OH	0	µM	Acylcarnitine	Biocrates	0,018	0,0005
C18:1-OH	120	µM	Acylcarnitine	Biocrates	0,835	0,0239
C18:1-OH	15	µM	Acylcarnitine	Biocrates	0,715	-0,0204
C18:1-OH	240	µM	Acylcarnitine	Biocrates	0,242	-0,0069
C18:1-OH	30	µM	Acylcarnitine	Biocrates	0,228	0,0065
C18:1-OH	60	µM	Acylcarnitine	Biocrates	0,791	0,0226
C18:1-OH	90	µM	Acylcarnitine	Biocrates	0,273	-0,0078
C18:2	0	µM	Acylcarnitine	Biocrates	0,452	-0,0129
C18:2	120	µM	Acylcarnitine	Biocrates	0,545	0,0156
C18:2	15	µM	Acylcarnitine	Biocrates	0,384	-0,0110
C18:2	240	µM	Acylcarnitine	Biocrates	0,269	-0,0077
C18:2	30	µM	Acylcarnitine	Biocrates	0,318	0,0091
C18:2	60	µM	Acylcarnitine	Biocrates	0,835	0,0239
C18:2	90	µM	Acylcarnitine	Biocrates	0,015	0,0004
C18:2	0	µM	Acylcarnitine	LC-MS/MS	0,211	-0,0060
C18:2	120	µM	Acylcarnitine	LC-MS/MS	0,595	-0,0170
C18:2	15	µM	Acylcarnitine	LC-MS/MS	0,067	-0,0019
C18:2	240	µM	Acylcarnitine	LC-MS/MS	0,318	0,0091
C18:2	30	µM	Acylcarnitine	LC-MS/MS	0,524	-0,0150
C18:2	60	µM	Acylcarnitine	LC-MS/MS	0,081	-0,0023
C18:2	90	µM	Acylcarnitine	LC-MS/MS	0,114	-0,0033
C18:2 n-6	fasting	µg/mL	Lipid metabolism	GC-FID	0,361	-0,0103
C18:2,n-6	fasting	%	Lipid metabolism	GC-FID	2,514	0,0719
C18:3 n-3	fasting	µg/mL	Lipid metabolism	GC-FID	1,681	-0,0481
C18:3 n-6	fasting	µg/mL	Lipid metabolism	GC-FID	1,172	-0,0335
C18:3,n-3	fasting	%	Lipid metabolism	GC-FID	0,807	-0,0231
C18:3,n-6	fasting	%	Lipid metabolism	GC-FID	0,134	-0,0038
C2	0	µM	Acylcarnitine	LC-MS/MS	0,637	-0,0182
C2	120	µM	Acylcarnitine	LC-MS/MS	1,512	-0,0432
C2	15	µM	Acylcarnitine	LC-MS/MS	0,518	-0,0148
C2	240	µM	Acylcarnitine	LC-MS/MS	0,409	0,0117
C2	30	µM	Acylcarnitine	LC-MS/MS	0,733	-0,0210
C2	60	µM	Acylcarnitine	LC-MS/MS	1,047	-0,0299
C2	90	µM	Acylcarnitine	LC-MS/MS	1,263	-0,0361

Supplemental Table 1. Variables included in the PLS-DA model. Variables are presented with their respective VIP values and loadings, method of detection and units.

C20:0	fasting	%	Lipid metabolism	GC-FID	1,601	0,0458
C20:0	fasting	µg/mL	Lipid metabolism	GC-FID	0,540	-0,0154
C20:1 n-9	fasting	µg/mL	Lipid metabolism	GC-FID	1,670	-0,0477
C20:1,n-9	fasting	%	Lipid metabolism	GC-FID	0,071	-0,0020
C20:2 n-6	fasting	µg/mL	Lipid metabolism	GC-FID	1,692	-0,0484
Primary ID	**Sampling time**	**Unit**	**Category**	**Method**	**VIP**	**Loadings**
C20:2,n-6	fasting	%	Lipid metabolism	GC-FID	0,481	-0,0137
C20:3 n-6	fasting	µg/mL	Lipid metabolism	GC-FID	1,514	-0,0433
C20:3,n-6	fasting	%	Lipid metabolism	GC-FID	0,032	0,0009
C20:4 n-6	fasting	µg/mL	Lipid metabolism	GC-FID	0,644	-0,0184
C20:4,n-6	fasting	%	Lipid metabolism	GC-FID	1,351	0,0386
C20:5 n-3	fasting	µg/mL	Lipid metabolism	GC-FID	0,815	-0,0233
C20:5,n-3	fasting	%	Lipid metabolism	GC-FID	0,083	0,0024
C22:0	fasting	%	Lipid metabolism	GC-FID	2,036	0,0582
C22:0	fasting	µg/mL	Lipid metabolism	GC-FID	0,222	0,0063
C22:5 n-3	fasting	µg/mL	Lipid metabolism	GC-FID	2,351	-0,0672
C22:5,n-3	fasting	%	Lipid metabolism	GC-FID	0,908	-0,0260
C22:6 n-3	fasting	µg/mL	Lipid metabolism	GC-FID	1,369	-0,0392
C22:6,n-3	fasting	%	Lipid metabolism	GC-FID	0,132	-0,0038
C23:0	fasting	%	Lipid metabolism	GC-FID	1,960	0,0560
C23:0	fasting	µg/mL	Lipid metabolism	GC-FID	0,250	0,0072
C24:0	fasting	%	Lipid metabolism	GC-FID	1,842	0,0527
C24:0	fasting	µg/mL	Lipid metabolism	GC-FID	0,034	-0,0010
C24:1 n-9	fasting	µg/mL	Lipid metabolism	GC-FID	1,126	0,0322
C24:1,n-9	fasting	%	Lipid metabolism	GC-FID	2,738	0,0783
C3	0	µM	Acylcarnitine	LC-MS/MS	1,945	-0,0556
C3	120	µM	Acylcarnitine	LC-MS/MS	1,534	-0,0439
C3	15	µM	Acylcarnitine	LC-MS/MS	1,935	-0,0553
C3	240	µM	Acylcarnitine	LC-MS/MS	1,227	-0,0351
C3	30	µM	Acylcarnitine	LC-MS/MS	1,992	-0,0570
C3	60	µM	Acylcarnitine	LC-MS/MS	1,641	-0,0469
C3	90	µM	Acylcarnitine	LC-MS/MS	1,614	-0,0461
C3:1	0	µM	Acylcarnitine	Biocrates	0,226	0,0065
C3:1	120	µM	Acylcarnitine	Biocrates	0,659	0,0188
C3:1	15	µM	Acylcarnitine	Biocrates	0,148	-0,0042
C3:1	240	µM	Acylcarnitine	Biocrates	0,195	0,0056
C3:1	30	µM	Acylcarnitine	Biocrates	0,528	0,0151
C3:1	60	µM	Acylcarnitine	Biocrates	0,996	0,0285
C3:1	90	µM	Acylcarnitine	Biocrates	0,196	0,0056
C3-DC-M	0	µM	Acylcarnitine	LC-MS/MS	0,815	-0,0233
C3-DC-M	120	µM	Acylcarnitine	LC-MS/MS	0,862	-0,0246
C3-DC-M	15	µM	Acylcarnitine	LC-MS/MS	1,004	-0,0287
C3-DC-M	240	µM	Acylcarnitine	LC-MS/MS	1,246	-0,0356
C3-DC-M	30	µM	Acylcarnitine	LC-MS/MS	0,746	-0,0213
C3-DC-M	60	µM	Acylcarnitine	LC-MS/MS	1,072	-0,0306
C3-DC-M	90	µM	Acylcarnitine	LC-MS/MS	0,177	0,0051
C3-OH	0	µM	Acylcarnitine	Biocrates	0,036	0,0010
C3-OH	120	µM	Acylcarnitine	Biocrates	0,450	0,0129
C3-OH	15	µM	Acylcarnitine	Biocrates	0,602	-0,0172
C3-OH	240	µM	Acylcarnitine	Biocrates	0,080	-0,0023
C3-OH	30	µM	Acylcarnitine	Biocrates	0,124	0,0035
C3-OH	60	µM	Acylcarnitine	Biocrates	0,726	0,0208
C3-OH	90	µM	Acylcarnitine	Biocrates	0,134	-0,0038
C4	0	µM	Acylcarnitine	LC-MS/MS	1,161	-0,0332
C4	120	µM	Acylcarnitine	LC-MS/MS	1,710	-0,0489
C4	15	µM	Acylcarnitine	LC-MS/MS	1,213	-0,0347
C4	240	µM	Acylcarnitine	LC-MS/MS	1,328	-0,0380
C4	30	µM	Acylcarnitine	LC-MS/MS	1,391	-0,0398
C4	60	µM	Acylcarnitine	LC-MS/MS	1,510	-0,0432
C4	90	µM	Acylcarnitine	LC-MS/MS	1,616	-0,0462
C4:1	0	µM	Acylcarnitine	Biocrates	0,247	0,0071
C4:1	120	µM	Acylcarnitine	Biocrates	0,172	0,0049
C4:1	15	µM	Acylcarnitine	Biocrates	0,310	-0,0089
C4:1	240	µM	Acylcarnitine	Biocrates	0,158	0,0045
C4:1	30	µM	Acylcarnitine	Biocrates	0,122	0,0035
C4:1	60	µM	Acylcarnitine	Biocrates	0,546	0,0156
C4:1	90	µM	Acylcarnitine	Biocrates	0,246	-0,0070
C4-DC	0	µM	Acylcarnitine	LC-MS/MS	2,035	-0,0582
C4-DC	120	µM	Acylcarnitine	LC-MS/MS	1,462	-0,0418
C4-DC	15	µM	Acylcarnitine	LC-MS/MS	1,804	-0,0516
C4-DC	240	µM	Acylcarnitine	LC-MS/MS	1,447	-0,0414

Supplemental Table 1. Variables included in the PLS-DA model. Variables are presented with their respective VIP values and loadings, method of detection and units.

C4-DC	30	µM	Acylcarnitine	LC-MS/MS	1,813	-0,0518
C4-DC	60	µM	Acylcarnitine	LC-MS/MS	0,708	-0,0203
C4-DC	90	µM	Acylcarnitine	LC-MS/MS	0,063	-0,0018
C4-OH - a	0	µM	Acylcarnitine	LC-MS/MS	0,286	-0,0082
C4-OH - a	120	µM	Acylcarnitine	LC-MS/MS	0,787	-0,0225
C4-OH - a	15	µM	Acylcarnitine	LC-MS/MS	0,091	0,0026
Primary ID	**Sampling time**	**Unit**	**Category**	**Method**	**VIP**	**Loadings**
C4-OH - a	240	µM	Acylcarnitine	LC-MS/MS	0,407	0,0117
C4-OH - a	30	µM	Acylcarnitine	LC-MS/MS	0,240	-0,0069
C4-OH - a	60	µM	Acylcarnitine	LC-MS/MS	0,118	-0,0034
C4-OH - a	90	µM	Acylcarnitine	LC-MS/MS	0,275	-0,0079
C4-OH - b	0	µM	Acylcarnitine	LC-MS/MS	0,432	-0,0123
C4-OH - b	120	µM	Acylcarnitine	LC-MS/MS	0,431	-0,0123
C4-OH - b	15	µM	Acylcarnitine	LC-MS/MS	0,155	-0,0044
C4-OH - b	240	µM	Acylcarnitine	LC-MS/MS	0,461	0,0132
C4-OH - b	30	µM	Acylcarnitine	LC-MS/MS	0,092	-0,0026
C4-OH - b	60	µM	Acylcarnitine	LC-MS/MS	0,232	-0,0066
C4-OH - b	90	µM	Acylcarnitine	LC-MS/MS	0,294	-0,0084
C5	0	µM	Acylcarnitine	Biocrates	0,597	-0,0171
C5	120	µM	Acylcarnitine	Biocrates	0,429	-0,0123
C5	15	µM	Acylcarnitine	Biocrates	1,151	-0,0329
C5	240	µM	Acylcarnitine	Biocrates	0,910	-0,0260
C5	30	µM	Acylcarnitine	Biocrates	0,944	-0,0270
C5	60	µM	Acylcarnitine	Biocrates	0,068	-0,0020
C5	90	µM	Acylcarnitine	Biocrates	0,801	-0,0229
C5:1	0	µM	Acylcarnitine	Biocrates	0,354	0,0101
C5:1	120	µM	Acylcarnitine	Biocrates	0,101	0,0029
C5:1	15	µM	Acylcarnitine	Biocrates	0,999	-0,0286
C5:1	240	µM	Acylcarnitine	Biocrates	0,019	-0,0005
C5:1	30	µM	Acylcarnitine	Biocrates	0,373	0,0107
C5:1	60	µM	Acylcarnitine	Biocrates	0,127	0,0036
C5:1	90	µM	Acylcarnitine	Biocrates	0,825	-0,0236
C5:1-DC	0	µM	Acylcarnitine	Biocrates	0,063	0,0018
C5:1-DC	120	µM	Acylcarnitine	Biocrates	0,344	0,0098
C5:1-DC	15	µM	Acylcarnitine	Biocrates	0,504	-0,0144
C5:1-DC	240	µM	Acylcarnitine	Biocrates	0,220	-0,0063
C5:1-DC	30	µM	Acylcarnitine	Biocrates	0,179	0,0051
C5:1-DC	60	µM	Acylcarnitine	Biocrates	0,660	0,0189
C5:1-DC	90	µM	Acylcarnitine	Biocrates	0,157	-0,0045
C5-DC	0	µM	Acylcarnitine	LC-MS/MS	0,680	-0,0194
C5-DC	120	µM	Acylcarnitine	LC-MS/MS	0,477	-0,0136
C5-DC	15	µM	Acylcarnitine	LC-MS/MS	0,663	-0,0190
C5-DC	240	µM	Acylcarnitine	LC-MS/MS	0,336	-0,0096
C5-DC	30	µM	Acylcarnitine	LC-MS/MS	0,615	-0,0176
C5-DC	60	µM	Acylcarnitine	LC-MS/MS	0,423	-0,0121
C5-DC	90	µM	Acylcarnitine	LC-MS/MS	0,262	-0,0075
C5-M-DC	0	µM	Acylcarnitine	LC-MS/MS	0,510	-0,0146
C5-M-DC	120	µM	Acylcarnitine	LC-MS/MS	0,428	-0,0123
C5-M-DC	15	µM	Acylcarnitine	LC-MS/MS	0,565	-0,0161
C5-M-DC	240	µM	Acylcarnitine	LC-MS/MS	0,481	-0,0137
C5-M-DC	30	µM	Acylcarnitine	LC-MS/MS	0,490	-0,0140
C5-M-DC	60	µM	Acylcarnitine	LC-MS/MS	0,439	-0,0126
C5-M-DC	90	µM	Acylcarnitine	LC-MS/MS	0,186	0,0053
C5-OH	0	µM	Acylcarnitine	LC-MS/MS	0,106	-0,0030
C5-OH	120	µM	Acylcarnitine	LC-MS/MS	0,304	-0,0087
C5-OH	15	µM	Acylcarnitine	LC-MS/MS	0,259	-0,0074
C5-OH	240	µM	Acylcarnitine	LC-MS/MS	0,474	-0,0136
C5-OH	30	µM	Acylcarnitine	LC-MS/MS	0,593	-0,0169
C5-OH	60	µM	Acylcarnitine	LC-MS/MS	0,398	-0,0114
C5-OH	90	µM	Acylcarnitine	LC-MS/MS	0,193	-0,0055
C5-OH (C3-DC-M)	0	µM	Acylcarnitine	Biocrates	0,085	-0,0024
C5-OH (C3-DC-M)	120	µM	Acylcarnitine	Biocrates	0,589	0,0168
C5-OH (C3-DC-M)	15	µM	Acylcarnitine	Biocrates	0,588	-0,0168
C5-OH (C3-DC-M)	240	µM	Acylcarnitine	Biocrates	0,163	0,0047
C5-OH (C3-DC-M)	30	µM	Acylcarnitine	Biocrates	0,059	0,0017
C5-OH (C3-DC-M)	60	µM	Acylcarnitine	Biocrates	0,782	0,0224
C5-OH (C3-DC-M)	90	µM	Acylcarnitine	Biocrates	0,321	0,0092
C6	0	µM	Acylcarnitine	LC-MS/MS	1,213	-0,0347
C6	120	µM	Acylcarnitine	LC-MS/MS	1,884	-0,0539
C6	15	µM	Acylcarnitine	LC-MS/MS	1,363	-0,0390
C6	240	µM	Acylcarnitine	LC-MS/MS	0,506	-0,0145

Supplemental Table 1. Variables included in the PLS-DA model. Variables are presented with their respective VIP values and loadings, method of detection and units.

C6	30	µM	Acylcarnitine	LC-MS/MS	1,656	-0,0473
C6	60	µM	Acylcarnitine	LC-MS/MS	2,023	-0,0578
C6	90	µM	Acylcarnitine	LC-MS/MS	1,936	-0,0554
C6 (C4:1-DC)	0	µM	Acylcarnitine	LC-MS/MS	0,327	0,0094
C6 (C4:1-DC)	120	µM	Acylcarnitine	LC-MS/MS	0,256	0,0073
C6 (C4:1-DC)	15	µM	Acylcarnitine	LC-MS/MS	0,091	0,0026
C6 (C4:1-DC)	240	µM	Acylcarnitine	LC-MS/MS	0,435	0,0124
Primary ID	**Sampling time**	**Unit**	**Category**	**Method**	**VIP**	**Loadings**
C6 (C4:1-DC)	30	µM	Acylcarnitine	LC-MS/MS	0,458	0,0131
C6 (C4:1-DC)	60	µM	Acylcarnitine	LC-MS/MS	0,284	0,0081
C6 (C4:1-DC)	90	µM	Acylcarnitine	LC-MS/MS	0,314	-0,0090
C6:1	0	µM	Acylcarnitine	Biocrates	1,096	0,0313
C6:1	120	µM	Acylcarnitine	Biocrates	0,545	0,0156
C6:1	15	µM	Acylcarnitine	Biocrates	0,287	0,0082
C6:1	240	µM	Acylcarnitine	Biocrates	0,734	0,0210
C6:1	30	µM	Acylcarnitine	Biocrates	0,811	0,0232
C6:1	60	µM	Acylcarnitine	Biocrates	0,905	0,0259
C6:1	90	µM	Acylcarnitine	Biocrates	0,120	-0,0034
C6-DC	0	µM	Acylcarnitine	LC-MS/MS	0,920	-0,0263
C6-DC	120	µM	Acylcarnitine	LC-MS/MS	0,898	-0,0257
C6-DC	15	µM	Acylcarnitine	LC-MS/MS	0,964	-0,0276
C6-DC	240	µM	Acylcarnitine	LC-MS/MS	0,798	-0,0228
C6-DC	30	µM	Acylcarnitine	LC-MS/MS	1,063	-0,0304
C6-DC	60	µM	Acylcarnitine	LC-MS/MS	0,866	-0,0248
C6-DC	90	µM	Acylcarnitine	LC-MS/MS	1,015	-0,0290
C7-DC	0	µM	Acylcarnitine	LC-MS/MS	0,102	-0,0029
C7-DC	120	µM	Acylcarnitine	LC-MS/MS	0,001	0,0000
C7-DC	15	µM	Acylcarnitine	LC-MS/MS	0,221	-0,0063
C7-DC	240	µM	Acylcarnitine	LC-MS/MS	0,194	0,0056
C7-DC	30	µM	Acylcarnitine	LC-MS/MS	0,077	-0,0022
C7-DC	60	µM	Acylcarnitine	LC-MS/MS	0,069	-0,0020
C7-DC	90	µM	Acylcarnitine	LC-MS/MS	0,165	0,0047
C8	0	µM	Acylcarnitine	LC-MS/MS	0,569	-0,0163
C8	120	µM	Acylcarnitine	LC-MS/MS	1,644	-0,0470
C8	15	µM	Acylcarnitine	LC-MS/MS	0,778	-0,0222
C8	240	µM	Acylcarnitine	LC-MS/MS	0,759	-0,0217
C8	30	µM	Acylcarnitine	LC-MS/MS	0,756	-0,0216
C8	60	µM	Acylcarnitine	LC-MS/MS	1,511	-0,0432
C8	90	µM	Acylcarnitine	LC-MS/MS	1,456	-0,0416
C9	0	µM	Acylcarnitine	Biocrates	0,229	0,0065
C9	120	µM	Acylcarnitine	Biocrates	0,704	0,0201
C9	15	µM	Acylcarnitine	Biocrates	0,094	-0,0027
C9	240	µM	Acylcarnitine	Biocrates	0,106	0,0030
C9	30	µM	Acylcarnitine	Biocrates	0,557	0,0159
C9	60	µM	Acylcarnitine	Biocrates	0,975	0,0279
C9	90	µM	Acylcarnitine	Biocrates	0,272	0,0078
CA	0	µM	Bile acid	LC-MS/MS	0,396	0,0113
CA	120	µM	Bile acid	LC-MS/MS	0,160	0,0046
CA	15	µM	Bile acid	LC-MS/MS	0,072	-0,0021
CA	240	µM	Bile acid	LC-MS/MS	0,423	0,0121
CA	30	µM	Bile acid	LC-MS/MS	0,124	0,0035
CA	60	µM	Bile acid	LC-MS/MS	0,154	0,0044
CA	90	µM	Bile acid	LC-MS/MS	0,106	0,0030
CA	0	%	Bile acid	LC-MS/MS	0,070	0,0020
CA	120	%	Bile acid	LC-MS/MS	0,324	-0,0093
CA	15	%	Bile acid	LC-MS/MS	0,157	-0,0045
CA	240	%	Bile acid	LC-MS/MS	0,203	-0,0058
CA	30	%	Bile acid	LC-MS/MS	0,070	-0,0020
CA	60	%	Bile acid	LC-MS/MS	0,328	-0,0094
CA	90	%	Bile acid	LC-MS/MS	0,499	-0,0143
CDCA	0	µM	Bile acid	LC-MS/MS	0,146	-0,0042
CDCA	120	µM	Bile acid	LC-MS/MS	0,266	0,0076
CDCA	15	µM	Bile acid	LC-MS/MS	0,258	-0,0074
CDCA	240	µM	Bile acid	LC-MS/MS	0,258	0,0074
CDCA	30	µM	Bile acid	LC-MS/MS	0,053	0,0015
CDCA	60	µM	Bile acid	LC-MS/MS	0,191	0,0055
CDCA	90	µM	Bile acid	LC-MS/MS	0,197	0,0056
CDCA	0	%	Bile acid	LC-MS/MS	0,784	-0,0224
CDCA	120	%	Bile acid	LC-MS/MS	0,882	-0,0252
CDCA	15	%	Bile acid	LC-MS/MS	0,779	-0,0223
CDCA	240	%	Bile acid	LC-MS/MS	1,008	-0,0288

Supplemental Table 1. Variables included in the PLS-DA model. Variables are presented with their respective VIP values and loadings, method of detection and units.

CDCA	30	%	Bile acid	LC-MS/MS	**0,542**	**-0,0155**
CDCA	60	%	Bile acid	LC-MS/MS	**0,377**	**-0,0108**
CDCA	90	%	Bile acid	LC-MS/MS	**0,679**	**-0,0194**
Cholesterol	fasting	mM	Lipid metabolism	GC-MS	**0,259**	**0,0074**
Cholesterol	0	AU	Lipid metabolism	GC-MS	**1,578**	**-0,0451**
Cholesterol	120	AU	Lipid metabolism	GC-MS	**0,928**	**-0,0265**
Cholesterol	15	AU	Lipid metabolism	GC-MS	**0,931**	**-0,0266**
Cholesterol	240	AU	Lipid metabolism	GC-MS	**0,925**	**-0,0264**
Primary ID	**Sampling time**	**Unit**	**Category**	**Method**	**VIP**	**Loadings**
Cholesterol	30	AU	Lipid metabolism	GC-MS	**1,625**	**-0,0465**
Cholesterol	60	AU	Lipid metabolism	GC-MS	**1,439**	**-0,0411**
Cholesterol	90	AU	Lipid metabolism	GC-MS	**1,357**	**-0,0388**
Cit	0	µM	Amino acid metabolism	Biocrates	**1,020**	**-0,0292**
Cit	120	µM	Amino acid metabolism	Biocrates	**0,462**	**-0,0132**
Cit	15	µM	Amino acid metabolism	Biocrates	**0,768**	**-0,0219**
Cit	240	µM	Amino acid metabolism	Biocrates	**1,053**	**-0,0301**
Cit	30	µM	Amino acid metabolism	Biocrates	**0,269**	**-0,0077**
Cit	60	µM	Amino acid metabolism	Biocrates	**0,437**	**-0,0125**
Cit	90	µM	Amino acid metabolism	Biocrates	**0,233**	**-0,0067**
Creatinine	0	µM	Biogenic amine	Biocrates	**1,046**	**-0,0299**
Creatinine	120	µM	Biogenic amine	Biocrates	**0,897**	**-0,0257**
Creatinine	15	µM	Biogenic amine	Biocrates	**1,268**	**-0,0363**
Creatinine	240	µM	Biogenic amine	Biocrates	**1,599**	**-0,0457**
Creatinine	30	µM	Biogenic amine	Biocrates	**0,724**	**-0,0207**
Creatinine	60	µM	Biogenic amine	Biocrates	**0,608**	**-0,0174**
Creatinine	90	µM	Biogenic amine	Biocrates	**0,971**	**-0,0278**
CRP	fasting	ng/ml	Inflammation	Enzymatic	**0,761**	**0,0218**
DBP	fasting	mmHg	General	Sphygmomanometer	**0,322**	**-0,0092**
DCA	0	nM	Bile acid	LC-MS/MS	**0,743**	**-0,0212**
DCA	120	nM	Bile acid	LC-MS/MS	**0,613**	**-0,0175**
DCA	15	nM	Bile acid	LC-MS/MS	**1,151**	**-0,0329**
DCA	240	nM	Bile acid	LC-MS/MS	**0,525**	**-0,0150**
DCA	30	nM	Bile acid	LC-MS/MS	**0,646**	**-0,0185**
DCA	60	nM	Bile acid	LC-MS/MS	**0,500**	**-0,0143**
DCA	90	nM	Bile acid	LC-MS/MS	**0,527**	**-0,0151**
DCA	0	%	Bile acid	LC-MS/MS	**0,911**	**-0,0261**
DCA	120	%	Bile acid	LC-MS/MS	**1,667**	**-0,0477**
DCA	15	%	Bile acid	LC-MS/MS	**0,589**	**-0,0168**
DCA	240	%	Bile acid	LC-MS/MS	**2,245**	**-0,0642**
DCA	30	%	Bile acid	LC-MS/MS	**0,006**	**-0,0002**
DCA	60	%	Bile acid	LC-MS/MS	**0,300**	**-0,0086**
DCA	90	%	Bile acid	LC-MS/MS	**1,003**	**-0,0287**
Eosinophil	0	giga/l	Leucocyte	Cell counter	**0,120**	**-0,0034**
Eosinophil	120	giga/l	Leucocyte	Cell counter	**0,139**	**-0,0040**
Eosinophil	15	giga/l	Leucocyte	Cell counter	**0,033**	**0,0009**
Eosinophil	240	giga/l	Leucocyte	Cell counter	**0,110**	**-0,0031**
Eosinophil	30	giga/l	Leucocyte	Cell counter	**0,199**	**-0,0057**
Eosinophil	60	giga/l	Leucocyte	Cell counter	**0,321**	**0,0092**
Eosinophil	90	giga/l	Leucocyte	Cell counter	**0,315**	**0,0090**
Fructose	0	AU	Glucose metabolism	GC-MS	**1,006**	**-0,0288**
Fructose	120	AU	Glucose metabolism	GC-MS	**0,720**	**-0,0206**
Fructose	15	AU	Glucose metabolism	GC-MS	**0,834**	**-0,0238**
Fructose	240	AU	Glucose metabolism	GC-MS	**0,236**	**0,0067**
Fructose	30	AU	Glucose metabolism	GC-MS	**0,993**	**-0,0284**
Fructose	60	AU	Glucose metabolism	GC-MS	**0,531**	**-0,0152**
Fructose	90	AU	Glucose metabolism	GC-MS	**0,649**	**-0,0186**
Gamma-glutamyl transpeptidase	fasting	U/L	General	Enzymatic	**0,808**	**-0,0231**
GCA	0	nM	Bile acid	LC-MS/MS	**0,432**	**0,0124**
GCA	120	nM	Bile acid	LC-MS/MS	**1,365**	**0,0390**
GCA	15	nM	Bile acid	LC-MS/MS	**1,050**	**0,0300**
GCA	240	nM	Bile acid	LC-MS/MS	**1,481**	**0,0423**
GCA	30	nM	Bile acid	LC-MS/MS	**0,483**	**0,0138**
GCA	60	nM	Bile acid	LC-MS/MS	**0,564**	**0,0161**
GCA	90	nM	Bile acid	LC-MS/MS	**0,880**	**0,0252**
GCA	0	%	Bile acid	LC-MS/MS	**0,454**	**0,0130**
GCA	120	%	Bile acid	LC-MS/MS	**1,313**	**0,0376**
GCA	15	%	Bile acid	LC-MS/MS	**1,262**	**0,0361**
GCA	240	%	Bile acid	LC-MS/MS	**1,480**	**0,0423**
GCA	30	%	Bile acid	LC-MS/MS	**0,370**	**0,0106**
GCA	60	%	Bile acid	LC-MS/MS	**0,717**	**0,0205**
GCA	90	%	Bile acid	LC-MS/MS	**1,010**	**0,0289**

Supplemental Table 1. Variables included in the PLS-DA model. Variables are presented with their respective VIP values and loadings, method of detection and units.

GCDCA	0	nM	Bile acid	LC-MS/MS	0,390	0,0111
GCDCA	120	nM	Bile acid	LC-MS/MS	1,804	0,0516
GCDCA	15	nM	Bile acid	LC-MS/MS	0,891	0,0255
GCDCA	240	nM	Bile acid	LC-MS/MS	2,244	0,0642
GCDCA	30	nM	Bile acid	LC-MS/MS	0,418	0,0120
GCDCA	60	nM	Bile acid	LC-MS/MS	0,163	0,0047
GCDCA	90	nM	Bile acid	LC-MS/MS	1,341	0,0383
GCDCA	0	%	Bile acid	LC-MS/MS	0,976	0,0279
GCDCA	120	%	Bile acid	LC-MS/MS	0,888	0,0254
Primary ID	**Sampling time**	**Unit**	**Category**	**Method**	**VIP**	**Loadings**
GCDCA	15	%	Bile acid	LC-MS/MS	1,065	0,0305
GCDCA	240	%	Bile acid	LC-MS/MS	0,953	0,0273
GCDCA	30	%	Bile acid	LC-MS/MS	0,610	0,0174
GCDCA	60	%	Bile acid	LC-MS/MS	0,377	0,0108
GCDCA	90	%	Bile acid	LC-MS/MS	0,649	0,0186
GDCA	0	nM	Bile acid	LC-MS/MS	0,141	0,0040
GDCA	120	nM	Bile acid	LC-MS/MS	1,721	0,0492
GDCA	15	nM	Bile acid	LC-MS/MS	0,029	0,0008
GDCA	240	nM	Bile acid	LC-MS/MS	1,897	0,0542
GDCA	30	nM	Bile acid	LC-MS/MS	0,432	-0,0124
GDCA	60	nM	Bile acid	LC-MS/MS	0,144	-0,0041
GDCA	90	nM	Bile acid	LC-MS/MS	1,024	0,0293
GDCA	0	%	Bile acid	LC-MS/MS	0,711	0,0203
GDCA	120	%	Bile acid	LC-MS/MS	0,984	0,0281
GDCA	15	%	Bile acid	LC-MS/MS	0,074	0,0021
GDCA	240	%	Bile acid	LC-MS/MS	1,192	0,0341
GDCA	30	%	Bile acid	LC-MS/MS	0,143	-0,0041
GDCA	60	%	Bile acid	LC-MS/MS	0,020	0,0006
GDCA	90	%	Bile acid	LC-MS/MS	0,622	0,0178
Gln	0	µM	Amino acid metabolism	Biocrates	1,026	0,0293
Gln	120	µM	Amino acid metabolism	Biocrates	1,720	0,0492
Gln	15	µM	Amino acid metabolism	Biocrates	1,568	0,0448
Gln	240	µM	Amino acid metabolism	Biocrates	1,254	0,0358
Gln	30	µM	Amino acid metabolism	Biocrates	2,172	0,0621
Gln	60	µM	Amino acid metabolism	Biocrates	1,495	0,0427
Gln	90	µM	Amino acid metabolism	Biocrates	1,268	0,0363
GLP-1	0	pM	Signalling/ hormone	RIA	0,538	0,0154
GLP-1	120	pM	Signalling/ hormone	RIA	1,012	0,0289
GLP-1	15	pM	Signalling/ hormone	RIA	0,074	-0,0021
GLP-1	240	pM	Signalling/ hormone	RIA	0,358	0,0102
GLP-1	30	pM	Signalling/ hormone	RIA	0,499	-0,0143
GLP-1	60	pM	Signalling/ hormone	RIA	0,606	0,0173
GLP-1	90	pM	Signalling/ hormone	RIA	1,030	0,0294
Glu	0	µM	Amino acid metabolism	Biocrates	2,490	-0,0712
Glu	120	µM	Amino acid metabolism	Biocrates	1,950	-0,0558
Glu	15	µM	Amino acid metabolism	Biocrates	2,471	-0,0707
Glu	240	µM	Amino acid metabolism	Biocrates	1,557	-0,0445
Glu	30	µM	Amino acid metabolism	Biocrates	2,592	-0,0741
Glu	60	µM	Amino acid metabolism	Biocrates	1,914	-0,0547
Glu	90	µM	Amino acid metabolism	Biocrates	2,215	-0,0633
Glucagon	0	pg/ml	Signalling/ hormone	RIA	0,857	-0,0245
Glucagon	120	pg/ml	Signalling/ hormone	RIA	0,837	-0,0239
Glucagon	15	pg/ml	Signalling/ hormone	RIA	1,105	-0,0316
Glucagon	240	pg/ml	Signalling/ hormone	RIA	0,102	-0,0029
Glucagon	30	pg/ml	Signalling/ hormone	RIA	1,111	-0,0318
Glucagon	60	pg/ml	Signalling/ hormone	RIA	1,008	-0,0288
Glucagon	90	pg/ml	Signalling/ hormone	RIA	0,623	-0,0178
Gluconic acid	0	AU	Glucose metabolism	GC-MS	0,019	0,0005
Gluconic acid	120	AU	Glucose metabolism	GC-MS	0,403	0,0115
Gluconic acid	15	AU	Glucose metabolism	GC-MS	0,567	-0,0162
Gluconic acid	240	AU	Glucose metabolism	GC-MS	0,479	-0,0137
Gluconic acid	30	AU	Glucose metabolism	GC-MS	1,371	-0,0392
Gluconic acid	60	AU	Glucose metabolism	GC-MS	1,455	-0,0416
Gluconic acid	90	AU	Glucose metabolism	GC-MS	0,459	0,0131
Glucose	**0**	**mM**	**Glucose metabolism**	**Enzymatic**	**Not used in the PLS-DA model**	
Glucose	**120**	**mM**	**Glucose metabolism**	**Enzymatic**		
Glucose	**15**	**mM**	**Glucose metabolism**	**Enzymatic**		
Glucose	**240**	**mM**	**Glucose metabolism**	**Enzymatic**		
Glucose	**30**	**mM**	**Glucose metabolism**	**Enzymatic**		
Glucose	**60**	**mM**	**Glucose metabolism**	**Enzymatic**		
Glucose	**90**	**mM**	**Glucose metabolism**	**Enzymatic**		

Supplemental Table 1. Variables included in the PLS-DA model. Variables are presented with their respective VIP values and loadings, method of detection and units.

Gly	0	µM	Amino acid metabolism	Biocrates	**1,508**	**0,0431**
Gly	120	µM	Amino acid metabolism	Biocrates	**1,676**	**0,0479**
Gly	15	µM	Amino acid metabolism	Biocrates	**1,598**	**0,0457**
Gly	240	µM	Amino acid metabolism	Biocrates	**1,485**	**0,0425**
Gly	30	µM	Amino acid metabolism	Biocrates	**1,937**	**0,0554**
Gly	60	µM	Amino acid metabolism	Biocrates	**1,756**	**0,0502**
Gly	90	µM	Amino acid metabolism	Biocrates	**1,875**	**0,0536**
Glycerol	0	AU	Lipid metabolism	GC-MS	**0,055**	**0,0016**
Glycerol	120	AU	Lipid metabolism	GC-MS	**0,769**	**-0,0220**
Glycerol	15	AU	Lipid metabolism	GC-MS	**0,084**	**-0,0024**
Primary ID	**Sampling time**	**Unit**	**Category**	**Method**	**VIP**	**Loadings**
Glycerol	240	AU	Lipid metabolism	GC-MS	**0,411**	**0,0118**
Glycerol	30	AU	Lipid metabolism	GC-MS	**0,522**	**-0,0149**
Glycerol	60	AU	Lipid metabolism	GC-MS	**0,809**	**-0,0231**
Glycerol	90	AU	Lipid metabolism	GC-MS	**0,837**	**-0,0239**
Gly-conj BA	0	%	Bile acid	LC-MS/MS	**1,157**	**0,0331**
Gly-conj BA	120	%	Bile acid	LC-MS/MS	**1,867**	**0,0534**
Gly-conj BA	15	%	Bile acid	LC-MS/MS	**1,302**	**0,0372**
Gly-conj BA	240	%	Bile acid	LC-MS/MS	**2,208**	**0,0631**
Gly-conj BA	30	%	Bile acid	LC-MS/MS	**0,642**	**0,0184**
Gly-conj BA	60	%	Bile acid	LC-MS/MS	**0,776**	**0,0222**
Gly-conj BA	90	%	Bile acid	LC-MS/MS	**1,411**	**0,0403**
Gly-conj. BA	0	nM	Bile acid	LC-MS/MS	**0,395**	**0,0113**
Gly-conj. BA	120	nM	Bile acid	LC-MS/MS	**1,958**	**0,0560**
Gly-conj. BA	15	nM	Bile acid	LC-MS/MS	**0,867**	**0,0248**
Gly-conj. BA	240	nM	Bile acid	LC-MS/MS	**2,229**	**0,0637**
Gly-conj. BA	30	nM	Bile acid	LC-MS/MS	**0,339**	**0,0097**
Gly-conj. BA	60	nM	Bile acid	LC-MS/MS	**0,330**	**0,0094**
Gly-conj. BA	90	nM	Bile acid	LC-MS/MS	**1,292**	**0,0369**
GUDCA	0	nM	Bile acid	LC-MS/MS	**0,473**	**0,0135**
GUDCA	120	nM	Bile acid	LC-MS/MS	**1,481**	**0,0424**
GUDCA	15	nM	Bile acid	LC-MS/MS	**0,649**	**0,0186**
GUDCA	240	nM	Bile acid	LC-MS/MS	**1,918**	**0,0549**
GUDCA	30	nM	Bile acid	LC-MS/MS	**0,732**	**0,0209**
GUDCA	60	nM	Bile acid	LC-MS/MS	**0,719**	**0,0206**
GUDCA	90	nM	Bile acid	LC-MS/MS	**1,047**	**0,0299**
GUDCA	0	%	Bile acid	LC-MS/MS	**0,825**	**0,0236**
GUDCA	120	%	Bile acid	LC-MS/MS	**0,707**	**0,0202**
GUDCA	15	%	Bile acid	LC-MS/MS	**0,658**	**0,0188**
GUDCA	240	%	Bile acid	LC-MS/MS	**0,914**	**0,0261**
GUDCA	30	%	Bile acid	LC-MS/MS	**0,608**	**0,0174**
GUDCA	60	%	Bile acid	LC-MS/MS	**0,586**	**0,0167**
GUDCA	90	%	Bile acid	LC-MS/MS	**0,495**	**0,0141**
HbA1c	fasting	mmol/mol Hb	Glucose metabolism	Enzymatic	**1,886**	**-0,0539**
HDL-chol	fasting	mM	Lipid metabolism	Enzymatic	**1,219**	**0,0349**
Hip	fasting	cm	Body composition	Measuring tape	**0,326**	**0,0093**
His	0	µM	Amino acid metabolism	Biocrates	**0,543**	**0,0155**
His	120	µM	Amino acid metabolism	Biocrates	**0,541**	**0,0155**
His	15	µM	Amino acid metabolism	Biocrates	**0,168**	**0,0048**
His	240	µM	Amino acid metabolism	Biocrates	**0,559**	**0,0160**
His	30	µM	Amino acid metabolism	Biocrates	**1,442**	**0,0412**
His	60	µM	Amino acid metabolism	Biocrates	**0,503**	**0,0144**
His	90	µM	Amino acid metabolism	Biocrates	**0,782**	**0,0224**
Histamine	0	µM	Biogenic amine	Biocrates	**0,270**	**-0,0077**
Histamine	120	µM	Biogenic amine	Biocrates	**0,034**	**-0,0010**
Histamine	15	µM	Biogenic amine	Biocrates	**0,419**	**-0,0120**
Histamine	240	µM	Biogenic amine	Biocrates	**0,187**	**-0,0053**
Histamine	30	µM	Biogenic amine	Biocrates	**0,267**	**-0,0076**
Histamine	60	µM	Biogenic amine	Biocrates	**0,477**	**-0,0136**
Histamine	90	µM	Biogenic amine	Biocrates	**0,034**	**-0,0010**
IAAT	fasting	%BW	Body composition	MRI	**2,201**	**-0,0629**
IAAT	fasting	%TBF	Body composition	MRI	**1,971**	**-0,0564**
IAAT	fasting	kg	Body composition	MRI	**2,228**	**-0,0637**
IAAT:ASAT	fasting	ratio	Body composition	MRI	**2,054**	**-0,0587**
ICAM-1	0	ng/ml	Inflammation	ELISA	**0,633**	**-0,0181**
ICAM-1	120	ng/ml	Inflammation	ELISA	**0,697**	**-0,0199**
ICAM-1	60	ng/ml	Inflammation	ELISA	**0,370**	**-0,0106**
IL-10	0	pg/ml	Inflammation	ELISA	**0,545**	**0,0156**
IL-10	120	pg/ml	Inflammation	ELISA	**0,766**	**0,0219**
IL-10	60	pg/ml	Inflammation	ELISA	**0,779**	**0,0223**
IL-18	fasting	pg/ml	Inflammation	ELISA	**0,894**	**-0,0256**

Supplemental Table 1. Variables included in the PLS-DA model. Variables are presented with their respective VIP values and loadings, method of detection and units.

IL1-RA	0	pg/ml	Inflammation	ELISA	**0,955**	**-0,0273**
IL1-RA	120	pg/ml	Inflammation	ELISA	**1,572**	**-0,0449**
IL1-RA	60	pg/ml	Inflammation	ELISA	**1,382**	**-0,0395**
IL-8	0	pg/ml	Inflammation	ELISA	**0,008**	**0,0002**
IL-8	120	pg/ml	Inflammation	ELISA	**0,551**	**0,0158**
IL-8	60	pg/ml	Inflammation	ELISA	**1,092**	**0,0312**
Ile	0	µM	Amino acid metabolism	Biocrates	**1,180**	**-0,0338**
Ile	120	µM	Amino acid metabolism	Biocrates	**1,584**	**-0,0453**
Ile	15	µM	Amino acid metabolism	Biocrates	**1,496**	**-0,0428**
Ile	240	µM	Amino acid metabolism	Biocrates	**0,472**	**-0,0135**
Ile	30	µM	Amino acid metabolism	Biocrates	**0,877**	**-0,0251**
Primary ID	**Sampling time**	**Unit**	**Category**	**Method**	**VIP**	**Loadings**
Ile	60	µM	Amino acid metabolism	Biocrates	**1,616**	**-0,0462**
Ile	90	µM	Amino acid metabolism	Biocrates	**1,663**	**-0,0476**
Insulin	**0**	**mIU/l**	**Signalling/ hormone**	**RIA**	**Not used in the PLS-DA model**	
Insulin	**120**	**mIU/l**	**Signalling/ hormone**	**RIA**		
Insulin	**15**	**mIU/l**	**Signalling/ hormone**	**RIA**		
Insulin	**240**	**mIU/l**	**Signalling/ hormone**	**RIA**		
Insulin	**30**	**mIU/l**	**Signalling/ hormone**	**RIA**		
Insulin	**60**	**mIU/l**	**Signalling/ hormone**	**RIA**		
Insulin	**90**	**mIU/l**	**Signalling/ hormone**	**RIA**		
Intern.: subcut. fat	fasting	ratio	Body composition	MRI	**1,953**	**-0,0559**
Internal	fasting	%TBF	Body composition	MRI	**1,975**	**-0,0565**
Internal body fat	fasting	%BW	Body composition	MRI	**2,167**	**-0,0620**
Internal body fat	fasting	kg	Body composition	MRI	**2,168**	**-0,0620**
Kynurenine	0	µM	Biogenic amine	Biocrates	**0,478**	**-0,0137**
Kynurenine	120	µM	Biogenic amine	Biocrates	**0,502**	**-0,0143**
Kynurenine	15	µM	Biogenic amine	Biocrates	**0,291**	**-0,0083**
Kynurenine	240	µM	Biogenic amine	Biocrates	**0,796**	**-0,0228**
Kynurenine	30	µM	Biogenic amine	Biocrates	**0,071**	**0,0020**
Kynurenine	60	µM	Biogenic amine	Biocrates	**0,170**	**-0,0049**
Kynurenine	90	µM	Biogenic amine	Biocrates	**0,210**	**-0,0060**
Lactic acid	0	AU	Glucose metabolism	GC-MS	**0,054**	**-0,0015**
Lactic acid	120	AU	Glucose metabolism	GC-MS	**0,782**	**-0,0224**
Lactic acid	15	AU	Glucose metabolism	GC-MS	**0,973**	**-0,0278**
Lactic acid	240	AU	Glucose metabolism	GC-MS	**0,554**	**-0,0158**
Lactic acid	30	AU	Glucose metabolism	GC-MS	**0,385**	**-0,0110**
Lactic acid	60	AU	Glucose metabolism	GC-MS	**1,300**	**-0,0372**
Lactic acid	90	AU	Glucose metabolism	GC-MS	**1,070**	**-0,0306**
LDL-chol	fasting	mM	Lipid metabolism	Enzymatic	**0,580**	**0,0166**
Leptin	fasting	ng/ml	Signalling/ hormone	ELISA	**0,362**	**-0,0104**
Leu	0	µM	Amino acid metabolism	Biocrates	**1,135**	**-0,0324**
Leu	120	µM	Amino acid metabolism	Biocrates	**1,508**	**-0,0431**
Leu	15	µM	Amino acid metabolism	Biocrates	**1,412**	**-0,0404**
Leu	240	µM	Amino acid metabolism	Biocrates	**0,729**	**-0,0208**
Leu	30	µM	Amino acid metabolism	Biocrates	**1,056**	**-0,0302**
Leu	60	µM	Amino acid metabolism	Biocrates	**1,616**	**-0,0462**
Leu	90	µM	Amino acid metabolism	Biocrates	**1,827**	**-0,0522**
Linoleic acid	0	AU	Lipid metabolism	GC-MS	**0,075**	**-0,0022**
Linoleic acid	120	AU	Lipid metabolism	GC-MS	**0,811**	**-0,0232**
Linoleic acid	15	AU	Lipid metabolism	GC-MS	**0,656**	**-0,0188**
Linoleic acid	240	AU	Lipid metabolism	GC-MS	**0,817**	**0,0233**
Linoleic acid	30	AU	Lipid metabolism	GC-MS	**0,781**	**-0,0223**
Linoleic acid	60	AU	Lipid metabolism	GC-MS	**1,126**	**-0,0322**
Linoleic acid	90	AU	Lipid metabolism	GC-MS	**0,708**	**-0,0202**
Lipid hydroperoxides	fasting	ng/ml	Oxidative stress	x	**0,125**	**0,0036**
Liver fat	fasting	ratio	Body composition	MRI	**2,830**	**-0,0809**
Liver T2	fasting	ratio	Body composition	MRI	**1,219**	**0,0349**
Lymphocyte	0	giga/l	Leucocyte	Cell counter	**1,073**	**-0,0307**
Lymphocyte	120	giga/l	Leucocyte	Cell counter	**0,413**	**-0,0118**
Lymphocyte	15	giga/l	Leucocyte	Cell counter	**1,108**	**-0,0317**
Lymphocyte	240	giga/l	Leucocyte	Cell counter	**1,594**	**-0,0456**
Lymphocyte	30	giga/l	Leucocyte	Cell counter	**1,242**	**-0,0355**
Lymphocyte	60	giga/l	Leucocyte	Cell counter	**0,761**	**-0,0217**
Lymphocyte	90	giga/l	Leucocyte	Cell counter	**0,400**	**-0,0114**
Lys	0	µM	Amino acid metabolism	Biocrates	**0,134**	**-0,0038**
Lys	120	µM	Amino acid metabolism	Biocrates	**0,257**	**-0,0074**
Lys	15	µM	Amino acid metabolism	Biocrates	**0,270**	**-0,0077**
Lys	240	µM	Amino acid metabolism	Biocrates	**0,340**	**-0,0097**
Lys	30	µM	Amino acid metabolism	Biocrates	**0,581**	**0,0166**
Lys	60	µM	Amino acid metabolism	Biocrates	**0,459**	**-0,0131**

Supplemental Table 1. Variables included in the PLS-DA model. Variables are presented with their respective VIP values and loadings, method of detection and units.

Lys	90	µM	Amino acid metabolism	Biocrates	0,227	-0,0065
Mannose	0	AU	Glucose metabolism	GC-MS	0,791	-0,0226
Mannose	120	AU	Glucose metabolism	GC-MS	1,323	-0,0378
Mannose	15	AU	Glucose metabolism	GC-MS	0,379	-0,0108
Mannose	240	AU	Glucose metabolism	GC-MS	0,686	-0,0196
Mannose	30	AU	Glucose metabolism	GC-MS	0,833	-0,0238
Mannose	60	AU	Glucose metabolism	GC-MS	1,837	-0,0525
Mannose	90	AU	Glucose metabolism	GC-MS	1,740	-0,0497
MCP-1	0	pg/ml	Inflammation	ELISA	0,417	0,0119
MCP-1	120	pg/ml	Inflammation	ELISA	0,477	0,0136
MCP-1	60	pg/ml	Inflammation	ELISA	0,552	0,0158
MDA	fasting	µM	Oxidative stress	x	1,567	-0,0448
Primary ID	**Sampling time**	**Unit**	**Category**	**Method**	**VIP**	**Loadings**
meso-Erythritol	0	AU	Glucose metabolism	GC-MS	1,405	-0,0402
meso-Erythritol	120	AU	Glucose metabolism	GC-MS	1,077	-0,0308
meso-Erythritol	15	AU	Glucose metabolism	GC-MS	1,161	-0,0332
meso-Erythritol	240	AU	Glucose metabolism	GC-MS	0,893	-0,0255
meso-Erythritol	30	AU	Glucose metabolism	GC-MS	1,296	-0,0370
meso-Erythritol	60	AU	Glucose metabolism	GC-MS	1,737	-0,0497
meso-Erythritol	90	AU	Glucose metabolism	GC-MS	1,348	-0,0386
Met	0	µM	Amino acid metabolism	Biocrates	0,314	-0,0090
Met	120	µM	Amino acid metabolism	Biocrates	0,636	-0,0182
Met	15	µM	Amino acid metabolism	Biocrates	0,557	-0,0159
Met	240	µM	Amino acid metabolism	Biocrates	0,042	-0,0012
Met	30	µM	Amino acid metabolism	Biocrates	0,277	0,0079
Met	60	µM	Amino acid metabolism	Biocrates	0,564	-0,0161
Met	90	µM	Amino acid metabolism	Biocrates	0,582	-0,0166
Met-SO	0	µM	Amino acid metabolism	Biocrates	0,051	0,0015
Met-SO	120	µM	Amino acid metabolism	Biocrates	0,088	-0,0025
Met-SO	15	µM	Amino acid metabolism	Biocrates	0,341	-0,0098
Met-SO	240	µM	Amino acid metabolism	Biocrates	0,051	0,0015
Met-SO	30	µM	Amino acid metabolism	Biocrates	0,099	-0,0028
Met-SO	60	µM	Amino acid metabolism	Biocrates	0,232	0,0066
Met-SO	90	µM	Amino acid metabolism	Biocrates	0,046	0,0013
Monocyte count	0	giga/l	Leucocyte	Cell counter	1,615	-0,0462
Monocyte count	120	giga/l	Leucocyte	Cell counter	0,930	-0,0266
Monocyte count	15	giga/l	Leucocyte	Cell counter	2,078	-0,0594
Monocyte count	240	giga/l	Leucocyte	Cell counter	2,579	-0,0737
Monocyte count	30	giga/l	Leucocyte	Cell counter	1,857	-0,0531
Monocyte count	60	giga/l	Leucocyte	Cell counter	1,238	-0,0354
Monocyte count	90	giga/l	Leucocyte	Cell counter	0,711	-0,0203
Myo-inositol	0	AU	Glucose metabolism	GC-MS	1,041	-0,0298
Myo-inositol	120	AU	Glucose metabolism	GC-MS	0,284	-0,0081
Myo-inositol	15	AU	Glucose metabolism	GC-MS	0,060	-0,0017
Myo-inositol	240	AU	Glucose metabolism	GC-MS	0,499	0,0143
Myo-inositol	30	AU	Glucose metabolism	GC-MS	0,558	-0,0160
Myo-inositol	60	AU	Glucose metabolism	GC-MS	0,533	-0,0153
Myo-inositol	90	AU	Glucose metabolism	GC-MS	0,424	-0,0121
NAIAT	fasting	%BW	Body composition	MRI	1,271	-0,0363
NAIAT	fasting	%TBF	Body composition	MRI	1,570	-0,0449
NAIAT (kg)	fasting	kg	Body composition	MRI	1,561	-0,0446
NASAT	fasting	%BW	Body composition	MRI	1,042	0,0298
NASAT	fasting	%TBF	Body composition	MRI	1,710	0,0489
NASAT (kg)	fasting	kg	Body composition	MRI	0,357	0,0102
NEFA	0	mM	Lipid metabolism	Enzymatic	0,907	-0,0259
NEFA	120	mM	Lipid metabolism	Enzymatic	1,359	-0,0389
NEFA	15	mM	Lipid metabolism	Enzymatic	1,113	-0,0318
NEFA	240	mM	Lipid metabolism	Enzymatic	0,590	0,0169
NEFA	30	mM	Lipid metabolism	Enzymatic	1,857	-0,0531
NEFA	60	mM	Lipid metabolism	Enzymatic	2,406	-0,0688
NEFA	90	mM	Lipid metabolism	Enzymatic	1,864	-0,0533
Neutrophil count	0	giga/l	Leucocyte	Cell counter	1,473	-0,0421
Neutrophil count	120	giga/l	Leucocyte	Cell counter	1,315	-0,0376
Neutrophil count	15	giga/l	Leucocyte	Cell counter	1,629	-0,0466
Neutrophil count	240	giga/l	Leucocyte	Cell counter	1,637	-0,0468
Neutrophil count	30	giga/l	Leucocyte	Cell counter	1,503	-0,0430
Neutrophil count	60	giga/l	Leucocyte	Cell counter	1,381	-0,0395
Neutrophil count	90	giga/l	Leucocyte	Cell counter	1,231	-0,0352
Oleic acid	0	AU	Lipid metabolism	GC-MS	0,810	-0,0232
Oleic acid	120	AU	Lipid metabolism	GC-MS	1,681	-0,0481
Oleic acid	15	AU	Lipid metabolism	GC-MS	0,897	-0,0257

Supplemental Table 1. Variables included in the PLS-DA model. Variables are presented with their respective VIP values and loadings, method of detection and units.

Oleic acid	240	AU	Lipid metabolism	GC-MS	0,827	0,0237
Oleic acid	30	AU	Lipid metabolism	GC-MS	2,078	-0,0594
Oleic acid	60	AU	Lipid metabolism	GC-MS	2,112	-0,0604
Oleic acid	90	AU	Lipid metabolism	GC-MS	2,061	-0,0589
Orn	0	µM	Biogenic amine	Biocrates	0,030	0,0009
Orn	120	µM	Biogenic amine	Biocrates	0,146	0,0042
Orn	15	µM	Biogenic amine	Biocrates	0,713	0,0204
Orn	240	µM	Biogenic amine	Biocrates	0,488	0,0139
Orn	30	µM	Biogenic amine	Biocrates	0,949	0,0271
Orn	60	µM	Biogenic amine	Biocrates	0,721	0,0206
Orn	90	µM	Biogenic amine	Biocrates	1,034	0,0296
Palmitic acid	0	AU	Lipid metabolism	GC-MS	1,368	-0,0391
Palmitic acid	120	AU	Lipid metabolism	GC-MS	1,685	-0,0482
Primary ID	**Sampling time**	**Unit**	**Category**	**Method**	**VIP**	**Loadings**
Palmitic acid	15	AU	Lipid metabolism	GC-MS	1,133	-0,0324
Palmitic acid	240	AU	Lipid metabolism	GC-MS	0,065	0,0019
Palmitic acid	30	AU	Lipid metabolism	GC-MS	1,647	-0,0471
Palmitic acid	60	AU	Lipid metabolism	GC-MS	2,001	-0,0572
Palmitic acid	90	AU	Lipid metabolism	GC-MS	1,920	-0,0549
Pancreas fat	fasting	ratio	Body composition	MRI	0,069	-0,0020
Phe	0	µM	Amino acid metabolism	Biocrates	1,101	-0,0315
Phe	120	µM	Amino acid metabolism	Biocrates	1,360	-0,0389
Phe	15	µM	Amino acid metabolism	Biocrates	1,566	-0,0448
Phe	240	µM	Amino acid metabolism	Biocrates	0,735	-0,0210
Phe	30	µM	Amino acid metabolism	Biocrates	0,581	-0,0166
Phe	60	µM	Amino acid metabolism	Biocrates	1,364	-0,0390
Phe	90	µM	Amino acid metabolism	Biocrates	1,514	-0,0433
Pro	0	µM	Amino acid metabolism	Biocrates	0,686	-0,0196
Pro	120	µM	Amino acid metabolism	Biocrates	1,077	-0,0308
Pro	15	µM	Amino acid metabolism	Biocrates	1,023	-0,0293
Pro	240	µM	Amino acid metabolism	Biocrates	0,705	-0,0201
Pro	30	µM	Amino acid metabolism	Biocrates	0,439	-0,0126
Pro	60	µM	Amino acid metabolism	Biocrates	0,990	-0,0283
Pro	90	µM	Amino acid metabolism	Biocrates	1,081	-0,0309
Putrescine	0	µM	Biogenic amine	Biocrates	0,294	-0,0084
Putrescine	120	µM	Biogenic amine	Biocrates	0,236	0,0068
Putrescine	15	µM	Biogenic amine	Biocrates	0,154	0,0044
Putrescine	240	µM	Biogenic amine	Biocrates	0,420	0,0120
Putrescine	30	µM	Biogenic amine	Biocrates	0,190	-0,0054
Putrescine	60	µM	Biogenic amine	Biocrates	0,046	-0,0013
Putrescine	90	µM	Biogenic amine	Biocrates	0,624	0,0178
Pyruvate	0	AU	Glucose metabolism	GC-MS	0,861	-0,0246
Pyruvate	120	AU	Glucose metabolism	GC-MS	0,542	-0,0155
Pyruvate	15	AU	Glucose metabolism	GC-MS	0,420	-0,0120
Pyruvate	240	AU	Glucose metabolism	GC-MS	0,571	-0,0163
Pyruvate	30	AU	Glucose metabolism	GC-MS	1,413	-0,0404
Pyruvate	60	AU	Glucose metabolism	GC-MS	1,404	-0,0401
Pyruvate	90	AU	Glucose metabolism	GC-MS	1,646	-0,0471
PYY	0	pM	Signalling/ hormone	RIA	0,954	-0,0273
PYY	120	pM	Signalling/ hormone	RIA	0,003	0,0001
PYY	15	pM	Signalling/ hormone	RIA	0,952	-0,0272
PYY	240	pM	Signalling/ hormone	RIA	0,702	-0,0201
PYY	30	pM	Signalling/ hormone	RIA	0,365	-0,0104
PYY	60	pM	Signalling/ hormone	RIA	0,769	-0,0220
PYY	90	pM	Signalling/ hormone	RIA	0,612	-0,0175
Ribitol	0	AU	Glucose metabolism	GC-MS	0,457	-0,0131
Ribitol	120	AU	Glucose metabolism	GC-MS	0,665	-0,0190
Ribitol	15	AU	Glucose metabolism	GC-MS	0,519	-0,0148
Ribitol	240	AU	Glucose metabolism	GC-MS	0,253	-0,0072
Ribitol	30	AU	Glucose metabolism	GC-MS	0,357	-0,0102
Ribitol	60	AU	Glucose metabolism	GC-MS	0,431	-0,0123
Ribitol	90	AU	Glucose metabolism	GC-MS	0,925	-0,0264
SAT	fasting	%BW	Body composition	MRI	1	0,0294602
SAT	fasting	%TBF	Body composition	MRI	1,975	0,0565
SAT	fasting	kg	Body composition	MRI	0,333	0,0095
SBP	fasting	mmHg	General	Sphygmomanometer	0,008	0,0002
SDMA	0	µM	Biogenic amine	Biocrates	0,110	0,0031
SDMA	120	µM	Biogenic amine	Biocrates	1,145	0,0327
SDMA	15	µM	Biogenic amine	Biocrates	0,624	-0,0179
SDMA	240	µM	Biogenic amine	Biocrates	0,552	0,0158
SDMA	30	µM	Biogenic amine	Biocrates	0,804	-0,0230

Supplemental Table 1. Variables included in the PLS-DA model. Variables are presented with their respective VIP values and loadings, method of detection and units.

SDMA	60	µM	Biogenic amine	Biocrates	**0,273**	**0,0078**
SDMA	90	µM	Biogenic amine	Biocrates	**0,534**	**0,0153**
Ser	0	µM	Amino acid metabolism	Biocrates	**1,424**	**0,0407**
Ser	120	µM	Amino acid metabolism	Biocrates	**1,108**	**0,0317**
Ser	15	µM	Amino acid metabolism	Biocrates	**1,216**	**0,0348**
Ser	240	µM	Amino acid metabolism	Biocrates	**1,372**	**0,0392**
Ser	30	µM	Amino acid metabolism	Biocrates	**1,946**	**0,0556**
Ser	60	µM	Amino acid metabolism	Biocrates	**1,129**	**0,0323**
Ser	90	µM	Amino acid metabolism	Biocrates	**1,135**	**0,0325**
Serotonin	0	µM	Biogenic amine	Biocrates	**0,056**	**-0,0016**
Serotonin	120	µM	Biogenic amine	Biocrates	**0,882**	**0,0252**
Serotonin	15	µM	Biogenic amine	Biocrates	**0,045**	**-0,0013**
Serotonin	240	µM	Biogenic amine	Biocrates	**0,548**	**0,0157**
Serotonin	30	µM	Biogenic amine	Biocrates	**0,779**	**-0,0223**
Primary ID	**Sampling time**	**Unit**	**Category**	**Method**	**VIP**	**Loadings**
Serotonin	60	µM	Biogenic amine	Biocrates	**0,491**	**0,0140**
Serotonin	90	µM	Biogenic amine	Biocrates	**0,775**	**0,0222**
s-E-Selectin	fasting	ng/ml	Inflammation	ELISA	**1,551**	**-0,0444**
Soleus-IMCL	fasting	ratio	Body composition	MRI	**1,381**	**-0,0395**
Spermidine	0	µM	Biogenic amine	Biocrates	**1,267**	**-0,0362**
Spermidine	120	µM	Biogenic amine	Biocrates	**1,124**	**-0,0321**
Spermidine	15	µM	Biogenic amine	Biocrates	**1,267**	**-0,0362**
Spermidine	240	µM	Biogenic amine	Biocrates	**1,107**	**-0,0317**
Spermidine	30	µM	Biogenic amine	Biocrates	**1,421**	**-0,0406**
Spermidine	60	µM	Biogenic amine	Biocrates	**1,068**	**-0,0305**
Spermidine	90	µM	Biogenic amine	Biocrates	**0,588**	**-0,0168**
Spermine	0	µM	Biogenic amine	Biocrates	**1,477**	**-0,0422**
Spermine	120	µM	Biogenic amine	Biocrates	**1,359**	**-0,0389**
Spermine	15	µM	Biogenic amine	Biocrates	**1,239**	**-0,0354**
Spermine	240	µM	Biogenic amine	Biocrates	**1,332**	**-0,0381**
Spermine	30	µM	Biogenic amine	Biocrates	**1,405**	**-0,0402**
Spermine	60	µM	Biogenic amine	Biocrates	**1,167**	**-0,0334**
Spermine	90	µM	Biogenic amine	Biocrates	**1,174**	**-0,0336**
Stearic acid	0	AU	Lipid metabolism	GC-MS	**1,729**	**-0,0494**
Stearic acid	120	AU	Lipid metabolism	GC-MS	**1,976**	**-0,0565**
Stearic acid	15	AU	Lipid metabolism	GC-MS	**1,209**	**-0,0346**
Stearic acid	240	AU	Lipid metabolism	GC-MS	**0,246**	**-0,0070**
Stearic acid	30	AU	Lipid metabolism	GC-MS	**2,558**	**-0,0731**
Stearic acid	60	AU	Lipid metabolism	GC-MS	**2,360**	**-0,0675**
Stearic acid	90	AU	Lipid metabolism	GC-MS	**1,568**	**-0,0448**
Sum CA	0	nM	Bile acid	LC-MS/MS	**0,572**	**0,0163**
Sum CA	120	nM	Bile acid	LC-MS/MS	**1,142**	**0,0327**
Sum CA	15	nM	Bile acid	LC-MS/MS	**0,430**	**0,0123**
Sum CA	240	nM	Bile acid	LC-MS/MS	**1,277**	**0,0365**
Sum CA	30	nM	Bile acid	LC-MS/MS	**0,386**	**0,0110**
Sum CA	60	nM	Bile acid	LC-MS/MS	**0,488**	**0,0139**
Sum CA	90	nM	Bile acid	LC-MS/MS	**0,783**	**0,0224**
Sum CDCA	0	nM	Bile acid	LC-MS/MS	**0,230**	**0,0066**
Sum CDCA	120	nM	Bile acid	LC-MS/MS	**1,553**	**0,0444**
Sum CDCA	15	nM	Bile acid	LC-MS/MS	**0,495**	**0,0142**
Sum CDCA	240	nM	Bile acid	LC-MS/MS	**1,960**	**0,0561**
Sum CDCA	30	nM	Bile acid	LC-MS/MS	**0,220**	**0,0063**
Sum CDCA	60	nM	Bile acid	LC-MS/MS	**0,146**	**0,0042**
Sum CDCA	90	nM	Bile acid	LC-MS/MS	**1,203**	**0,0344**
Sum DCA	0	nM	Bile acid	LC-MS/MS	**0,470**	**-0,0134**
Sum DCA	120	nM	Bile acid	LC-MS/MS	**1,064**	**0,0304**
Sum DCA	15	nM	Bile acid	LC-MS/MS	**0,619**	**-0,0177**
Sum DCA	240	nM	Bile acid	LC-MS/MS	**1,276**	**0,0365**
Sum DCA	30	nM	Bile acid	LC-MS/MS	**0,574**	**-0,0164**
Sum DCA	60	nM	Bile acid	LC-MS/MS	**0,272**	**-0,0078**
Sum DCA	90	nM	Bile acid	LC-MS/MS	**0,754**	**0,0216**
Sum lyso PC	0	µM	Glycerophopspholipid	Biocrates	**0,630**	**0,0180**
Sum lyso PC	120	µM	Glycerophopspholipid	Biocrates	**0,666**	**0,0190**
Sum lyso PC	15	µM	Glycerophopspholipid	Biocrates	**0,303**	**0,0087**
Sum lyso PC	240	µM	Glycerophopspholipid	Biocrates	**0,502**	**0,0143**
Sum lyso PC	30	µM	Glycerophopspholipid	Biocrates	**0,972**	**0,0278**
Sum lyso PC	60	µM	Glycerophopspholipid	Biocrates	**1,170**	**0,0334**
Sum lyso PC	90	µM	Glycerophopspholipid	Biocrates	**0,467**	**0,0134**
Sum PC aa	0	µM	Glycerophopspholipid	Biocrates	**0,131**	**0,0037**
Sum PC aa	120	µM	Glycerophopspholipid	Biocrates	**0,097**	**-0,0028**
Sum PC aa	15	µM	Glycerophopspholipid	Biocrates	**0,036**	**0,0010**

Supplemental Table 1. Variables included in the PLS-DA model. Variables are presented with their respective VIP values and loadings, method of detection and units.

Sum PC aa	240	µM	Glycerophopspholipid	Biocrates	**0,347**	**0,0099**
Sum PC aa	30	µM	Glycerophopspholipid	Biocrates	**0,421**	**0,0120**
Sum PC aa	60	µM	Glycerophopspholipid	Biocrates	**0,826**	**0,0236**
Sum PC aa	90	µM	Glycerophopspholipid	Biocrates	**0,357**	**0,0102**
Sum PC ae	0	µM	Glycerophopspholipid	Biocrates	**0,575**	**0,0164**
Sum PC ae	120	µM	Glycerophopspholipid	Biocrates	**0,564**	**0,0161**
Sum PC ae	15	µM	Glycerophopspholipid	Biocrates	**0,597**	**0,0171**
Sum PC ae	240	µM	Glycerophopspholipid	Biocrates	**1,013**	**0,0290**
Sum PC ae	30	µM	Glycerophopspholipid	Biocrates	**0,982**	**0,0281**
Sum PC ae	60	µM	Glycerophopspholipid	Biocrates	**1,314**	**0,0376**
Sum PC ae	90	µM	Glycerophopspholipid	Biocrates	**0,940**	**0,0269**
Sum sphingomyelins	0	µM	Sphingomyelin	Biocrates	**0,490**	**0,0140**
Sum sphingomyelins	120	µM	Sphingomyelin	Biocrates	**0,598**	**0,0171**
Sum sphingomyelins	15	µM	Sphingomyelin	Biocrates	**0,531**	**0,0152**
Sum sphingomyelins	240	µM	Sphingomyelin	Biocrates	**0,856**	**0,0245**
Primary ID	**Sampling time**	**Unit**	**Category**	**Method**	**VIP**	**Loadings**
Sum sphingomyelins	30	µM	Sphingomyelin	Biocrates	**0,820**	**0,0235**
Sum sphingomyelins	60	µM	Sphingomyelin	Biocrates	**1,648**	**0,0471**
Sum sphingomyelins	90	µM	Sphingomyelin	Biocrates	**0,752**	**0,0215**
Sum UDCA	0	nM	Bile acid	LC-MS/MS	**0,125**	**0,0036**
Sum UDCA	120	nM	Bile acid	LC-MS/MS	**1,774**	**0,0507**
Sum UDCA	15	nM	Bile acid	LC-MS/MS	**0,013**	**0,0004**
Sum UDCA	240	nM	Bile acid	LC-MS/MS	**1,943**	**0,0556**
Sum UDCA	30	nM	Bile acid	LC-MS/MS	**0,340**	**-0,0097**
Sum UDCA	60	nM	Bile acid	LC-MS/MS	**0,058**	**-0,0017**
Sum UDCA	90	nM	Bile acid	LC-MS/MS	**1,074**	**0,0307**
T4	fasting	pM	Signalling/ hormone	x	**0,244**	**-0,0070**
TAT	fasting	%BW	Body composition	MRI	**0,552**	**0,0158**
TAT	fasting	kg	Body composition	MRI	**0,243**	**-0,0069**
Tau-conj. BA	0	%	Bile acid	LC-MS/MS	**0,017**	**-0,0005**
Tau-conj. BA	120	%	Bile acid	LC-MS/MS	**0,211**	**-0,0060**
Tau-conj. BA	15	%	Bile acid	LC-MS/MS	**0,748**	**-0,0214**
Tau-conj. BA	240	%	Bile acid	LC-MS/MS	**0,206**	**-0,0059**
Tau-conj. BA	30	%	Bile acid	LC-MS/MS	**0,973**	**-0,0278**
Tau-conj. BA	60	%	Bile acid	LC-MS/MS	**0,670**	**-0,0191**
Tau-conj. BA	90	%	Bile acid	LC-MS/MS	**0,441**	**-0,0126**
Tau-conj. BA	0	nM	Bile acid	LC-MS/MS	**0,063**	**0,0018**
Tau-conj. BA	120	nM	Bile acid	LC-MS/MS	**1,011**	**0,0289**
Tau-conj. BA	15	nM	Bile acid	LC-MS/MS	**0,339**	**-0,0097**
Tau-conj. BA	240	nM	Bile acid	LC-MS/MS	**1,148**	**0,0328**
Tau-conj. BA	30	nM	Bile acid	LC-MS/MS	**0,375**	**-0,0107**
Tau-conj. BA	60	nM	Bile acid	LC-MS/MS	**0,055**	**-0,0016**
Tau-conj. BA	90	nM	Bile acid	LC-MS/MS	**0,710**	**0,0203**
Taurine	0	µM	Amino acid metabolism	Biocrates	**0,285**	**-0,0081**
Taurine	120	µM	Amino acid metabolism	Biocrates	**0,405**	**0,0116**
Taurine	15	µM	Amino acid metabolism	Biocrates	**0,795**	**-0,0227**
Taurine	240	µM	Amino acid metabolism	Biocrates	**0,355**	**0,0102**
Taurine	30	µM	Amino acid metabolism	Biocrates	**0,514**	**-0,0147**
Taurine	60	µM	Amino acid metabolism	Biocrates	**0,247**	**0,0071**
Taurine	90	µM	Amino acid metabolism	Biocrates	**0,323**	**0,0092**
TCA	0	nM	Bile acid	LC-MS/MS	**0,415**	**0,0119**
TCA	120	nM	Bile acid	LC-MS/MS	**0,843**	**0,0241**
TCA	15	nM	Bile acid	LC-MS/MS	**0,350**	**-0,0100**
TCA	240	nM	Bile acid	LC-MS/MS	**0,806**	**0,0231**
TCA	30	nM	Bile acid	LC-MS/MS	**0,231**	**0,0066**
TCA	60	nM	Bile acid	LC-MS/MS	**0,365**	**0,0104**
TCA	90	nM	Bile acid	LC-MS/MS	**0,540**	**0,0154**
TCA	0	%	Bile acid	LC-MS/MS	**0,057**	**0,0016**
TCA	120	%	Bile acid	LC-MS/MS	**0,413**	**0,0118**
TCA	15	%	Bile acid	LC-MS/MS	**0,578**	**-0,0165**
TCA	240	%	Bile acid	LC-MS/MS	**0,024**	**0,0007**
TCA	30	%	Bile acid	LC-MS/MS	**0,427**	**-0,0122**
TCA	60	%	Bile acid	LC-MS/MS	**0,203**	**-0,0058**
TCA	90	%	Bile acid	LC-MS/MS	**0,447**	**-0,0128**
TCDCA	0	nM	Bile acid	LC-MS/MS	**0,230**	**-0,0066**
TCDCA	120	nM	Bile acid	LC-MS/MS	**0,836**	**0,0239**
TCDCA	15	nM	Bile acid	LC-MS/MS	**0,011**	**0,0003**
TCDCA	240	nM	Bile acid	LC-MS/MS	**1,054**	**0,0301**
TCDCA	30	nM	Bile acid	LC-MS/MS	**0,376**	**-0,0107**
TCDCA	60	nM	Bile acid	LC-MS/MS	**0,159**	**-0,0045**
TCDCA	90	nM	Bile acid	LC-MS/MS	**0,730**	**0,0209**

Supplemental Table 1. Variables included in the PLS-DA model. Variables are presented with their respective VIP values and loadings, method of detection and units.

TCDCA	0	%	Bile acid	LC-MS/MS	0,292	-0,0084
TCDCA	120	%	Bile acid	LC-MS/MS	0,588	-0,0168
TCDCA	15	%	Bile acid	LC-MS/MS	0,542	-0,0155
TCDCA	240	%	Bile acid	LC-MS/MS	0,501	-0,0143
TCDCA	30	%	Bile acid	LC-MS/MS	0,828	-0,0237
TCDCA	60	%	Bile acid	LC-MS/MS	0,673	-0,0193
TCDCA	90	%	Bile acid	LC-MS/MS	0,510	-0,0146
TDCA	0	nM	Bile acid	LC-MS/MS	0,296	0,0085
TDCA	120	nM	Bile acid	LC-MS/MS	1,208	0,0345
TDCA	15	nM	Bile acid	LC-MS/MS	0,485	-0,0139
TDCA	240	nM	Bile acid	LC-MS/MS	1,420	0,0406
TDCA	30	nM	Bile acid	LC-MS/MS	0,782	-0,0224
TDCA	60	nM	Bile acid	LC-MS/MS	0,321	-0,0092
TDCA	90	nM	Bile acid	LC-MS/MS	0,826	0,0236
TDCA	0	%	Bile acid	LC-MS/MS	0,426	0,0122
TDCA	120	%	Bile acid	LC-MS/MS	0,005	0,0001
Primary ID	**Sampling time**	**Unit**	**Category**	**Method**	**VIP**	**Loadings**
TDCA	15	%	Bile acid	LC-MS/MS	0,761	-0,0218
TDCA	240	%	Bile acid	LC-MS/MS	0,277	0,0079
TDCA	30	%	Bile acid	LC-MS/MS	0,966	-0,0276
TDCA	60	%	Bile acid	LC-MS/MS	0,518	-0,0148
TDCA	90	%	Bile acid	LC-MS/MS	0,090	0,0026
Thr	0	µM	Amino acid metabolism	Biocrates	0,295	-0,0084
Thr	120	µM	Amino acid metabolism	Biocrates	0,046	0,0013
Thr	15	µM	Amino acid metabolism	Biocrates	0,302	-0,0086
Thr	240	µM	Amino acid metabolism	Biocrates	0,025	0,0007
Thr	30	µM	Amino acid metabolism	Biocrates	0,122	0,0035
Thr	60	µM	Amino acid metabolism	Biocrates	0,311	-0,0089
Thr	90	µM	Amino acid metabolism	Biocrates	0,406	0,0116
Threitol	0	AU	Glucose metabolism	GC-MS	1,126	-0,0322
Threitol	120	AU	Glucose metabolism	GC-MS	1,525	-0,0436
Threitol	15	AU	Glucose metabolism	GC-MS	1,330	-0,0380
Threitol	240	AU	Glucose metabolism	GC-MS	1,397	-0,0399
Threitol	30	AU	Glucose metabolism	GC-MS	1,026	-0,0293
Threitol	60	AU	Glucose metabolism	GC-MS	1,595	-0,0456
Threitol	90	AU	Glucose metabolism	GC-MS	1,347	-0,0385
Tibialis-IMCL	fasting	ratio	Body composition	MRI	1,243	-0,0355
TLCA	0	nM	Bile acid	LC-MS/MS	0,435	-0,0125
TLCA	120	nM	Bile acid	LC-MS/MS	1,164	0,0333
TLCA	15	nM	Bile acid	LC-MS/MS	0,625	0,0179
TLCA	240	nM	Bile acid	LC-MS/MS	1,246	0,0356
TLCA	30	nM	Bile acid	LC-MS/MS	0,258	0,0074
TLCA	60	nM	Bile acid	LC-MS/MS	0,216	0,0062
TLCA	90	nM	Bile acid	LC-MS/MS	0,981	0,0281
TLCA	0	%	Bile acid	LC-MS/MS	0,413	0,0118
TLCA	120	%	Bile acid	LC-MS/MS	0,212	-0,0061
TLCA	15	%	Bile acid	LC-MS/MS	0,072	-0,0021
TLCA	240	%	Bile acid	LC-MS/MS	0,585	-0,0167
TLCA	30	%	Bile acid	LC-MS/MS	0,155	-0,0044
TLCA	60	%	Bile acid	LC-MS/MS	0,151	-0,0043
TLCA	90	%	Bile acid	LC-MS/MS	0,194	-0,0055
TNF-alpha	fasting	pg/ml	Inflammation	ELISA	0,003	-0,0001
total DMA	0	µM	Biogenic amine	Biocrates	0,541	-0,0155
total DMA	120	µM	Biogenic amine	Biocrates	0,142	0,0041
total DMA	15	µM	Biogenic amine	Biocrates	0,009	-0,0003
total DMA	240	µM	Biogenic amine	Biocrates	0,386	-0,0110
total DMA	30	µM	Biogenic amine	Biocrates	0,365	-0,0104
total DMA	60	µM	Biogenic amine	Biocrates	0,257	-0,0074
total DMA	90	µM	Biogenic amine	Biocrates	0,301	0,0086
Total thiols	fasting	mM	Oxidative stress	x	0,653	0,0187
Triglycerides	0	mM	Lipid metabolism	Enzymatic	2,774	-0,0793
Triglycerides	120	mM	Lipid metabolism	Enzymatic	2,559	-0,0732
Triglycerides	15	mM	Lipid metabolism	Enzymatic	2,427	-0,0694
Triglycerides	240	mM	Lipid metabolism	Enzymatic	2,483	-0,0710
Triglycerides	30	mM	Lipid metabolism	Enzymatic	2,338	-0,0669
Triglycerides	60	mM	Lipid metabolism	Enzymatic	2,214	-0,0633
Triglycerides	90	mM	Lipid metabolism	Enzymatic	2,687	-0,0768
Trp	0	µM	Amino acid metabolism	Biocrates	1,538	-0,0440
Trp	120	µM	Amino acid metabolism	Biocrates	1,528	-0,0437
Trp	15	µM	Amino acid metabolism	Biocrates	1,546	-0,0442
Trp	240	µM	Amino acid metabolism	Biocrates	1,212	-0,0347

Supplemental Table 1. Variables included in the PLS-DA model. Variables are presented with their respective VIP values and loadings, method of detection and units.

Trp	30	µM	Amino acid metabolism	Biocrates	**1,136**	**-0,0325**
Trp	60	µM	Amino acid metabolism	Biocrates	**1,004**	**-0,0287**
Trp	90	µM	Amino acid metabolism	Biocrates	**1,895**	**-0,0542**
Trunk:periph. fat	fasting	ratio	Body composition	MRI	**1,178**	**-0,0337**
TSH	fasting	mIU/l	Signalling/ hormone	x	**0,227**	**0,0065**
TUDCA	120	nM	Bile acid	LC-MS/MS	**0,956**	**0,0273**
TUDCA	15	nM	Bile acid	LC-MS/MS	**0,766**	**-0,0219**
TUDCA	240	nM	Bile acid	LC-MS/MS	**1,005**	**0,0288**
TUDCA	30	nM	Bile acid	LC-MS/MS	**0,050**	**0,0014**
TUDCA	60	nM	Bile acid	LC-MS/MS	**0,147**	**-0,0042**
TUDCA	90	nM	Bile acid	LC-MS/MS	**0,484**	**0,0138**
TUDCA	120	%	Bile acid	LC-MS/MS	**1,258**	**-0,0360**
TUDCA	15	%	Bile acid	LC-MS/MS	**0,989**	**-0,0283**
TUDCA	240	%	Bile acid	LC-MS/MS	**1,682**	**-0,0481**
TUDCA	30	%	Bile acid	LC-MS/MS	**1,290**	**-0,0369**
TUDCA	60	%	Bile acid	LC-MS/MS	**1,366**	**-0,0391**
TUDCA	90	%	Bile acid	LC-MS/MS	**1,564**	**-0,0447**
Primary ID	**Sampling time**	**Unit**	**Category**	**Method**	**VIP**	**Loadings**
Tyr	0	µM	Amino acid metabolism	Biocrates	**1,416**	**-0,0405**
Tyr	120	µM	Amino acid metabolism	Biocrates	**1,437**	**-0,0411**
Tyr	15	µM	Amino acid metabolism	Biocrates	**1,013**	**-0,0290**
Tyr	240	µM	Amino acid metabolism	Biocrates	**0,746**	**-0,0213**
Tyr	30	µM	Amino acid metabolism	Biocrates	**0,428**	**-0,0122**
Tyr	60	µM	Amino acid metabolism	Biocrates	**0,944**	**-0,0270**
Tyr	90	µM	Amino acid metabolism	Biocrates	**1,371**	**-0,0392**
Urea	0	mM	Amino acid metabolism	Enzymatic	**1,067**	**-0,0305**
Urea	120	mM	Amino acid metabolism	Enzymatic	**1,237**	**-0,0354**
Urea	15	mM	Amino acid metabolism	Enzymatic	**1,123**	**-0,0321**
Urea	240	mM	Amino acid metabolism	Enzymatic	**1,290**	**-0,0369**
Urea	30	mM	Amino acid metabolism	Enzymatic	**1,180**	**-0,0337**
Urea	60	mM	Amino acid metabolism	Enzymatic	**1,359**	**-0,0389**
Urea	90	mM	Amino acid metabolism	Enzymatic	**1,210**	**-0,0346**
Uric acid	fasting	µM	Amino acid metabolism	Enzymatic	**1,194**	**-0,0341**
Val	0	µM	Amino acid metabolism	Biocrates	**1,154**	**-0,0330**
Val	120	µM	Amino acid metabolism	Biocrates	**1,590**	**-0,0455**
Val	15	µM	Amino acid metabolism	Biocrates	**1,194**	**-0,0341**
Val	240	µM	Amino acid metabolism	Biocrates	**1,112**	**-0,0318**
Val	30	µM	Amino acid metabolism	Biocrates	**0,739**	**-0,0211**
Val	60	µM	Amino acid metabolism	Biocrates	**1,216**	**-0,0348**
Val	90	µM	Amino acid metabolism	Biocrates	**1,559**	**-0,0446**
VCAM	fasting	ng/ml	Inflammation	ELISA	**0,744**	**-0,0213**
Waist	fasting	cm	Body composition	Measuring tape	**1,373**	**-0,0393**
White blood cell	0	giga/l	Leucocyte	Cell counter	**1,716**	**-0,0491**
White blood cell	120	giga/l	Leucocyte	Cell counter	**1,401**	**-0,0401**
White blood cell	15	giga/l	Leucocyte	Cell counter	**1,859**	**-0,0532**
White blood cell	240	giga/l	Leucocyte	Cell counter	**2,174**	**-0,0622**
White blood cell	30	giga/l	Leucocyte	Cell counter	**1,750**	**-0,0501**
White blood cell	60	giga/l	Leucocyte	Cell counter	**1,495**	**-0,0428**
White blood cell	90	giga/l	Leucocyte	Cell counter	**1,260**	**-0,0360**